INFORMATION TO USERS

This manuscript has been reproduced from the microfilm master. UMI films the text directly from the original or copy submitted. Thus, some thesis and dissertation copies are in typewriter face, while others may be from any type of computer printer.

The quality of this reproduction is dependent upon the quality of the copy submitted. Broken or indistinct print, colored or poor quality illustrations and photographs, print bleedthrough, substandard margins, and improper alignment can adversely affect reproduction.

In the unlikely event that the author did not send UMI a complete manuscript and there are missing pages, these will be noted. Also, if unauthorized copyright material had to be removed, a note will indicate the deletion.

Oversize materials (e.g., maps, drawings, charts) are reproduced by sectioning the original, beginning at the upper left-hand corner and continuing from left to right in equal sections with small overlaps.

ProQuest Information and Learning
300 North Zeeb Road, Ann Arbor, MI 48106-1346 USA
800-521-0600

UNIVERSITY OF CINCINNATI

_____

_____ 19____

I hereby recommend that the thesis prepared under my supervision by JOHN DIETERLE HLADES

entitled FREQUENCY ENTRAINMENT

be accepted as fulfilling this part of the requirements for the degree of DOCTOR OF PHILOSOPHY

Approved by:

Carl A. Ludeke

D. A. Wells

Boris Podolsky

Form 668—G.S. and T.C.—1M—4-51

FREQUENCY ENTRAINMENT

A dissertation submitted to the
Graduate School of Arts and Sciences of the
University of Cincinnati

in partial fulfillment of the
requirements for the degree of

DOCTOR OF PHILOSOPHY

1954

by

John Dieterle Blades

B.S. Western Maryland College 1949
M.S. University of Cincinnati 1951

FREQUENCY ENTRAINMENT

OUTLINE

1. INTRODUCTION

If a periodic force of frequency ω_2 is applied to a self-excited nonlinear system of natural frequency ω_1, and if ω_2 is in the vicinity of ω_1, the familiar heterodyning effect will be observed. However, when the difference $|\omega_2-\omega_1|$ becomes smaller and reaches a specific value, $|\omega_2-\omega_1| \neq 0$, it has been observed that the forced self-excited system has the frequency of the forcing function, ω_2. With a further variation of ω_2 there is a range within which the self-excited system is synchronized with the frequency of the forcing function and within which the amplitude of vibration for specific values of ω_2 is constant. From the nonlinear mechanical[1,2] theory it has been found that for this range of ω_2 the free vibration of the nonlinear system is suppressed by the forcing vibration, i.e. the system gains its controlling energy from the forcing function, the limit cycle no longer existing.[3] This phenomenon is called by various authors[4] frequency entrainment and the range of domination by the forcing function is the zone of entrainment. From the linear theory $|\omega_2-\omega_1|=0$ only when $\omega_1=\omega_2$, hence, it does not account for frequency entrainment, and therefore, the phenomenon is attributed to the nonlinearity of the system. Fig. 1.1 demonstrates graphically frequency entrainment. The dotted lines

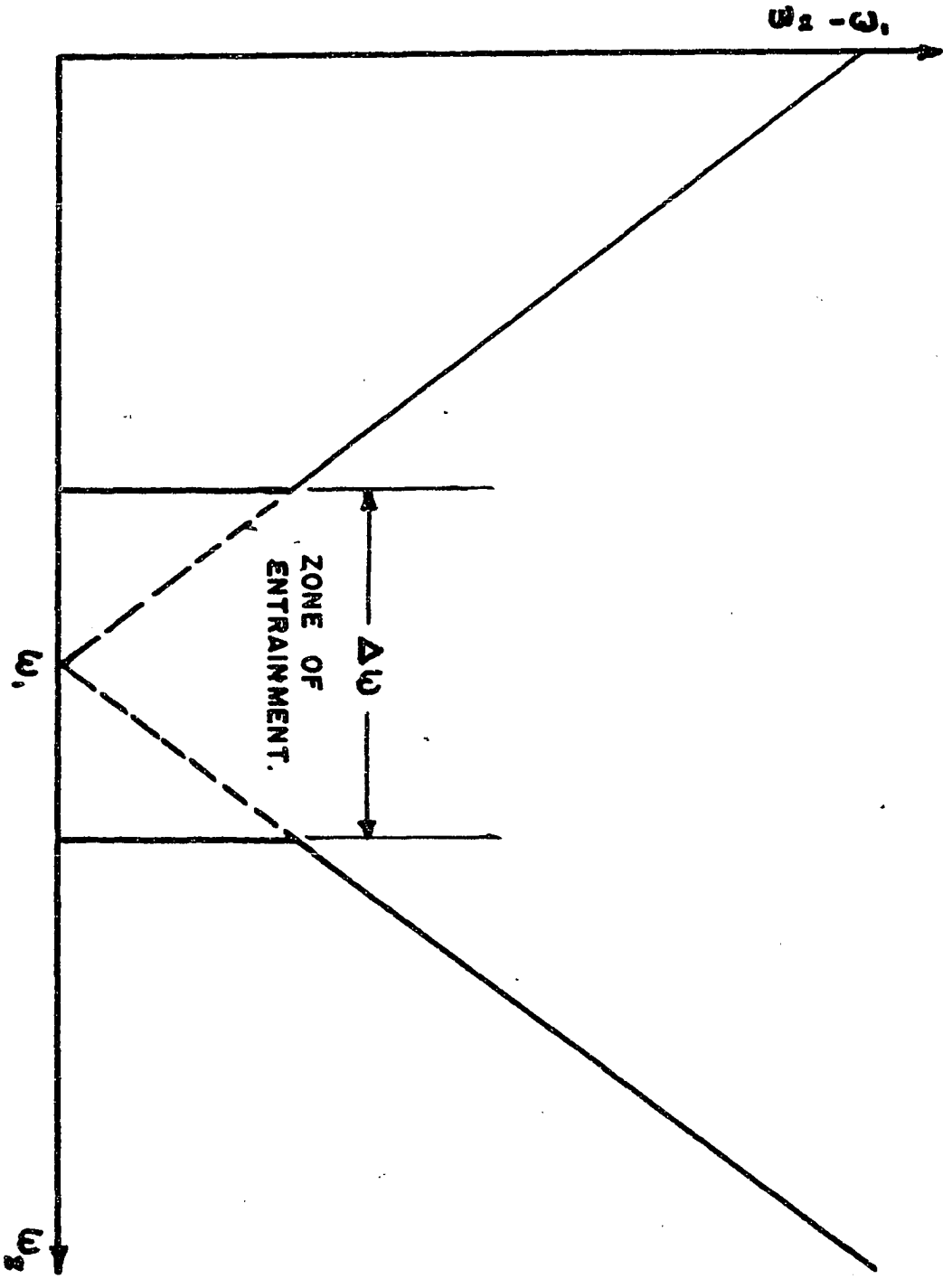

Fig. 1.1

indicating the expected linear behavior, while the solid lines indicate the nonlinear behavior.

Frequency entrainment is believed to have been observed in a number of cases. The earliest is that of Huygens' synchronous clocks.[5] Two pendulum clocks having slightly different frequencies when completely isolated from each other, will synchronize upon coupling, say by hanging them on the same wall. Later, Lord Rayleigh[6] noted that upon coupling two organ pipes of slightly different frequencies a synchronization occurs, and that electrically excited tuning forks of different natural frequencies will synchronize when coupled with a resonator. Vincent[7] in 1919 presented what is believed to be the first quantitative experimental measurements of the synchronization spread effect in connection with two capacitively coupled electronic oscillators. Möller, van der Pol, Appleton, Cartwright, and many Russian scientists have investigated frequency entrainment for one degree of freedom systems and have obtained predictions and interpretations with the approximation methods of nonlinear mechanics.

THERE IS THE QUESTION, HOWEVER, AS TO WHETHER IT IS CORRECT TO ASSUME THAT THE ABOVE DEFINED AND CURRENTLY ACCEPTED CONCEPT OF FREQUENCY ENTRAINMENT IS APPLICABLE TO NONLINEAR SYSTEMS OF TWO DEGREES OF FREEDOM. Is it

possible to have one clock entrain the other clock at the first clock's frequency, or does one oscillator entrain the other oscillator? It certainly does not seem justifiable to reduce a two degree of freedom system to a one degree of freedom system that is forced and then say that one self-oscillating system entrains the other. In comparing this procedure with the linear concepts, it is apparent that there are energy states that are neglected. Of course, the reduction is said to be justified in view of the present state of nonlinear theory for systems of two degrees of freedom. It is practically nonexistent. However, linear considerations, as well as nonlinear theory extended to systems of two degrees of freedom, should uncover a considerable amount of information in regards to the extension of the frequency entrainment concept. A complete physical interpretation should include the prediction of the existence of all energy states, as well as the entrainment phenomenon itself. Of course, the attainment of these predictions assumes (a.) previous knowledge of the specific types of coupling involved and (b.) an applicable analytical theory.

In order to obtain a clarification of the concept of frequency entrainment as applied to nonlinear systems of two degrees of freedom, it is proposed to (1.) investi-

gate and ascertain experimentally the coupling existing between two nonlinear self-excited systems, demonstrating the synchronization spread phenomenon, (2.) to consider the possible attainment of a theoretical quantitative interpretation of the synchronization spread effect and associated phenomenon, and (3.) compare these possible theoretical results with actual experimental results attained from two self-oscillating nonlinear systems with the necessary coupling. In the disertation to follow, the results of these investigations and considerations are presented.

2. THE UTILIZATION OF ELECTRO-MECHANICAL ANALOGS AND ADDITIONAL UNITS

2.1 Adaptation of the Analog to the van der Pol System

For the purpose of obtaining frequency entrainment experimentally in a nonlinear system of one degree of freedom, it was decided to adapt an electro-mechanical analog of the type developed by Ludeke and Morrison[8] to a forced van der Pol self-excited nonlinear system, and if successful, then couple a second identical analog to it, so that the two degree of freedom case can be investigated. There are a number of advantages in following this procedure. First of all, if successful, a measurable mechanical frequency entrainment will be obtained, secondly, the physical system itself is visually perceived which on many types of analogs cannot be done and thus, is physically a disadvantage, and thirdly, all parameters of the analoged system are conveniently controllable.

In order to achieve the above purpose a number of additions and alterations to the original electro-mechanical analog are required. The differential equation of motion of the displacement of the shaft of the basic analog is

$$\ddot{\theta} + \alpha_1 \dot{\theta} + \omega^2 \theta = 0, \qquad (2.1)$$

and the homogeneous van der Pol equation of motion is

$$\ddot{\theta} - \alpha \dot{\theta} + \omega^2 \theta + \beta \theta^2 \dot{\theta} = 0. \qquad (2.2)$$

By comparing eq (2.1) and eq (2.2), it can be seen that negative damping and nonlinearity torques are required.

The conversion of eq (2.1) to a negatively damped system has been achieved by affixing at right angles to the moveable coil in the main magnetic field a similar coil. The current induced in it will be proportional to the damping of the system. This current is then amplified by a dc amplifier and injected into a second coil connected to the main analog shaft and within a permanent radial magnetic field, located above the main field coils, with the correct polarity to give a torque that is proportional to the negative of the damping. It should be mentioned that coulombic damping is to be neglected in the system.

To obtain the nonlinearity torque a displacement function generator similar to that described by Ludeke and Evans[9] is utilized, giving a current that is proportional to $f(\theta) = \theta^3$. A simple RC differentiator circuit is then employed to differentiate θ^3 with respect to time, giving a current that is proportional to $\theta^2\dot{\theta}$. In order to have the required magnitude of this current, two dc amplifiers are utilized, the output of which drives another coil attached to the analog shaft and within the previously mentioned permanent radial magnet. A block diagram illustrating the analoged van der Pol system is given in fig. 2.1. The displacement as a function of time is also

$$\ddot{\theta} - \alpha\dot{\theta} + \omega^2\theta + \beta\theta^2\dot{\theta} = 0$$

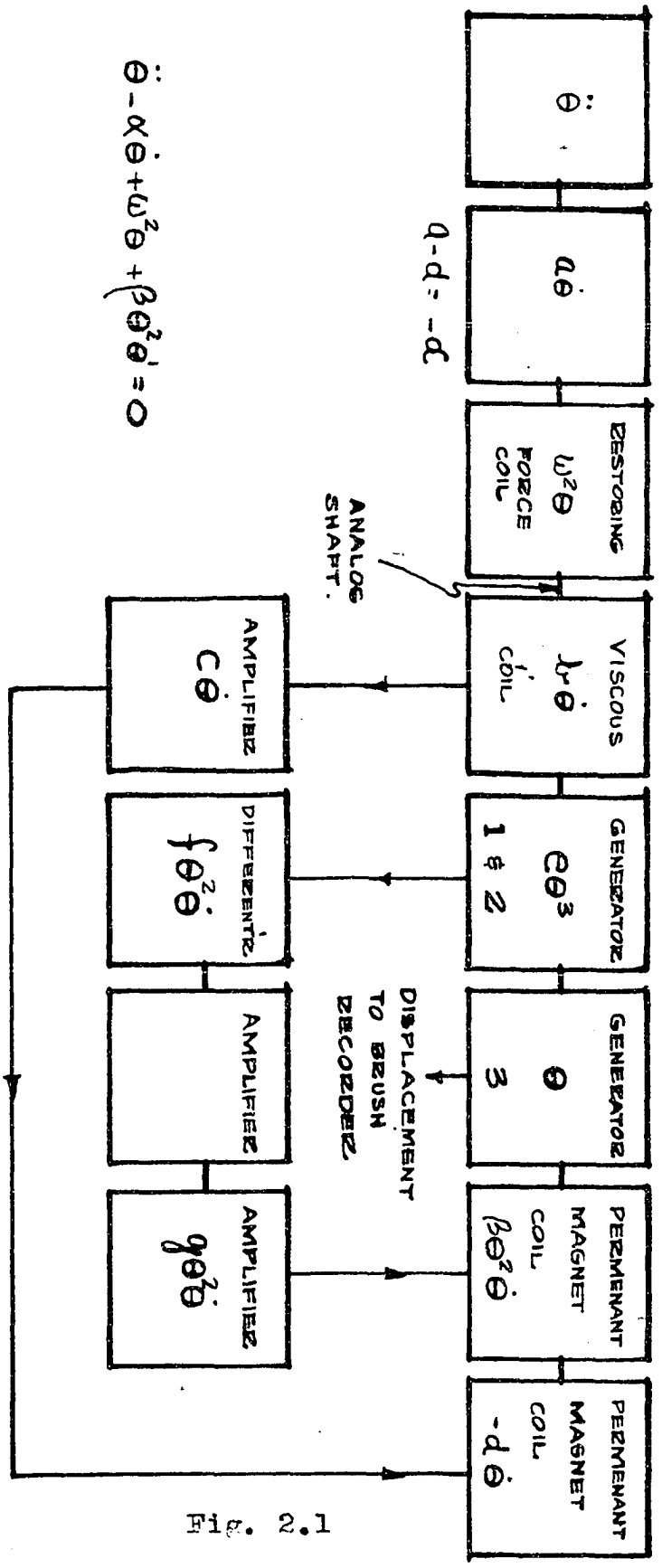

Fig. 2.1

obtained from a displacement function generator, the output of which is used to drive a Brush recording instrument for permanent records.

2.2 Displacement Function Generators

Due to the fact that for two degrees of freedom an increased number of function generators is required, the problem of their location becomes important. Each one requires a shutter connected to the analog shaft, causing a crowded condition. This difficulty is overcome by employing a light source, having the direction of the analog shaft. A circular shutter is then attached to the bottom of the analog shaft, and a mirror arrangement constructed such that the light from the mask attached to the shutter is reflected into the collector cylinders located vertically around the bottom of the shaft. Fig. 2.2 illustrates the arrangement of the collector units, mirrors, shutter and light source.

The masks now instead of having rectangular coordinates require polar coordinates. If the shutter has an opening cut in it, which is bounded by $r_1 = f_1(\theta)$ and $r_2 = f_2(\theta)$, then the quantity of light which passes through the opening is proportional to

$$\varphi(\theta) = \int_0^{\theta} (r_2^2 - r_1^2)\, d\varphi$$

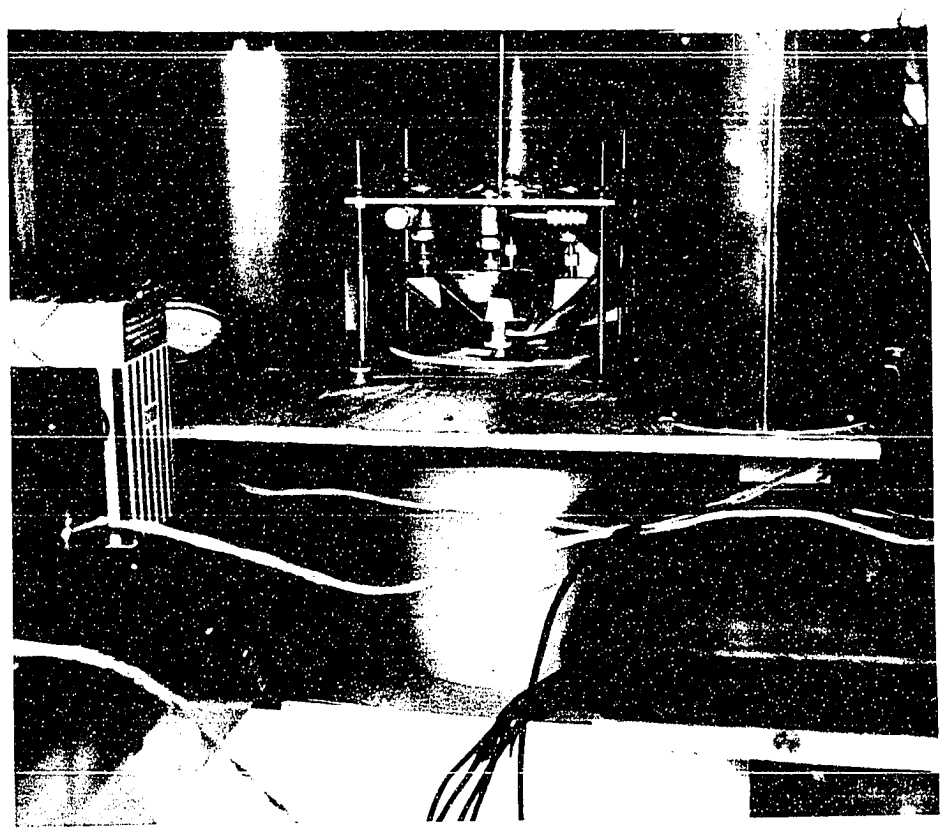

Fig. 2.2

and if $r_1 = r_0 + \varphi^2$ and $r_2 = r_0 - \varphi^2$, then $\varphi(\theta) = k\theta^3$, k a constant.

One more difficulty must be considered and that is the fact that θ^3 is an odd function. When θ is negative the photo cell will not give a negative current. Hence, by having a separate mask for positive θ and another for negative θ the photocell circuits can be arranged such that their output is proportional to θ^3.

The final construction of each analog unit utilizes four displacement function generators. Two are employed to obtain the nonlinearity, one for displacement as a function of time, and the final one later on for coupling.

2.3 Operation of the Analog Units

A number of experiments have been performed to demonstrate that the respective units of the analog are operating correctly and with the required degree of accuracy. Fig. 2.3 gives the typical response of a collector cylinder. Figs. 2.4 and 2.5 give the expected and experimental response of the nonlinearity displacement function generator. Fig. 2.6 demonstrates the cubic accuracy with a plot of $y = k\theta^3$. Fig. 2.7 is a representation of the curve $y = \theta^2\dot{\theta}$ when the displacement is $\theta = \sin \omega t$. Fig. 2.8 is the actual output of the differentiator circuit when the analog shaft

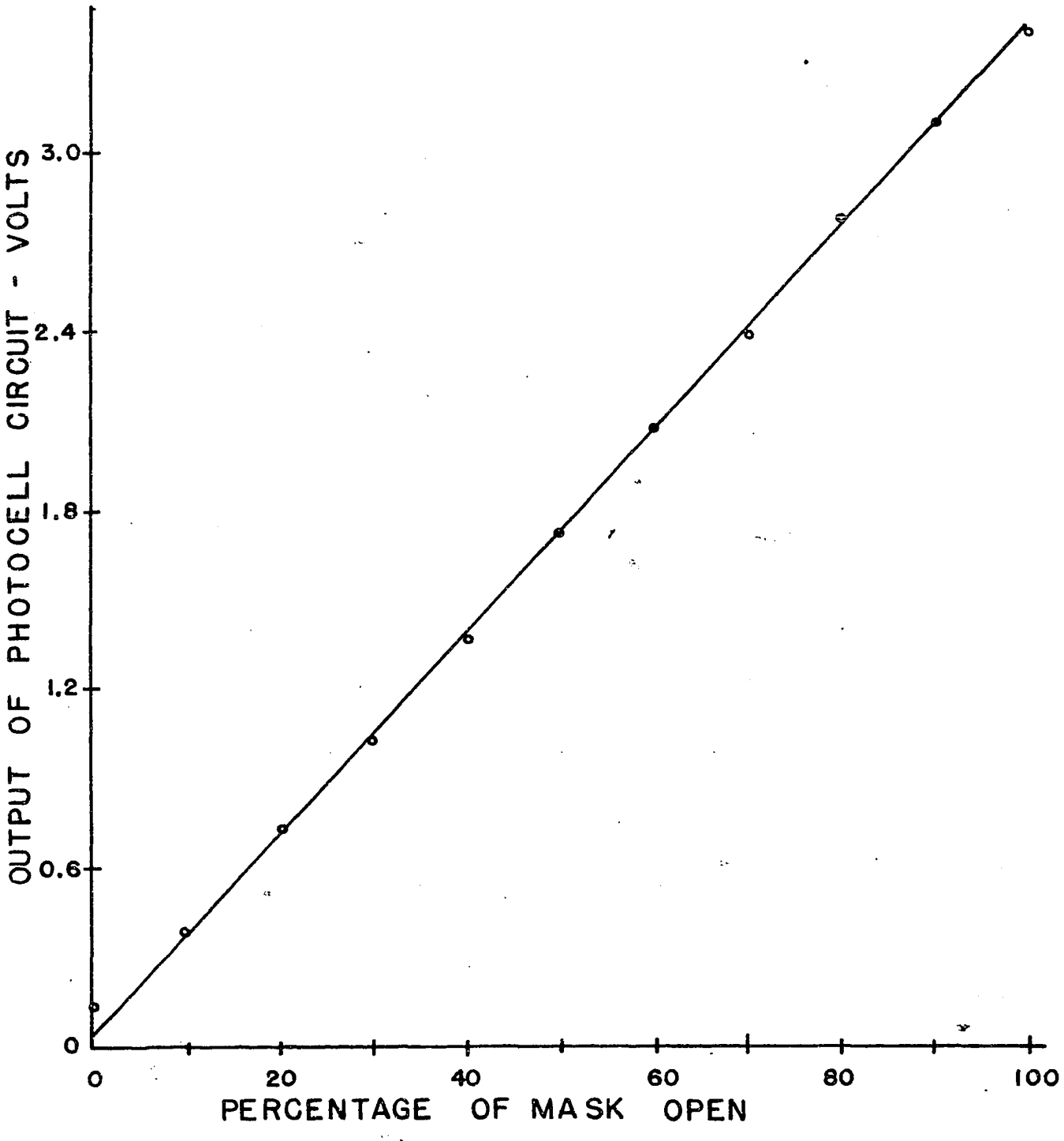

Fig. 2.3

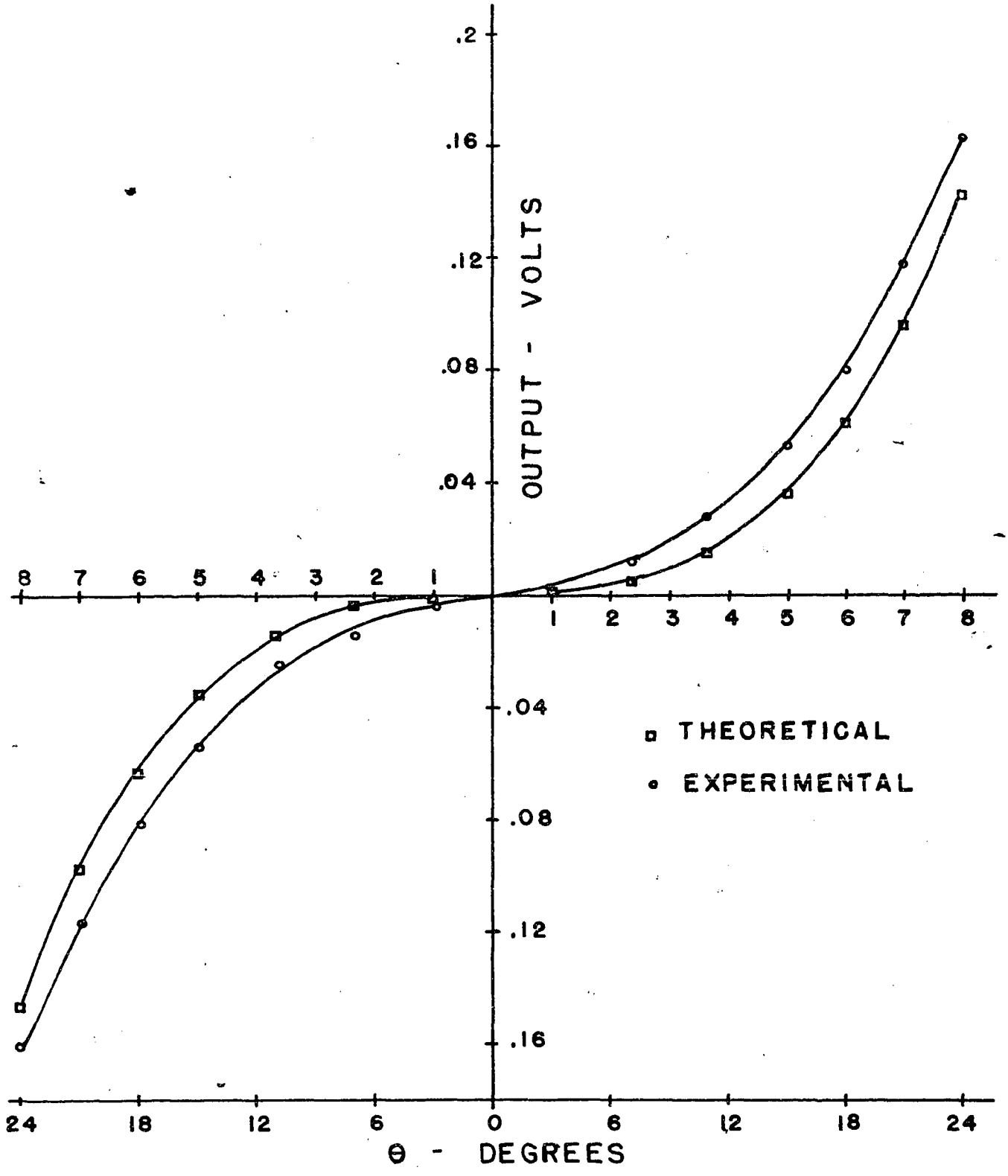

Fig. 2.4

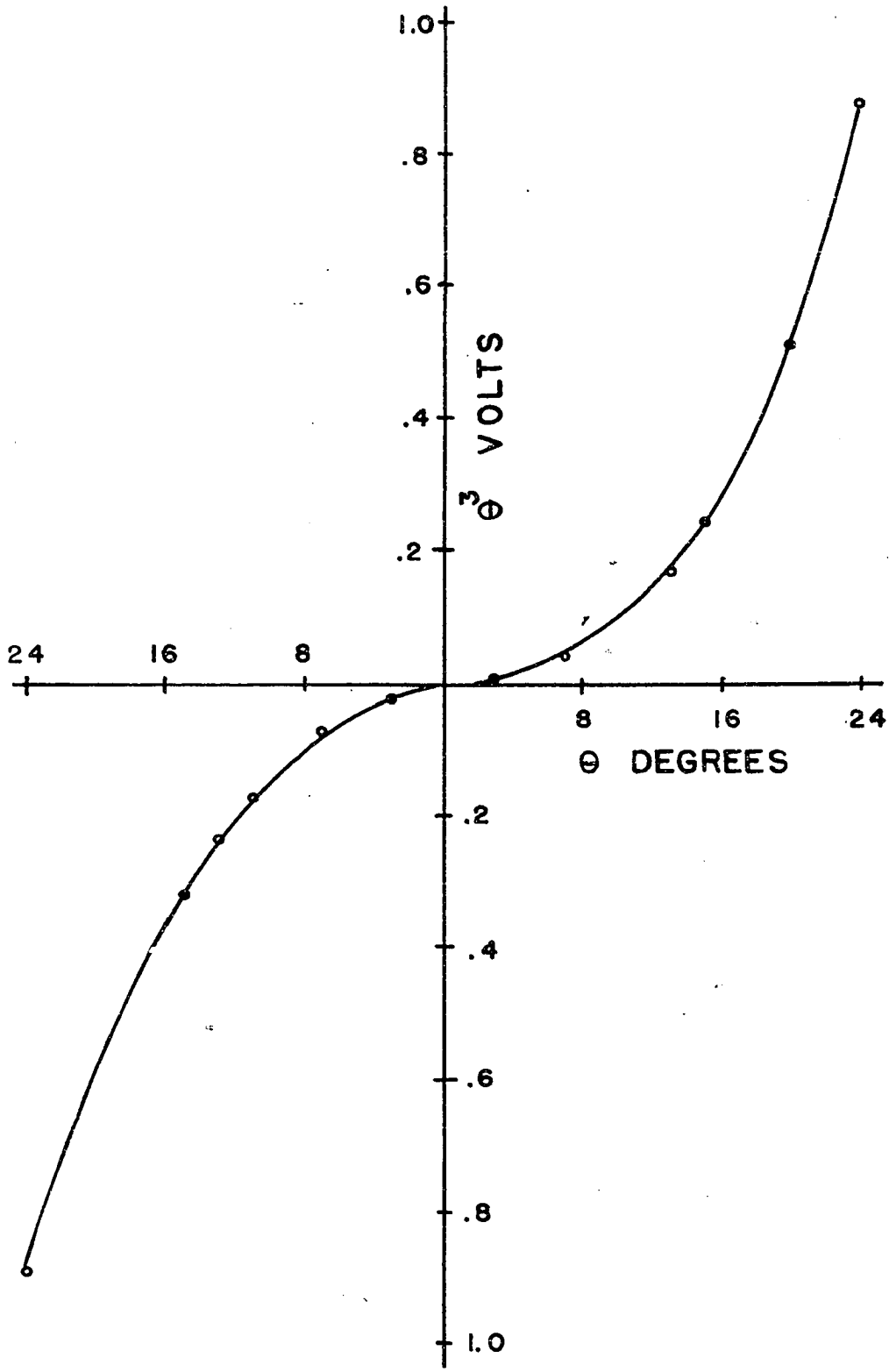

Fig. 2.5

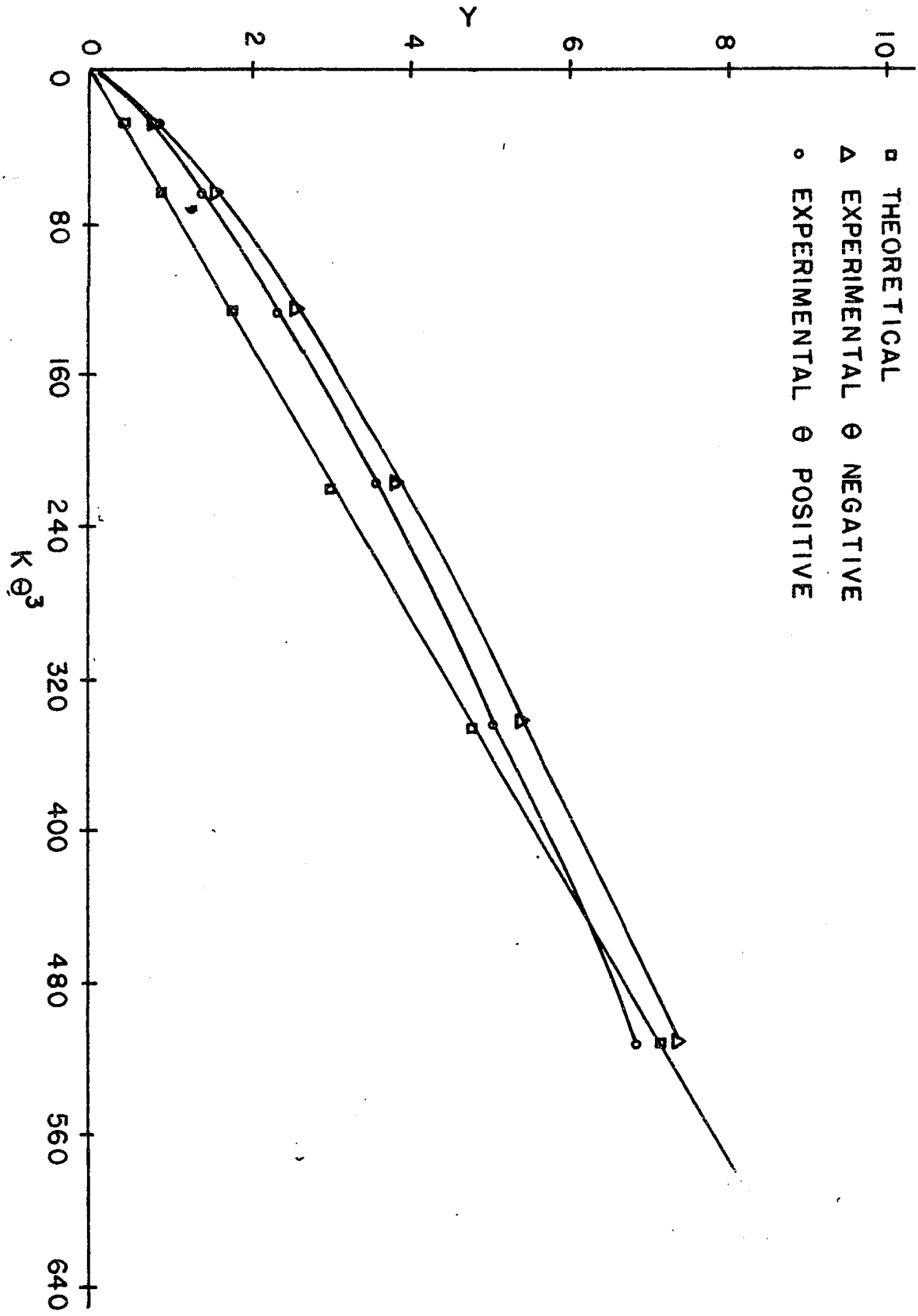

Fig. 2.6

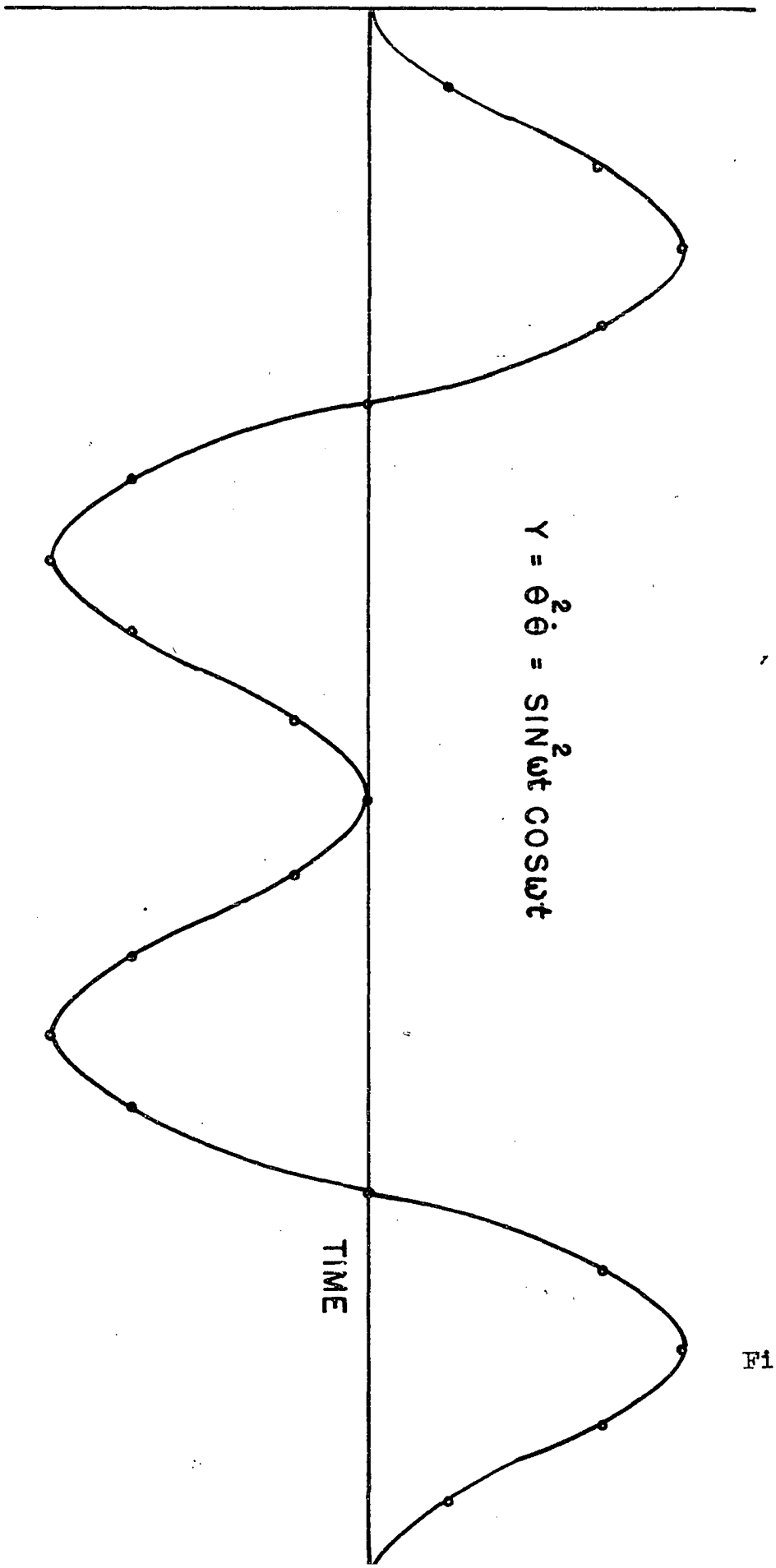

Fig. 2.7

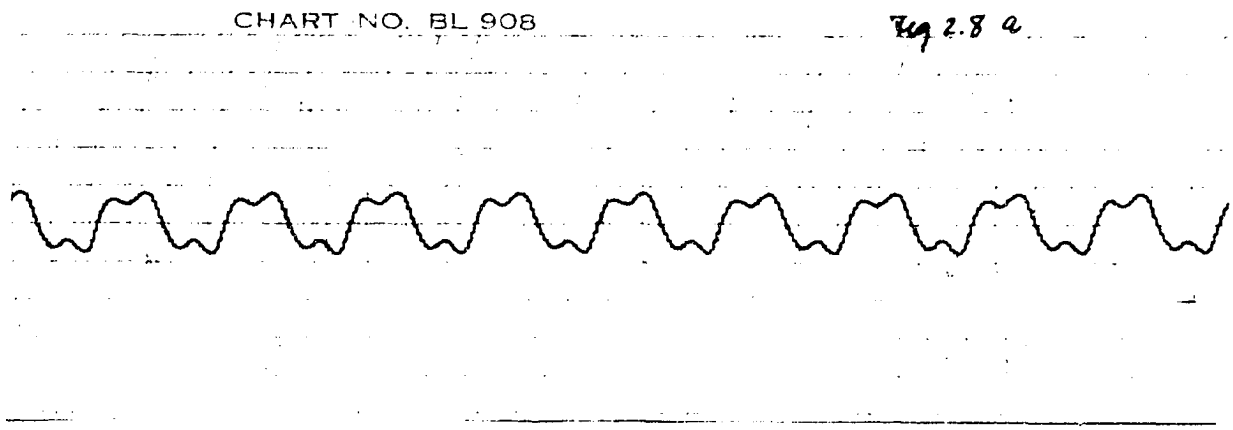

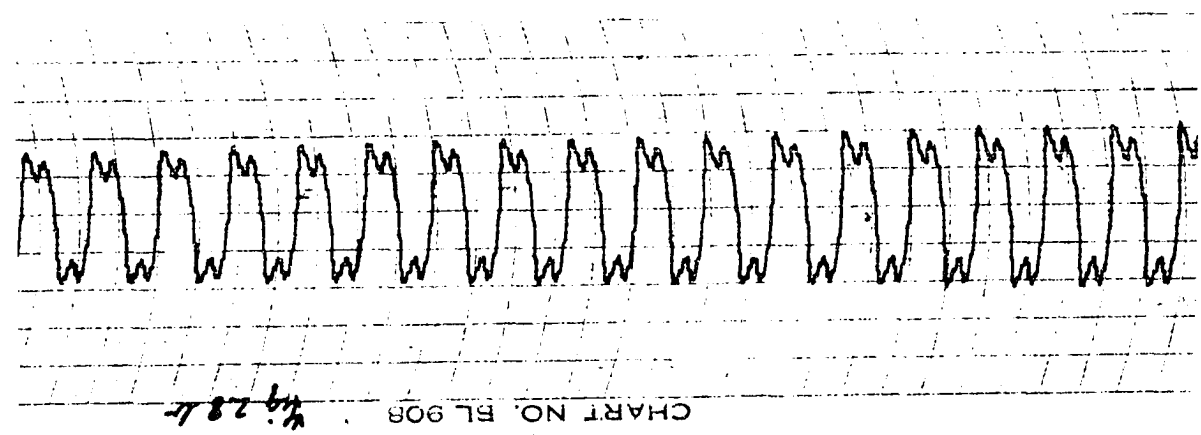

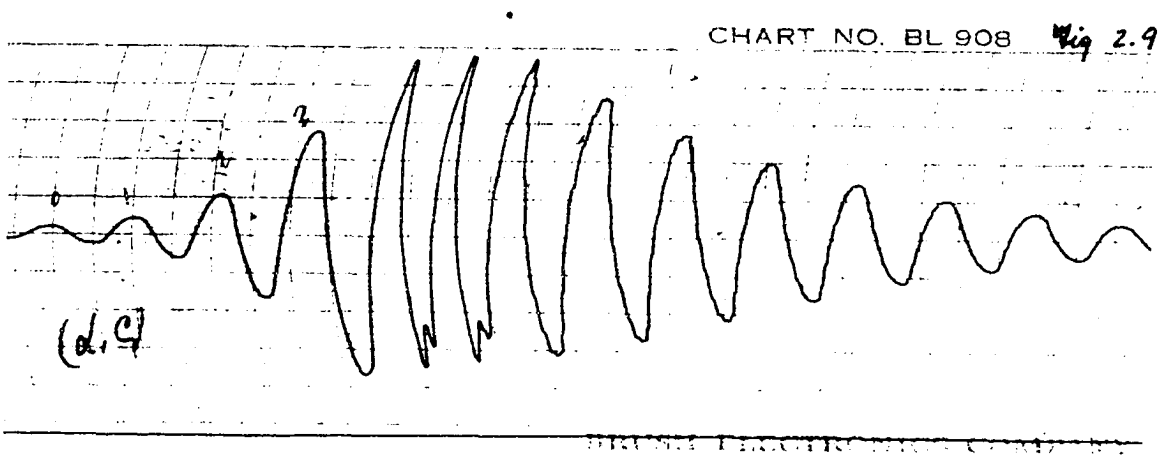

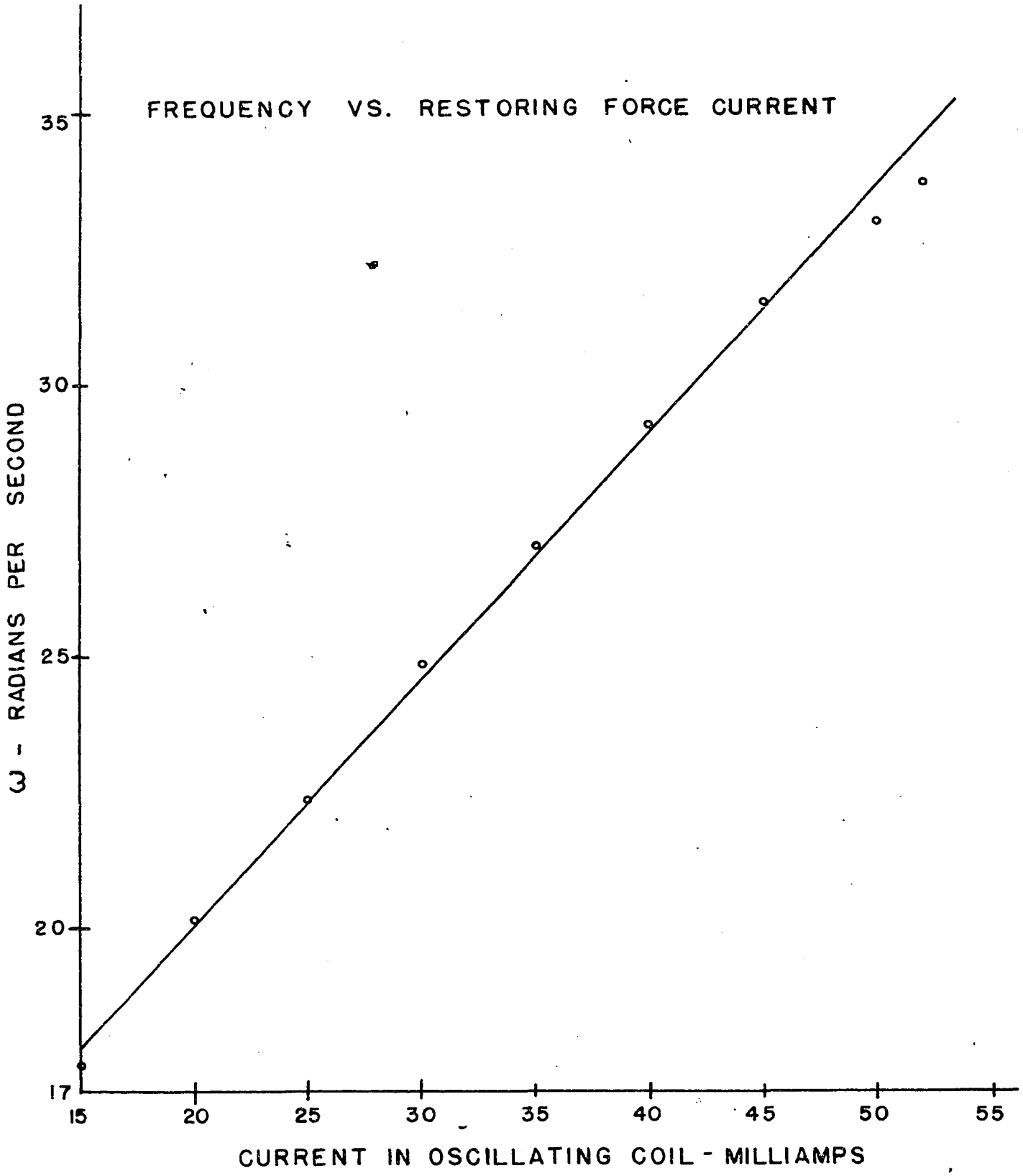

Fig. 2.10

displacement is sinusoidal. Fig. 2.9 illustrates that the negative damping unit is functioning correctly by the fact that the displacement builds up indefinitely to the limits of the analog as time increases. Fig. 2.10 demonstrates that the natural frequency of the basic analog system is a linear function of the current in the restoring force coil.

3. THE VAN DER POL SYSTEM

The differential equation of the self-excited van der Pol system can be written in the form

$$\ddot{\theta} + \omega^2\theta + (-\alpha + \beta\theta^2)\dot{\theta} = 0. \qquad (3.1)$$

When the system has $|\beta\theta^2| < |\alpha|$, the negative damping predominates and the vibration builds up in amplitude. When $|\beta\theta^2| > |\alpha|$ then positive damping predominates, limiting the amplitude of the vibration. For a steady state condition the amplitude of vibration will be a specific amount, depending upon α and β , for the steady state solution of eq (3.1) is

$$\theta = 2\left(\frac{\alpha}{\beta}\right)^{1/2} \sin(\omega t + \psi_0) \qquad (3.2)$$

in the first approximation. This is the usual limit cycle phenomenon. Having adapted the Ludeke-Morrison electro-mechanical analog to the van der Pol system above, limit cycle records were obtained. Figs. 3.1 and 3.2 demonstrate the achievement of this limit cycle amplitude by the analog for the transition both for an increase and decrease in amplitude to the limit cycle amplitude respectively.

A quantitative experimental verification of the analoged van der Pol system is obtained by considering β fixed, varying α in a known manner, and determining maximum θ , for each of these values of α , both by calculation and experimental measurement. For two specific

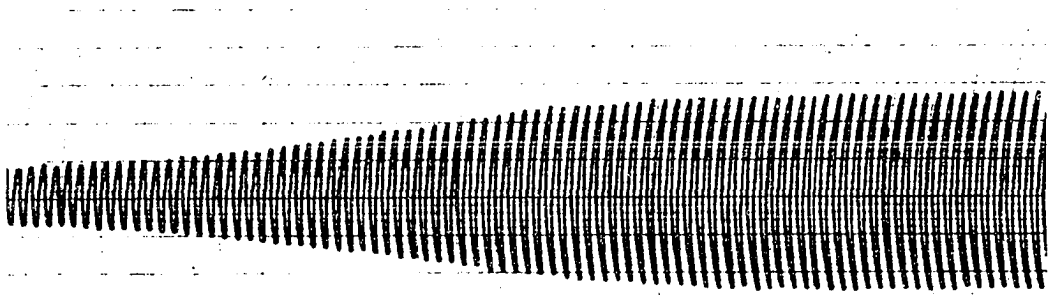

FIG. 3.1

OMPANY PRINTED IN U.S.A.

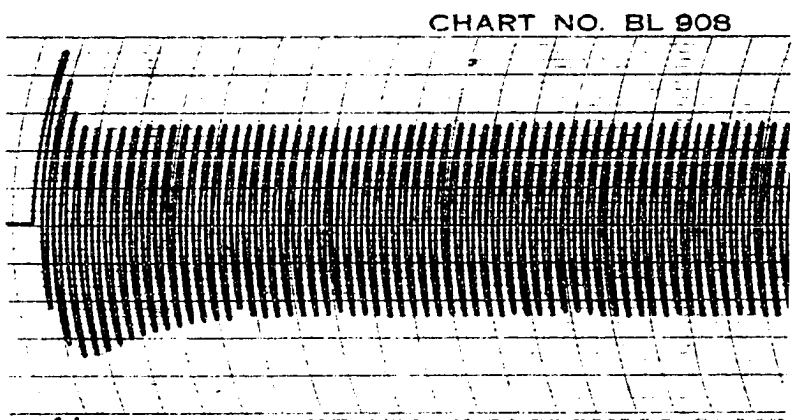

Fig. 3.2 BRUSH ELECTRONICS COMP

values of α , the relation

$$\hat{\theta}_1/\hat{\theta}_2 = \left(\alpha_1/\alpha_2\right)^{1/2} \tag{3.3}$$

holds, where $\hat{\theta}_1$ and $\hat{\theta}_2$ are peak values of the amplitudes of vibration, i.e., the amplitudes of the limit cycles. α_1 and α_2 can be determined experimentally by employing the logarithmic decrement method[10] in the reverse direction. Accurate values of α are obtained by plotting the logarithmic decrements against time.

Two quantitative experimental verifications of the analoged van der Pol system are now presented. Figs. 3.3 to 3.10 and fig. 3.19 represent the performance of the analog for the first experiment. Figs. 3.11 to 3.18 and fig. 3.20 represent data for the second experiment. Table 3.1 is a collection of the logarithmic decrement data for the first experiment, table 3.2 for the second experiment and table 3.3 compares the experimental values of $\hat{\theta}_1/\hat{\theta}_2$ and those calculated by eq (3.3). The ratios $\hat{\theta}_1/\hat{\theta}_2$ experimentally are determined from the limit cycles in figs. 3.3, 3.11, 3.12. Figs. 3.4 and 3.13 demonstrate the differentiator outputs for each experiment. Figs. 3.5 to 3.10 and figs. 3.14 to 3.18, fig. 2.9 are employed to determine the various values of α . Figs. 3.19 and 3.20 demonstrate the plots of the logarithmic decrement against time.

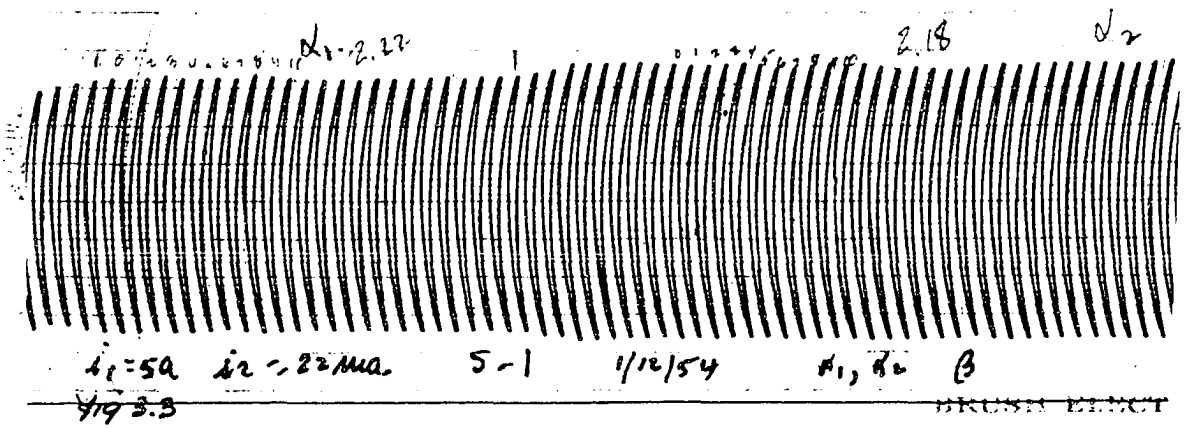

Fig 3.3

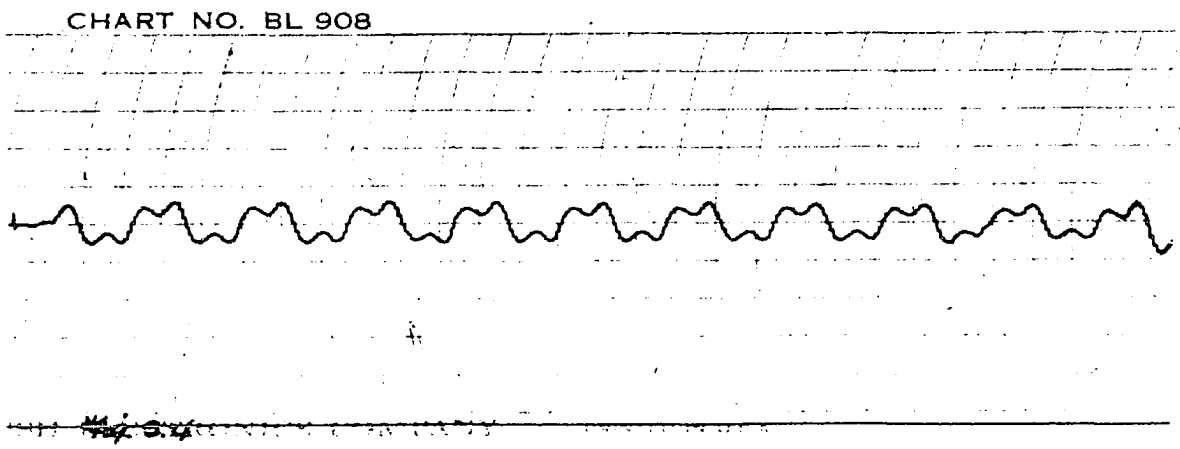

Fig 3.4

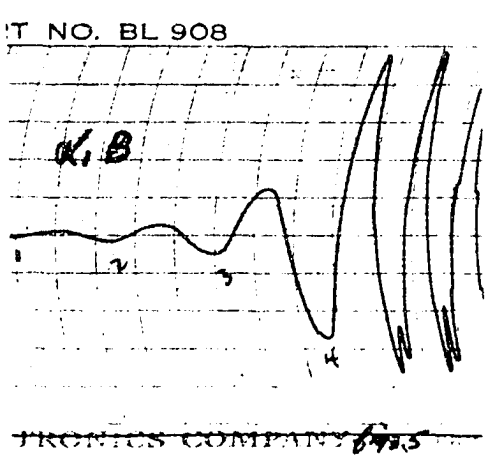

Fig 3.5

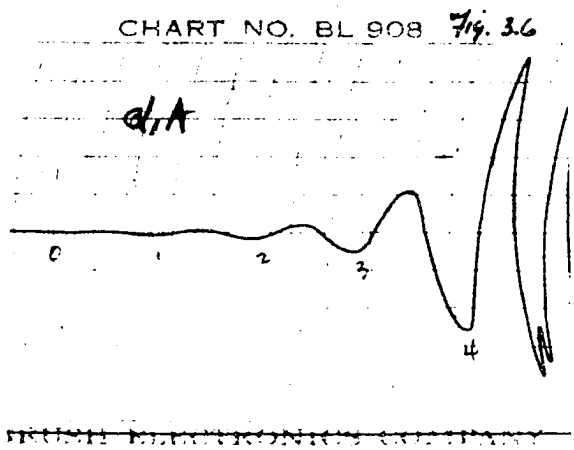

Fig. 3.6

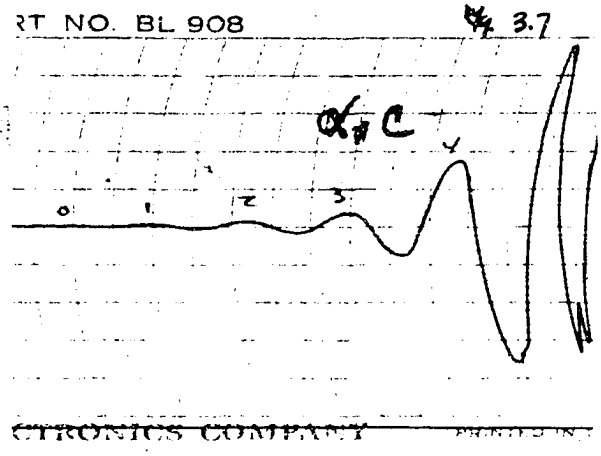

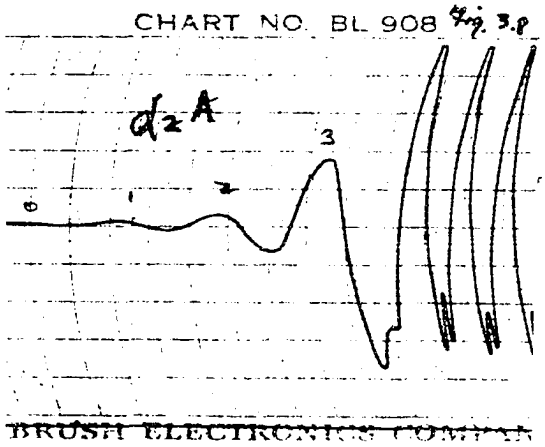

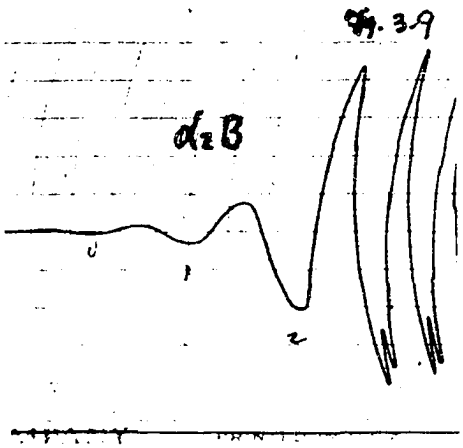

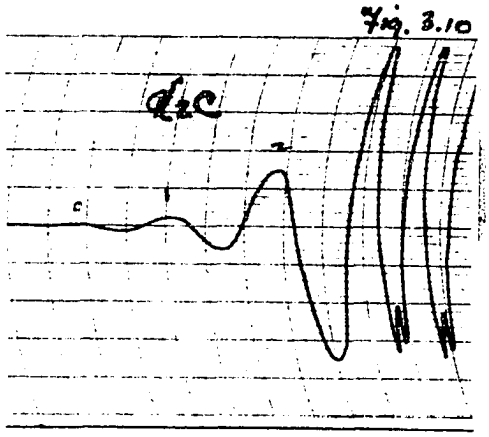

Fig. 3.11 CHART

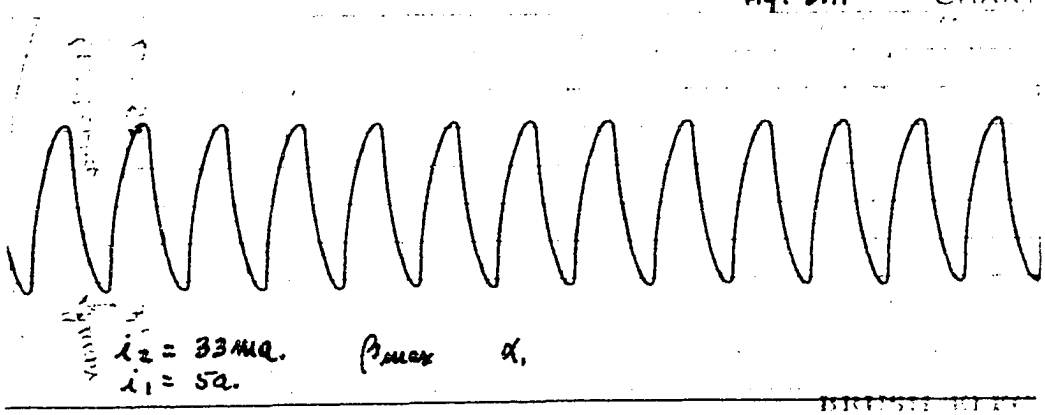

Fig. 3.12

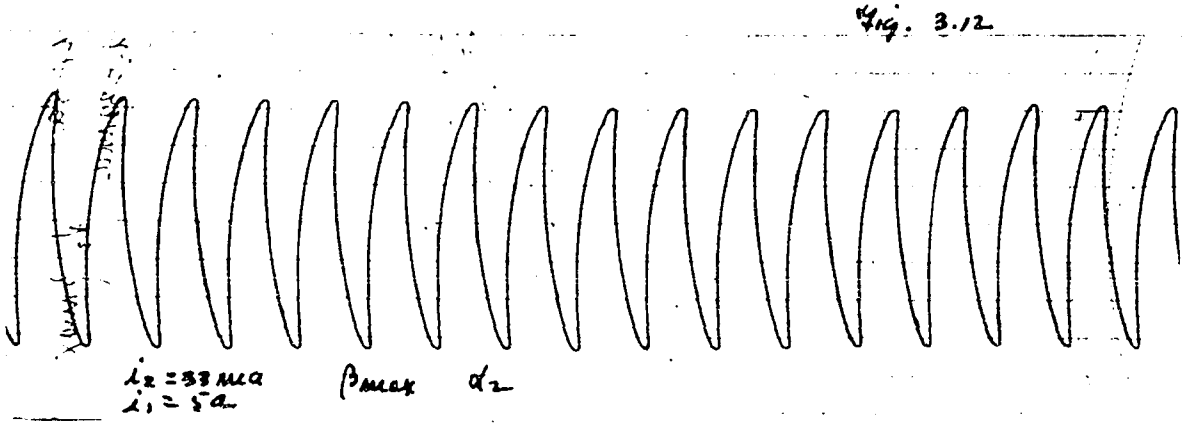

908

Fig. 3.13

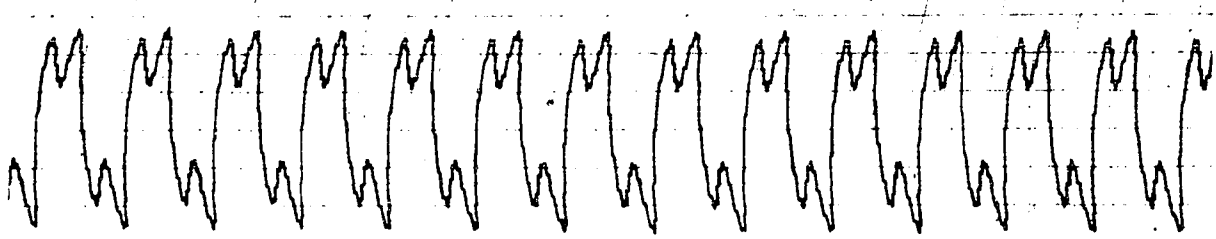

Fig. 3.14

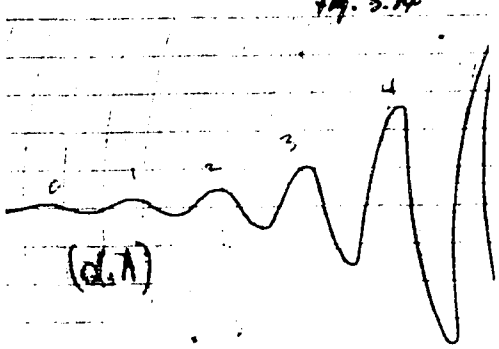

Fig. 3.15

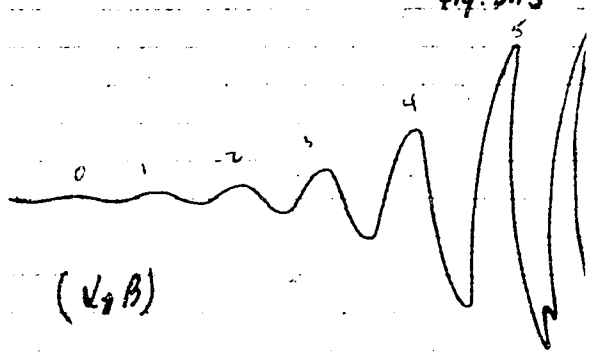

Fig. 3.16

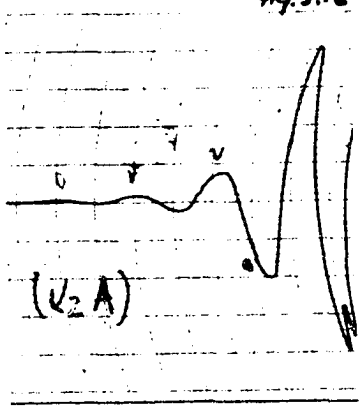

Fig. 3.17. CH

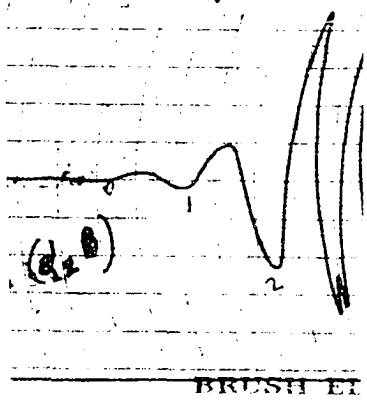

Fig. 3.18

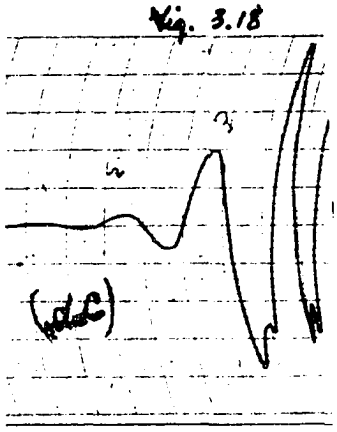

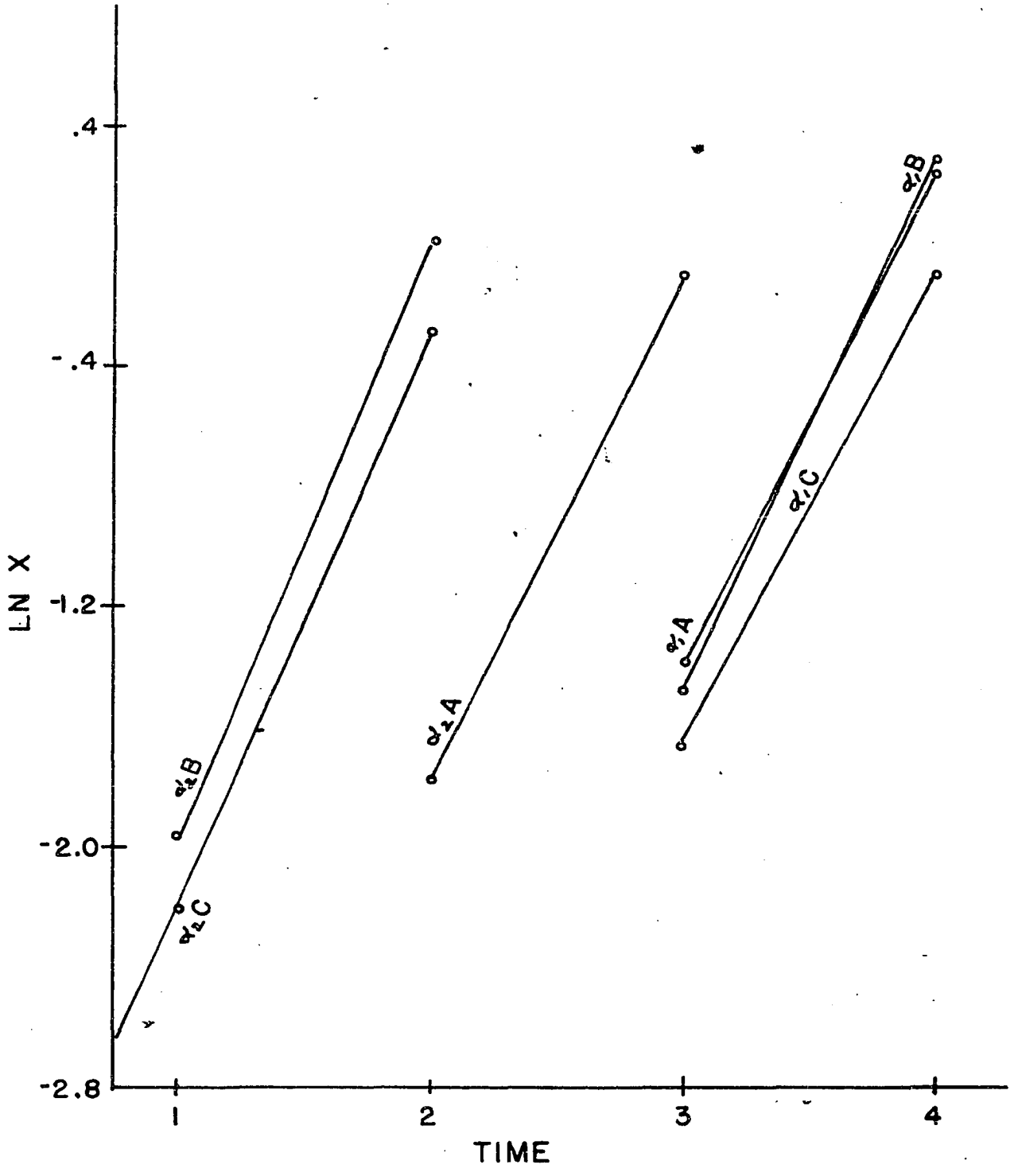

Fig. 3.19

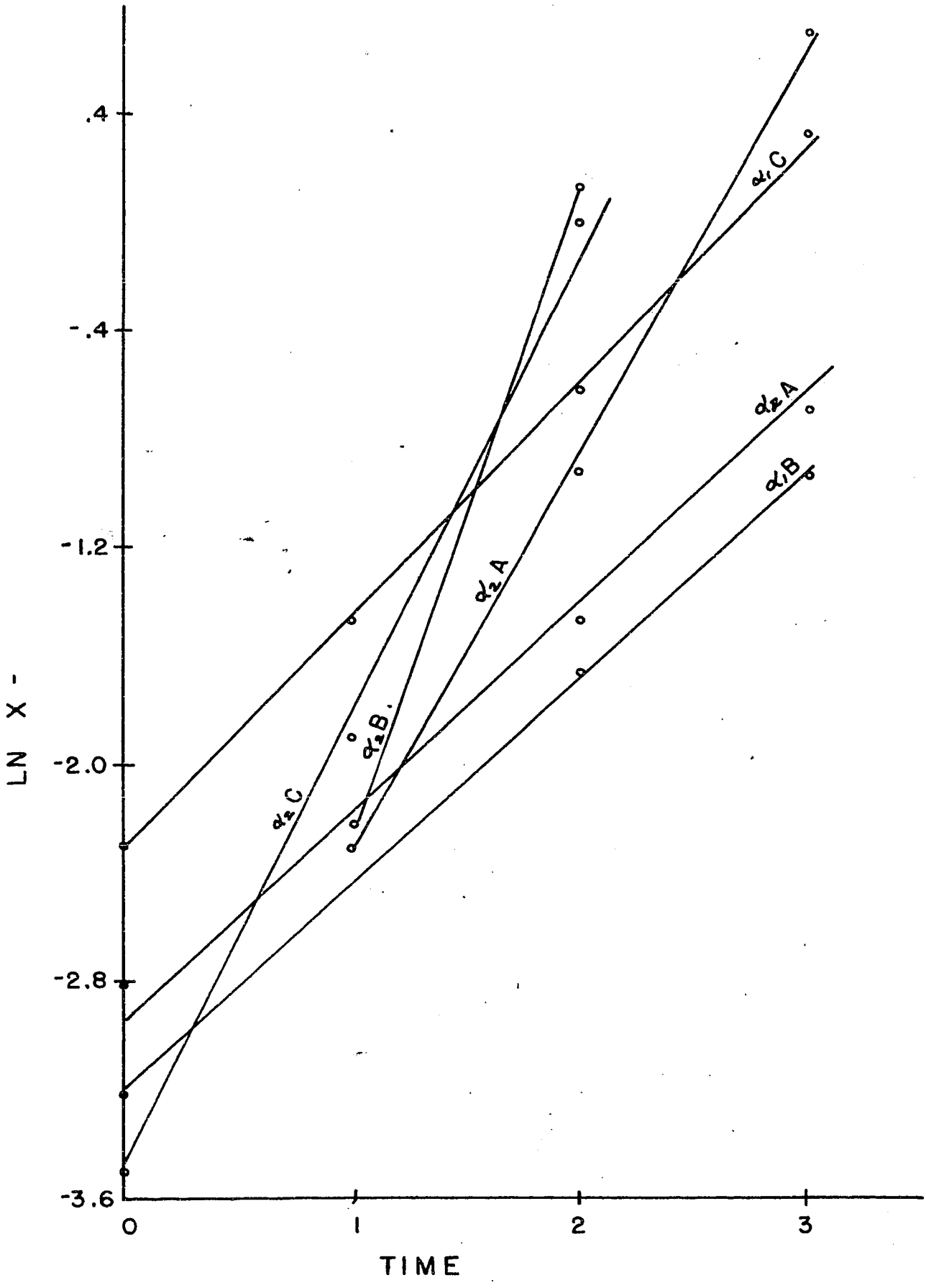

Fig. 3.20

Table 3.1

α_1	X	ln X	δ_1	α_2	X	ln X	δ_2
(A)	.02	-3.912		(A)	.03	-3.507	
	.04	-3.219			.08	-2.526	
	.09	-2.408			.17	-1.772	
	.25	-1.386			.90	- .105	
	1.29	.255	1.641	(B)	.03	-3.507	
(B)	.02	-3.912			.14	-1.966	1.986
	.03	-3.507			1.02	.020	
	.08	-2.526		(C)	.02	-3.912	
	.23	-1.469			.11	-2.207	1.919
	1.34	.293			.75	- .288	
(C)	.02	-3.912					
	.04	-3.219					
	.09	-2.408	1.544				
	.19	-1.661					
	.89	- .117					
			(1.59)				(1.95)

Table 3.2

α_1	X	ln X	δ_1		α_2	X	ln X	δ_2
(A)	.06	-2.813			(A)	.04	-3.219	
	.11	-2.207				.10	-2.303	
	.23	-1.470				.39	- .942	
	.50	- .693				2.02	.703	1.645
	1.31	.270			(B)	.03	-3.507	
(B)	.04	-3.219				.10	-2.303	
	.10	-2.303				1.14	.131	
	.19	-1.661	.719		(C)	.03	-3.507	
	.39	- .942				.15	-1.897	
	.90	- .105				.99	- .010	
	2.02	.703						
(C)	.10	-2.303						
	.23	-1.470						
	.53	- .635						
	1.39	.329						

Table 3.3

Calculations from Table 3.1:	
$\omega_1 = 14.13$ radians/second	$\omega_1 = 14.40$ radians/second
$\alpha_1 = 7.14$	$\alpha_2 = 8.44$
$\frac{\alpha_1}{\alpha_2} = .845$	$\left(\frac{\alpha_1}{\alpha_2}\right)^{1/2} = .916$
	$\hat{\theta}_1/\hat{\theta}_2 = .906$
Calculations from Table 3.2:	
$\omega_1 = 16.05$ radians/second	$\omega_1 = 18.00$ radians/second
$\alpha_1 = 3.68$	$\alpha_2 = 9.20$
$\alpha_1/\alpha_2 = .400$	$\left(\alpha_1/\alpha_2\right)^{1/2} = .630$
	$\hat{\theta}_1/\hat{\theta}_2 = .690$
	4.5% mean deviation

4. THE FORCED VAN DER POL SYSTEM

For a forced van der Pol system, one which possesses frequency entrainment in the region of resonance, we have the following nonlinear differential equation

$$\ddot{\theta} - \alpha\dot{\theta} + \beta\theta^2\dot{\theta} + \omega_1^2\theta = F \sin \omega_2 t. \qquad (4.1)$$

The right hand side of eq (4.1) is obtained on the analog by use of a time function generator, the output of which is placed in a coil in the radial permanent magnet. Figs. 4.1 and 4.2 demonstrate the entrainment of the van der Pol system by the forcing function. The lower curve represents the forcing function response as it drives a relay in the Brush equipment, and the upper curve the van der Pol system's response. The frequency of the forcing function ω_2 is varied from below ω_1 to a point above ω_1. Notice that the expected variations in amplitude are obtained on either side of the range of entrainment $\Delta\omega_2$. Within the range of entrainment ω_2 has been varied.

In order to determine the amplitude frequency response within the range of entrainment and the dependency of the width of the range of entrainment upon the magnitude of the forcing function, a set of records was obtained from the analog with ω_1, α and β fixed for various values of F, varying ω_2 through the range of entrainment from below ω_1 and then from above ω_1 in each instance. The response curves for these various values of F are presented

Fig. 4.1

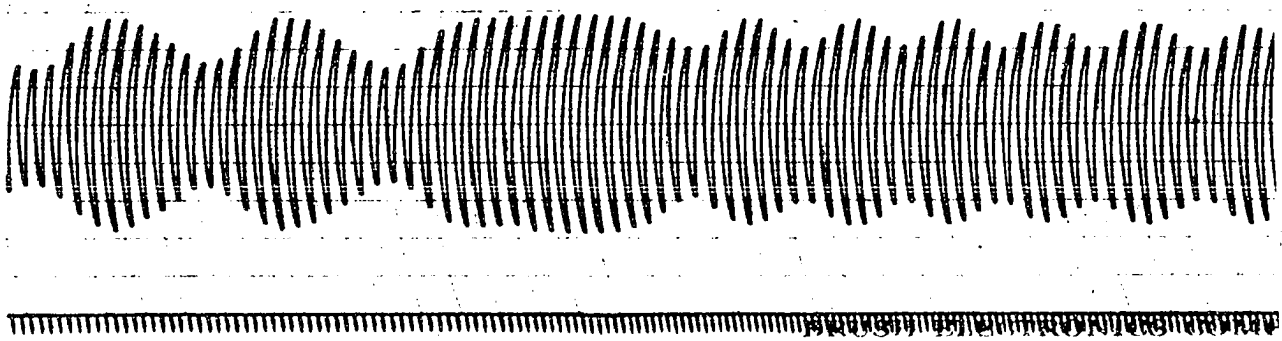

Fig 4.2 - 1

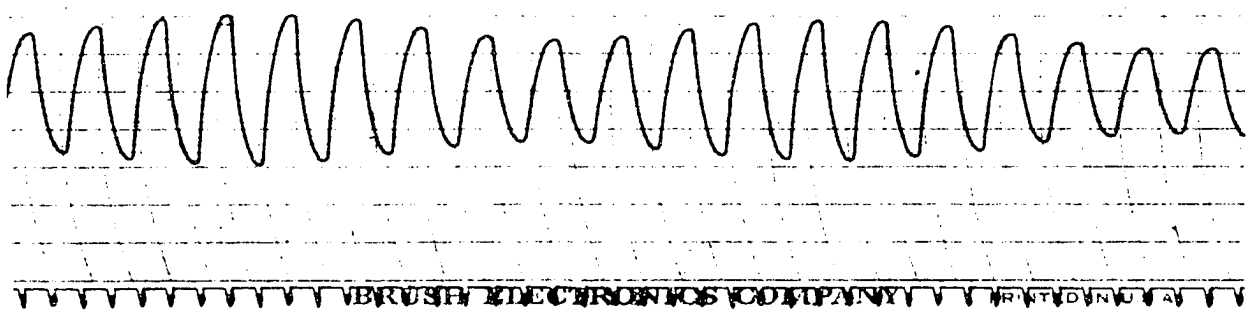

Fig 4.2 - 2

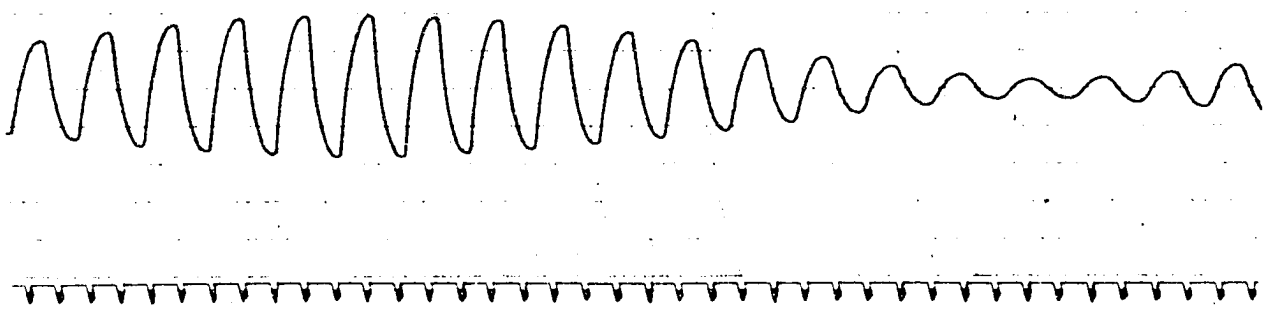

Fig. 4.2-3 CHART NO. BL 908

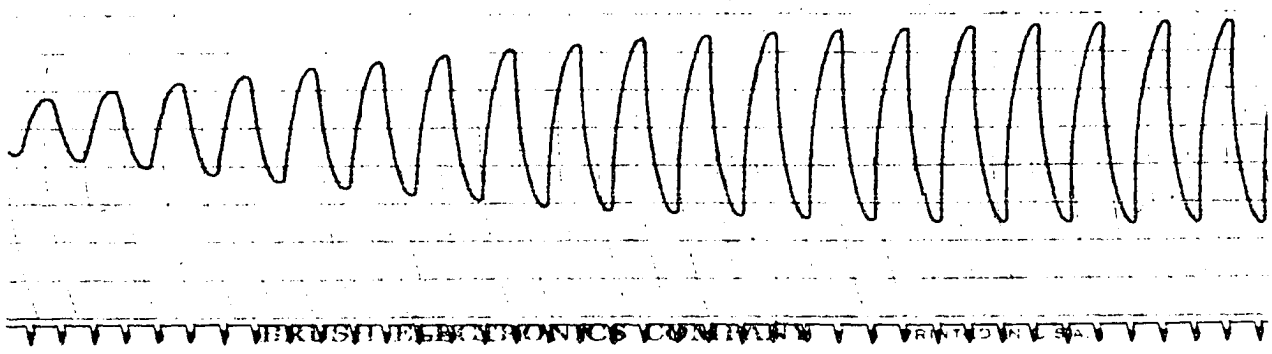

Fig. 4.2-4

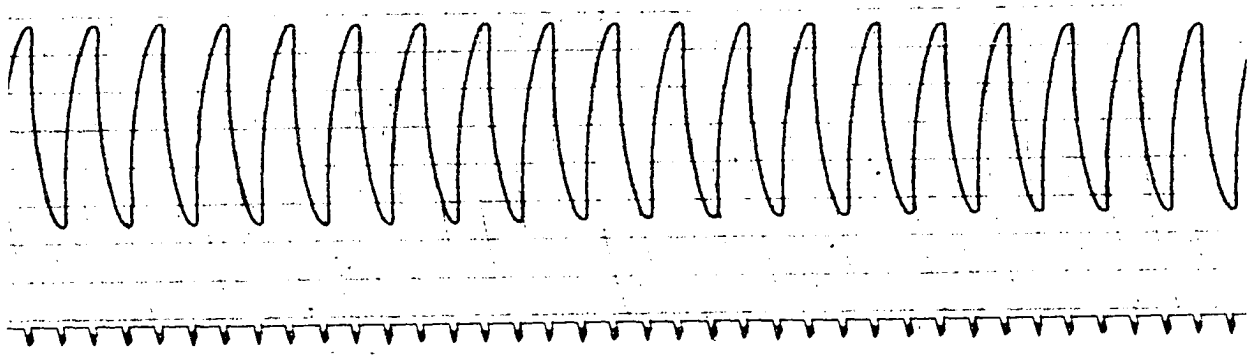

Fig. 4.2-5 CHART NO. BL 903

W_2 increasing

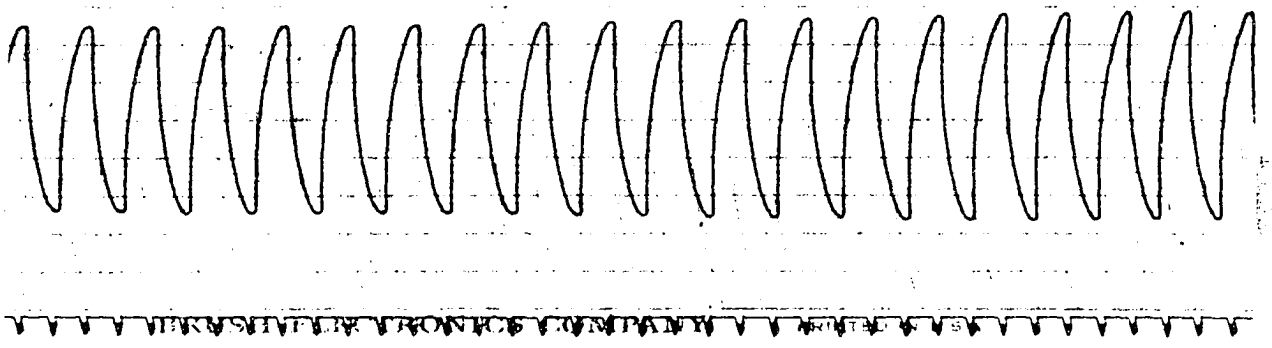

Fig. 4.2-6

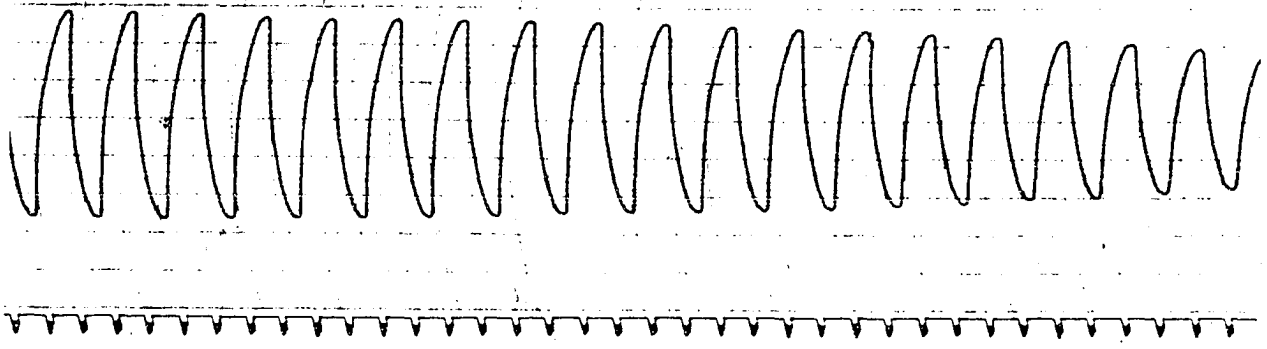

Fig. 4.2-7 CHART NO. BL 908

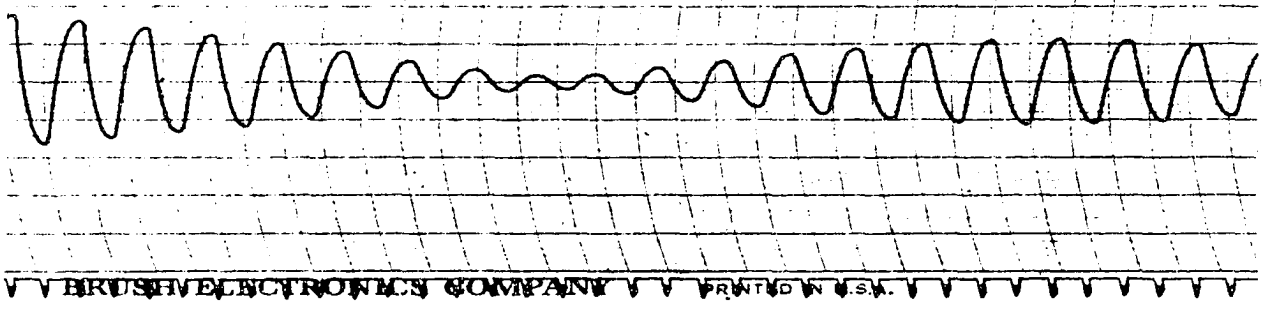

Fig. 4.2-8

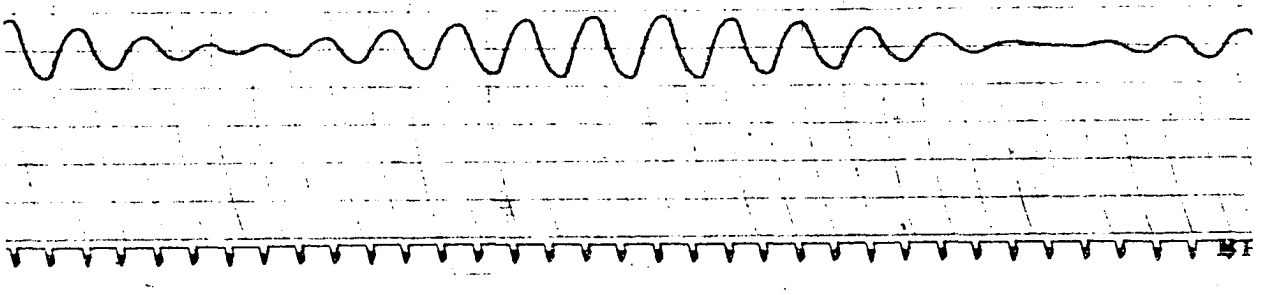

in figs. 4.3 to 4.10. Fig. 4.11 presents an overall view of the amplitude frequency response of the forced van der Pol system within the region of entrainment as a function of the amplitude of the forcing function.

The amplitude of the forcing function was determined experimentally by employing the static case of eq (4.1), which gives the relation

$$\omega_1^2 \theta = F. \tag{4.2}$$

F is proportional to the current in the coil within the permanent magnet. Varying this current, ω_1 and θ were measured and F evaluated by eq (4.2). Fig. 4.12 is a plot of the magnitude of the forcing function as a function of the forcing current in milliamperes.

The negative damping coeficient, α , was determined experimentally by the reverse logarithmic decrement method as demonstrated in section 3, both before and after the response curve data was taken from the analog. Table 4.1 presents this information and figs. 4.13 and 4.14 give the logarithmic decrement curves.

Assuming a solution of eq (4.1) of the form

$$\theta = b_1(t) \sin \omega_2 t + b_2(t) \cos \omega_2 t, \tag{4.3}$$

and imposing the periodicity conditions[11], the response relationship

$$\rho \left[a^2 + (1-\rho)^2 \right] = A^2 \tag{4.4}$$

is obtained, where $A = -F/\alpha a_0 \omega_2$; $\rho = \frac{3\beta}{4\alpha}(b_1^2 + b_2^2)$; $a = \frac{2(\omega_1 - \omega_2)}{\alpha}$; $a_0 = \left(\frac{4\alpha}{3\beta}\right)^{1/2}$.

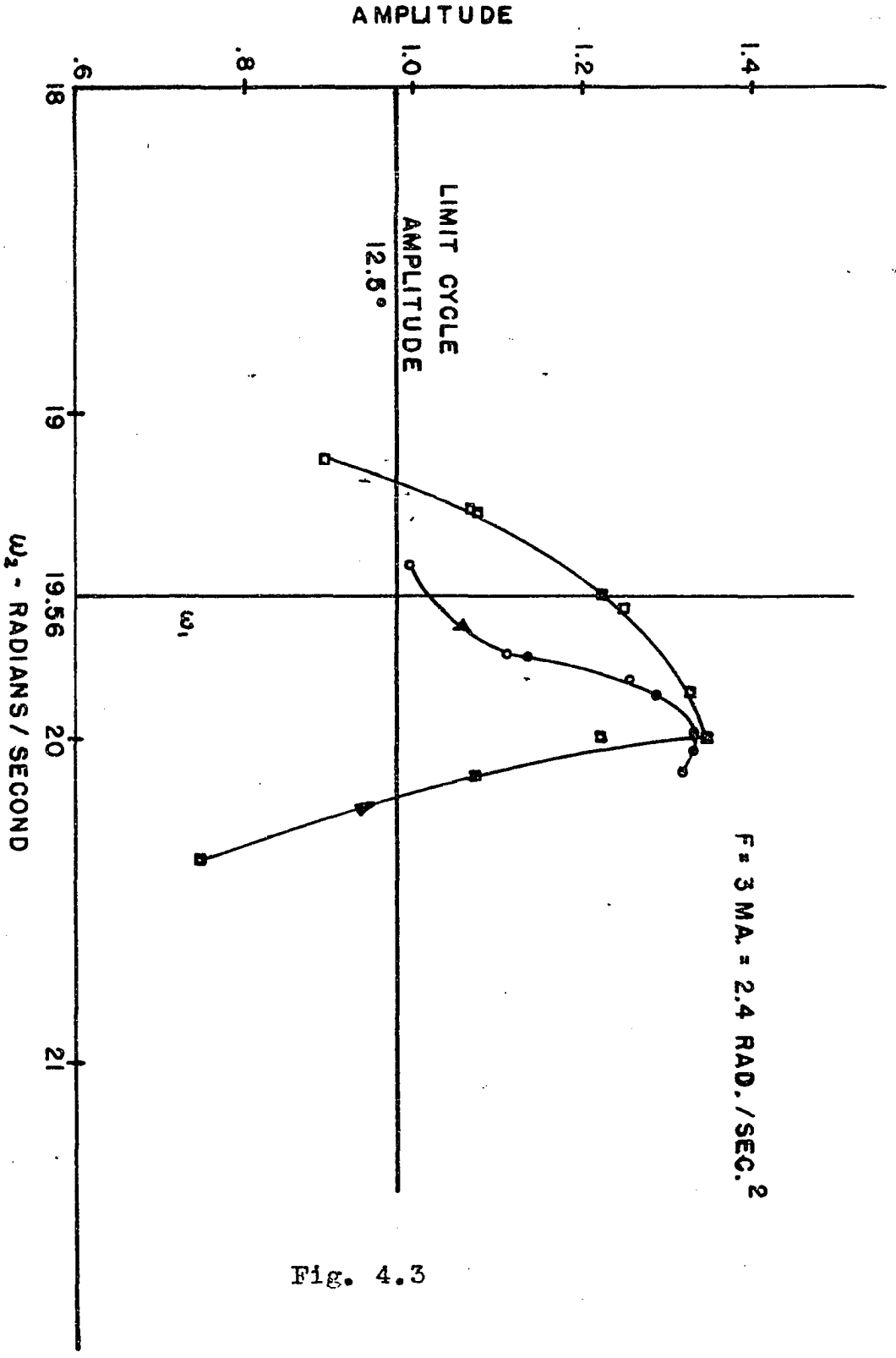

Fig. 4.3

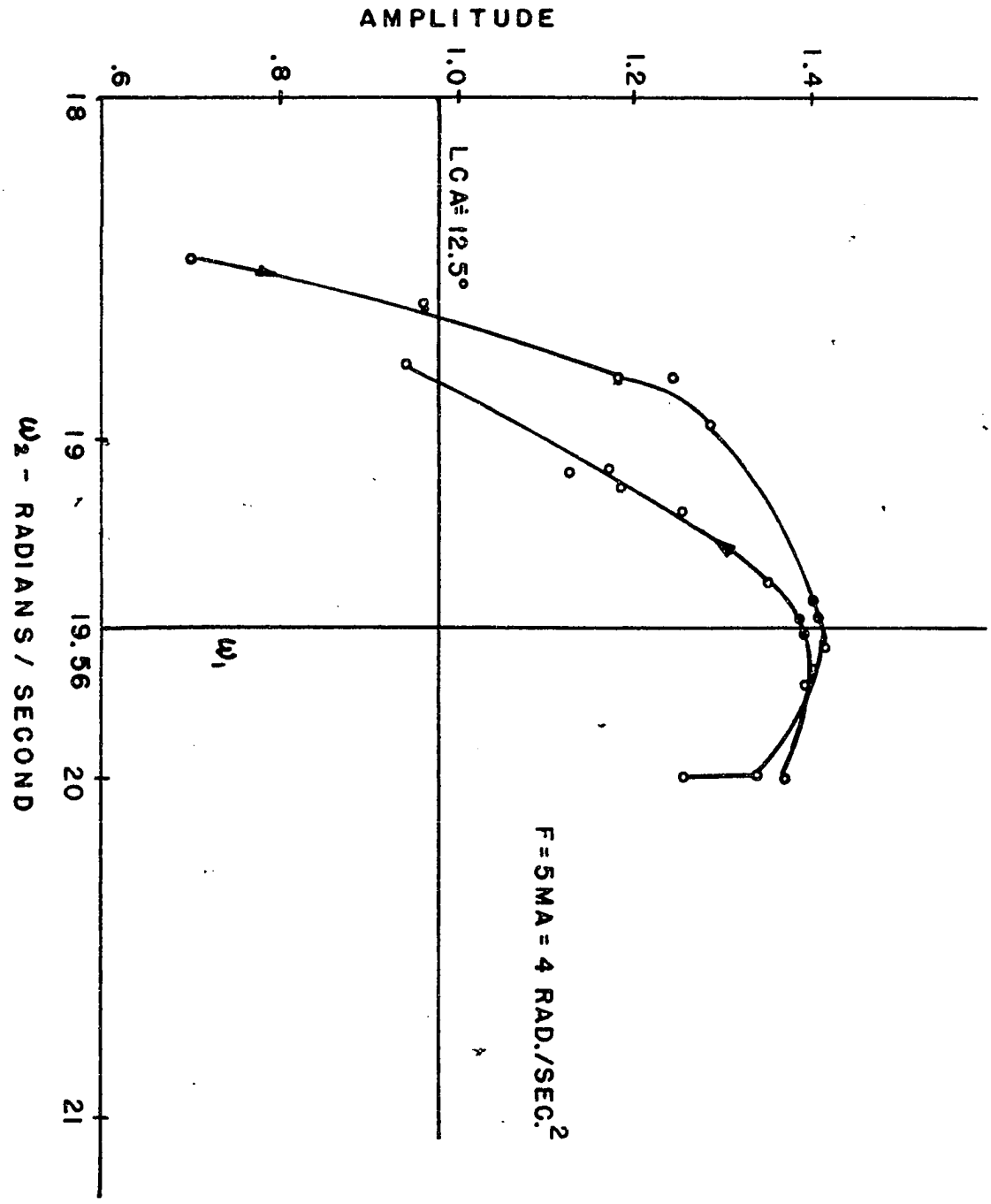

Fig. 4.4

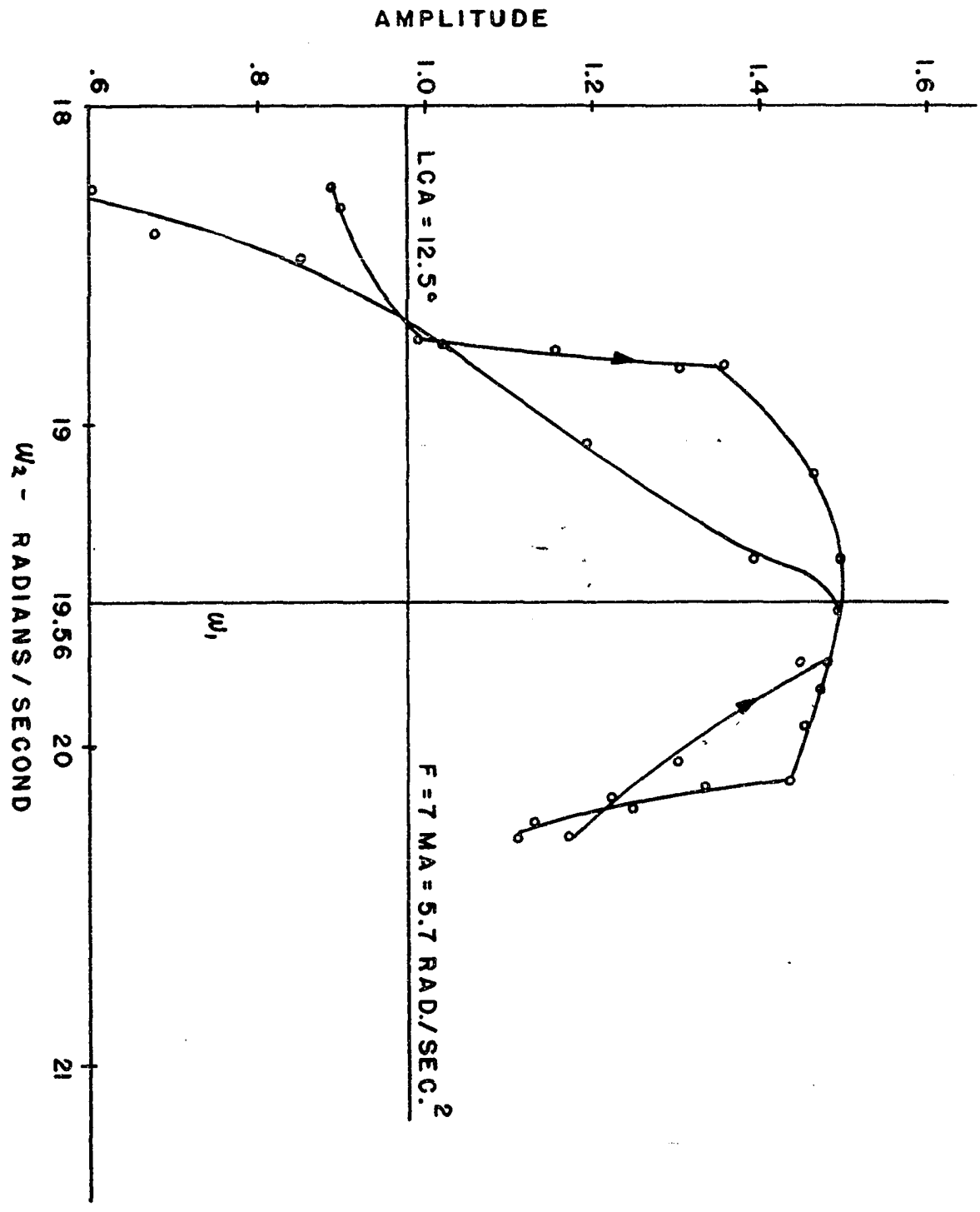

Fig. 4.5

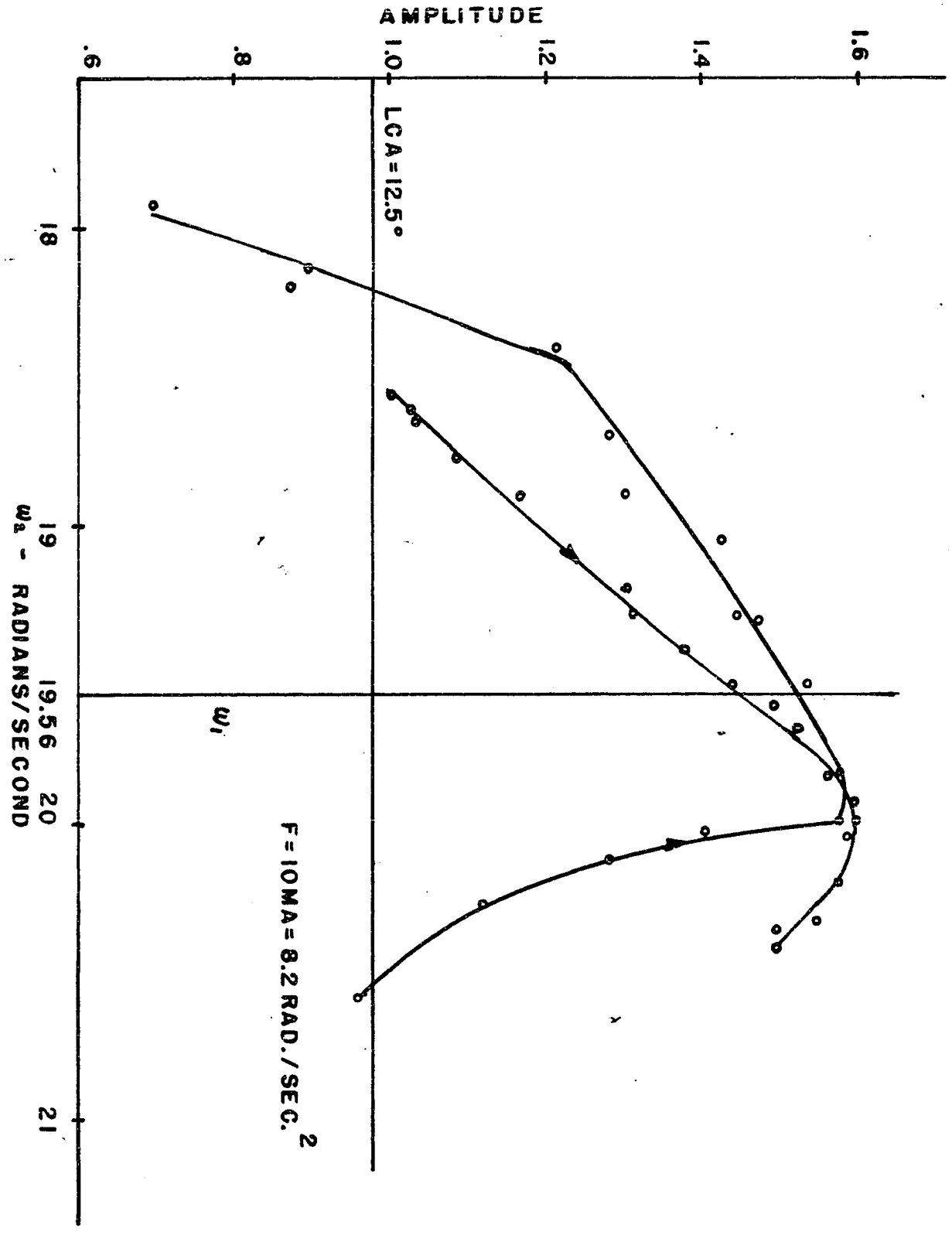

Fig. 4.6

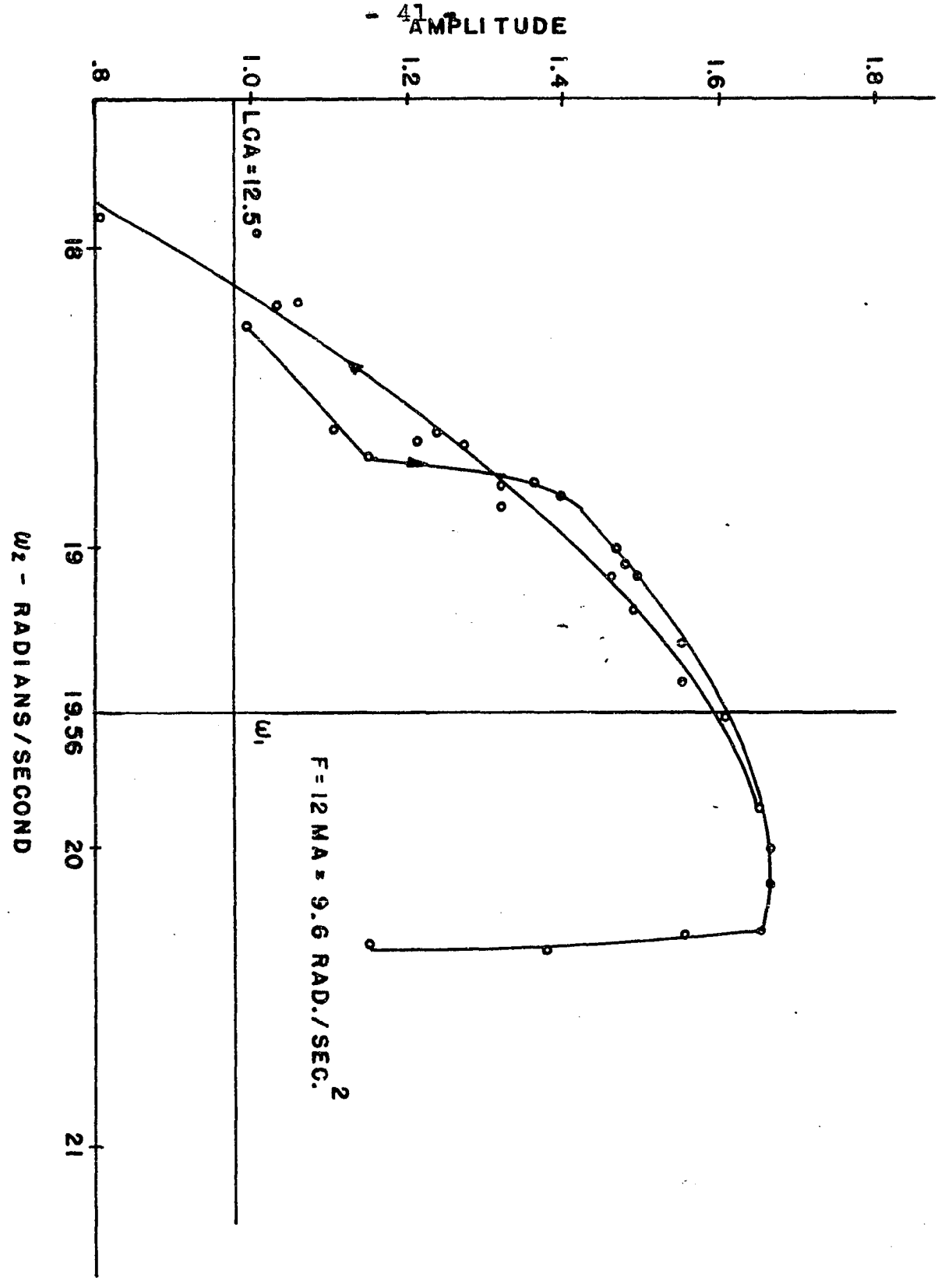

Fig. 4.7

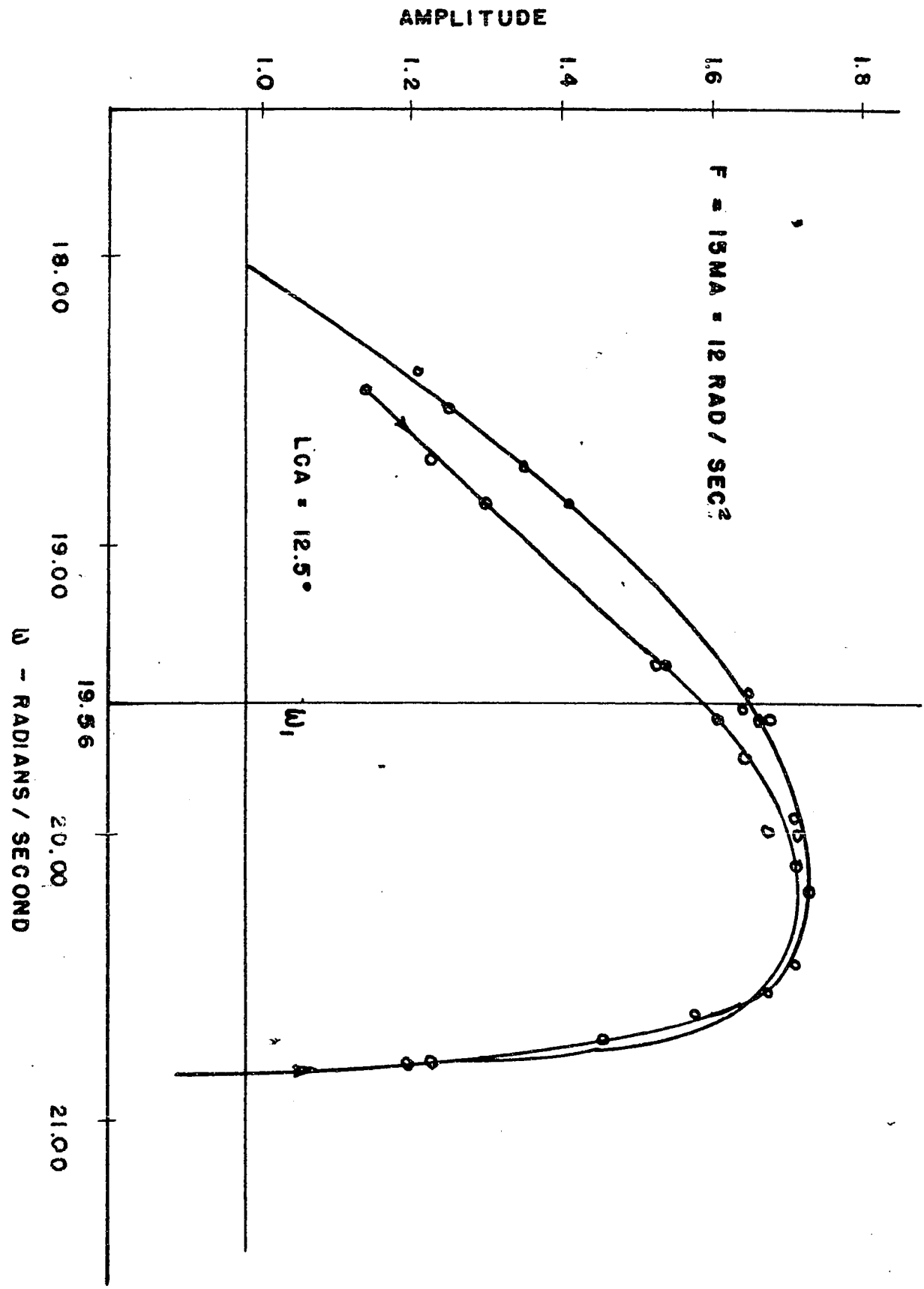

Fig. 4.8

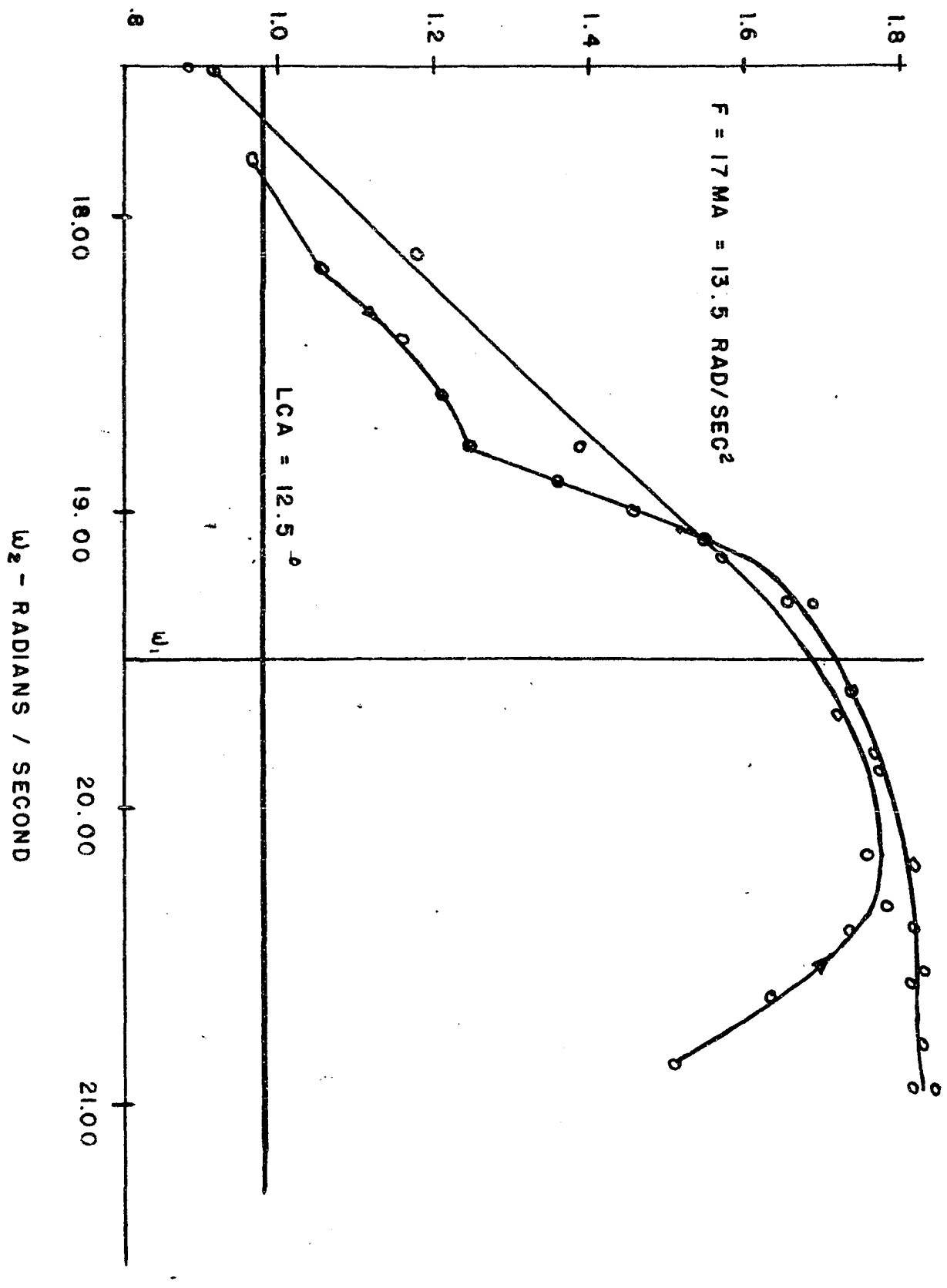

Fig. 4.9

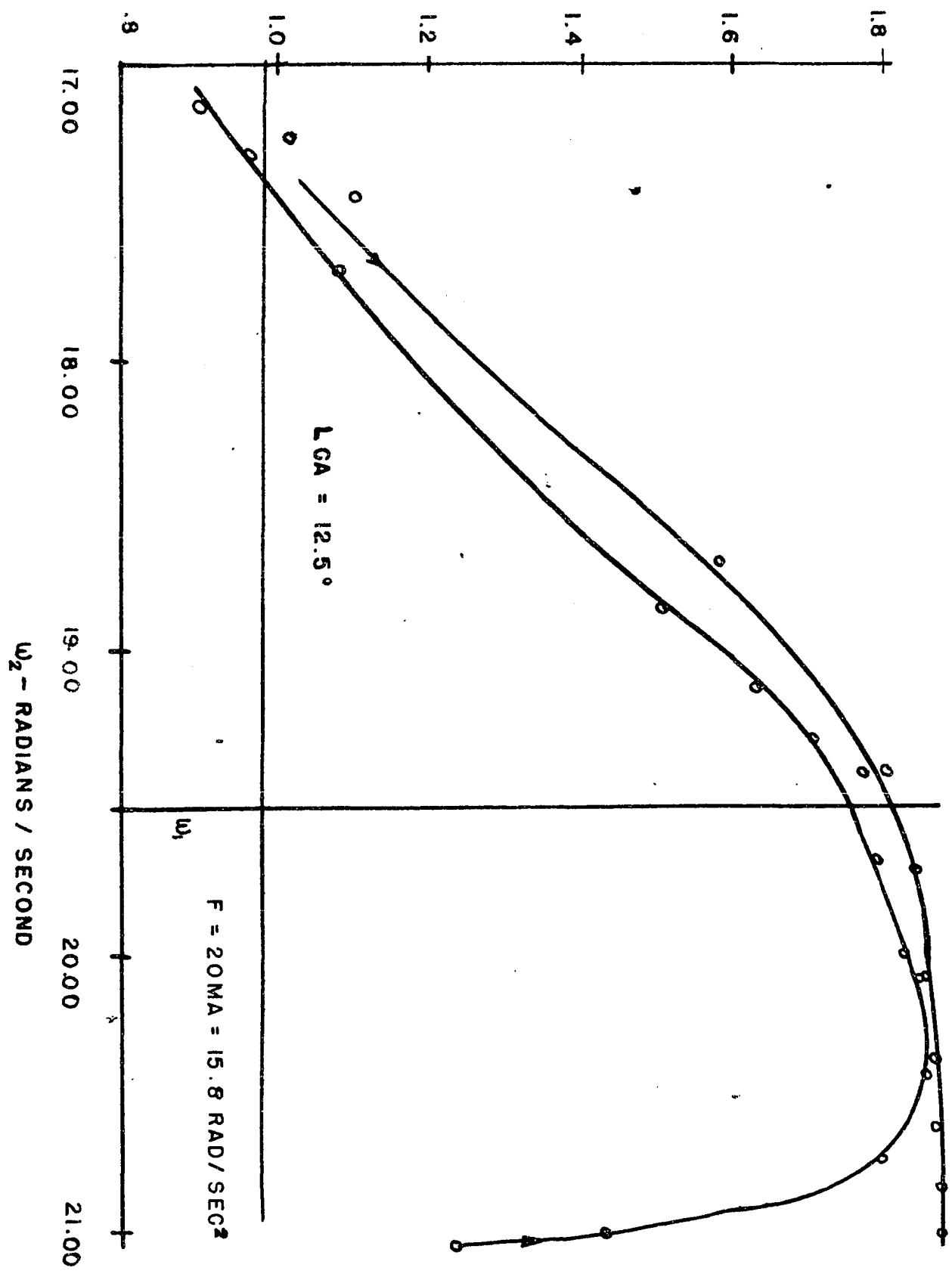

Fig. 4.10

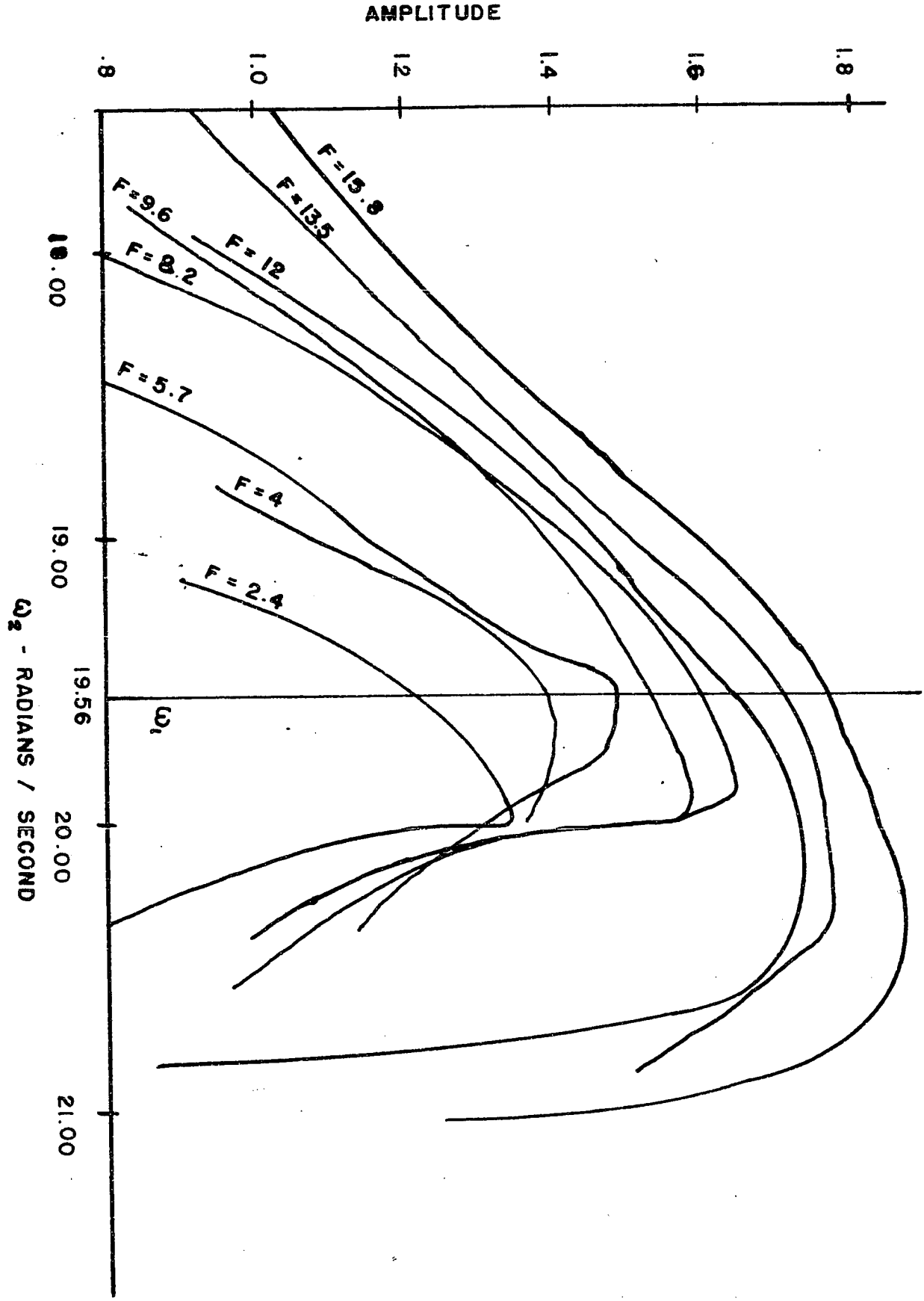

Fig. 4.11

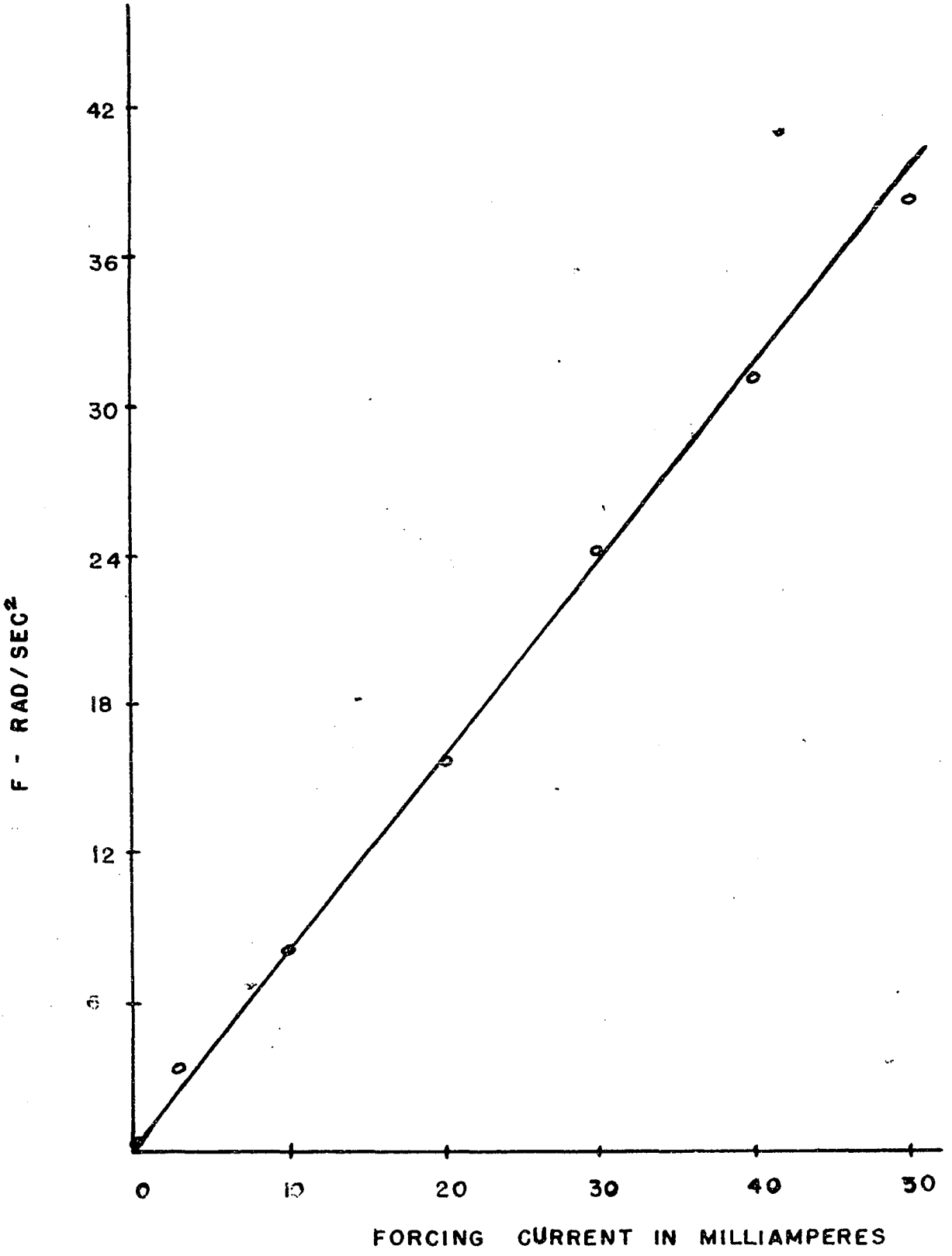

Fig. 4.12

Table 4.1

Pre-experimental value

α_A	X	ln X	α_B	X	ln X	α_C	X	ln X
0	.17	-1.772		.14	-1.966		.13	-2.040
3	.22	-1.514		.20	-1.609		.20	-1.609
6	.28	-1.273		.26	-1.347		.24	-1.427
9	.33	-1.109		.31	-1.171		.30	-1.204
12	.46	- .777		.42	- .868		.42	- .868
15	.67	- .400		.60	- .511		.61	- .494
18	.98	- .020		.90	- .105		.92	- .083
21	1.39	.329		1.31	.270		1.33	.285
24	1.81	.593					1.78	.577

$\omega_1 = 19.68$ rad./sec. $a_o = 1.025 = 12.5^\circ = .218$ rad

Post-experimental value

0	.18	-1.715		.17	-1.772		.18	-1.715
3	.22	-1.514		.21	-1.561		.22	-1.514
6	.26	-1.347		.23	-1.470		.29	-1.238
9	.33	-1.109		.30	-1.204		.31	-1.171
12	.46	- .777		.38	- .968		.37	- .994
15	.62	- .478		.50	- .693		.45	- .799
18	.83	- .186		.68	- .386		.62	- .478
21	1.19	.174		.94	- .062		.87	- .139
24	1.53	.425		1.30	.262		1.20	.182
27	1.80	.588		1.67	.513		1.53	.425

$\delta_{ave} = .101$ $\alpha = .630$

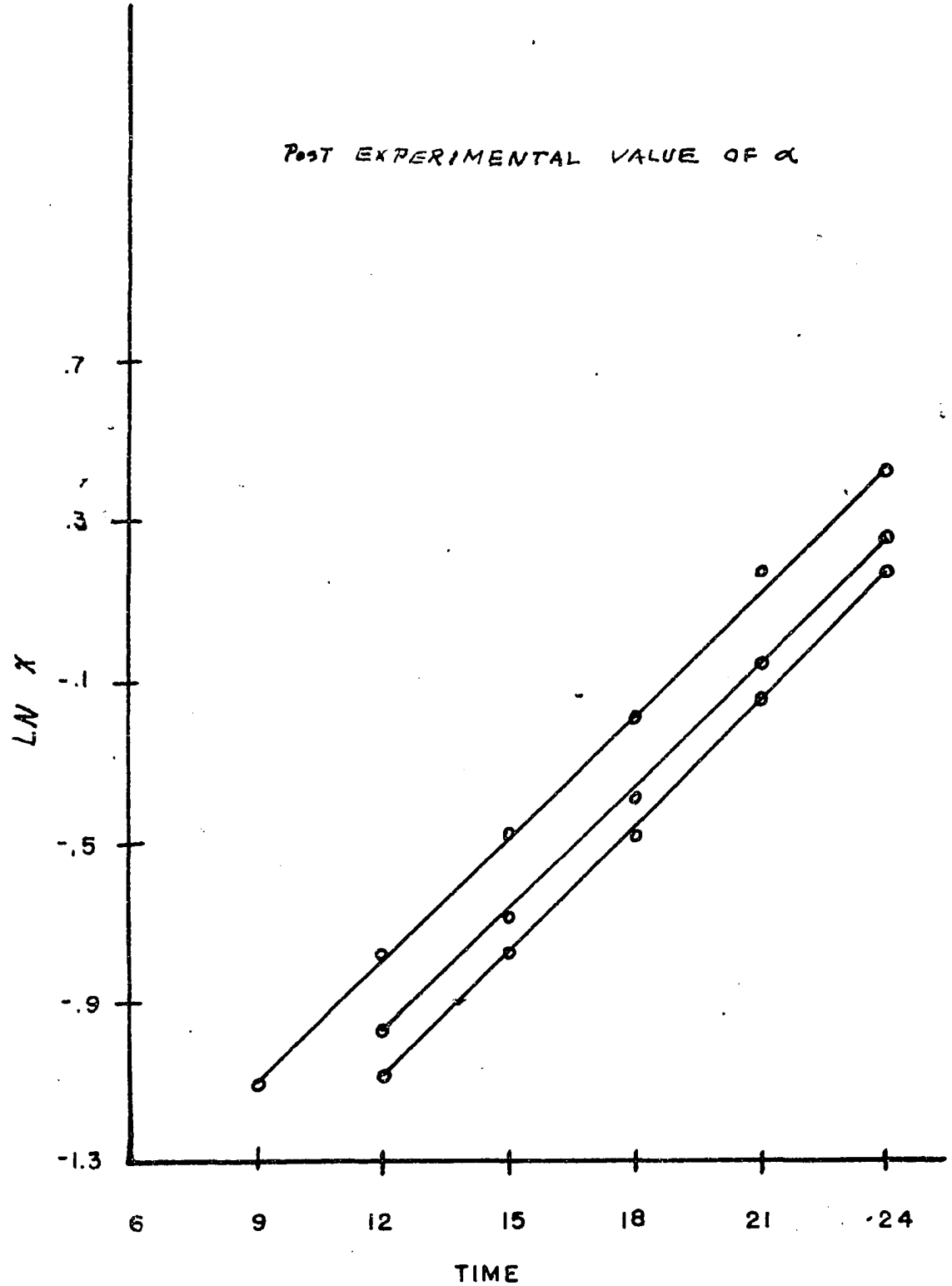

Fig. 4.13

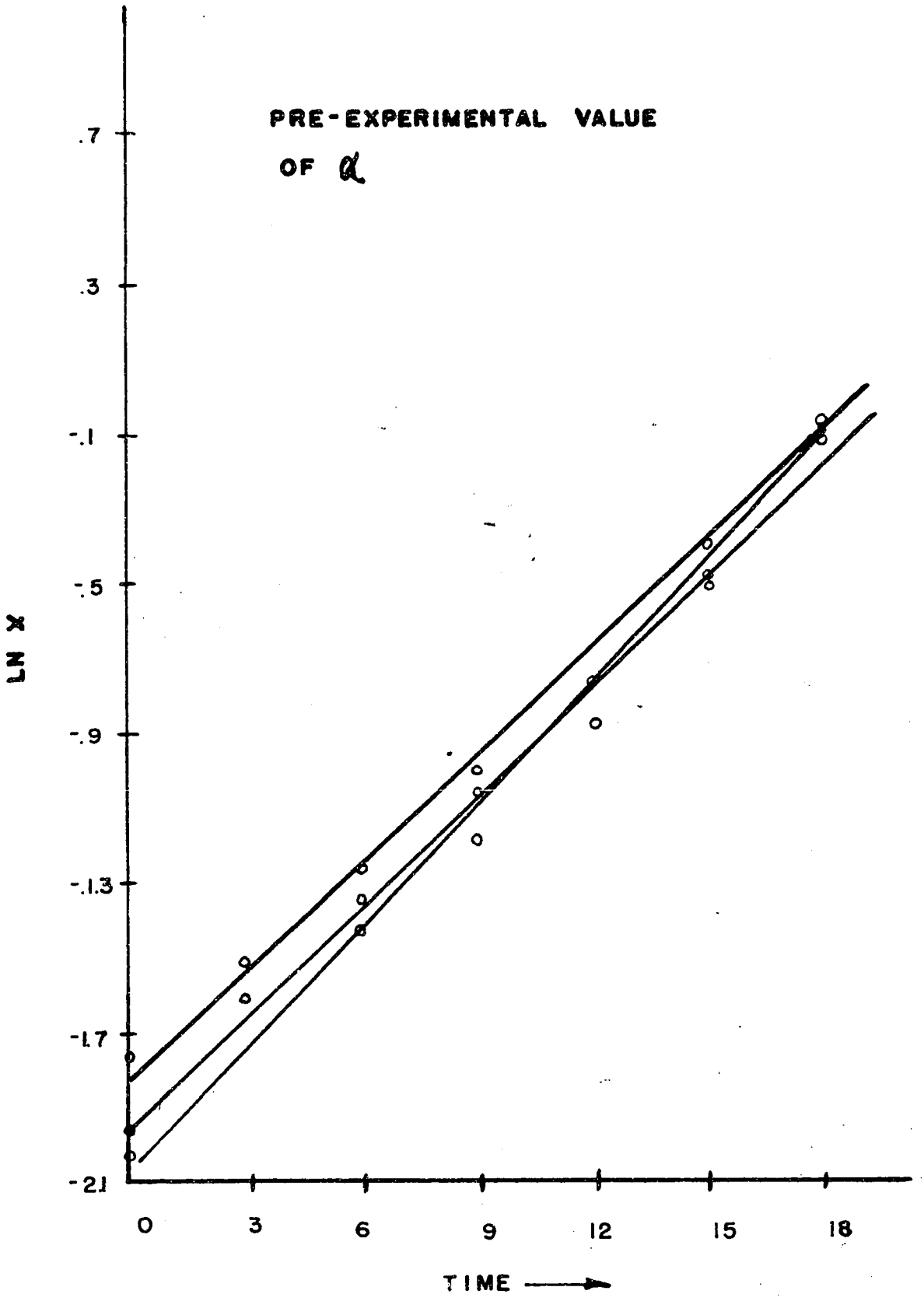

Fig. 4.14

These relationships are restricted by the fact that $\alpha<1$ and $\omega_1-\omega_2$ be small. It is well known from the theory that eq (4.4) for stable conditions, i.e. constant vibration amplitude is only valid for the range of frequency entrainment, the response relation being dependent upon oscillations having slowly varying amplitudes outside of this range.

Eq. (4.4) has as the dividing point between stable and unstable motion the line $\beta=1/2$. It is assumed that the range of entrainment begins and ends at these points. Substituting $\beta=1/2$ into eq (4.4) and considering the values for A and a from above, then

$$\omega_1-\omega_2 = \pm\frac{1}{2}\left(2F^2/\omega_2^2a_0^2 - \alpha^2/4\right)^{1/2}. \qquad (4.5)$$

ω_2 now is the frequency of the forcing function at which the system becomes entrained, and ω_1 is the natural frequency of the nonlinear system; thus, $\omega_1-\omega_2$ is one half the range or zone of entrainment.

Assuming the approximation $\omega_2\cong\omega_1$ under the radical in eq (4.5), then

$$\omega_1-\omega_2 = \pm\frac{1}{2}\left(2F^2/\omega_1^2a_0^2 - \alpha^2/4\right)^{1/2} \qquad (4.6)$$

Fig. 4.15 presents a plot of eq (4.6) for various values of F, employing values of $\alpha<1$, ω_1 and a_0 determined experimentally and held fixed throughout the experiment. Experimental values of the range of entrainment obtained from the response records of the previous experiment are plotted also in fig. 4.15, for various values of the magnitude of the forcing function.

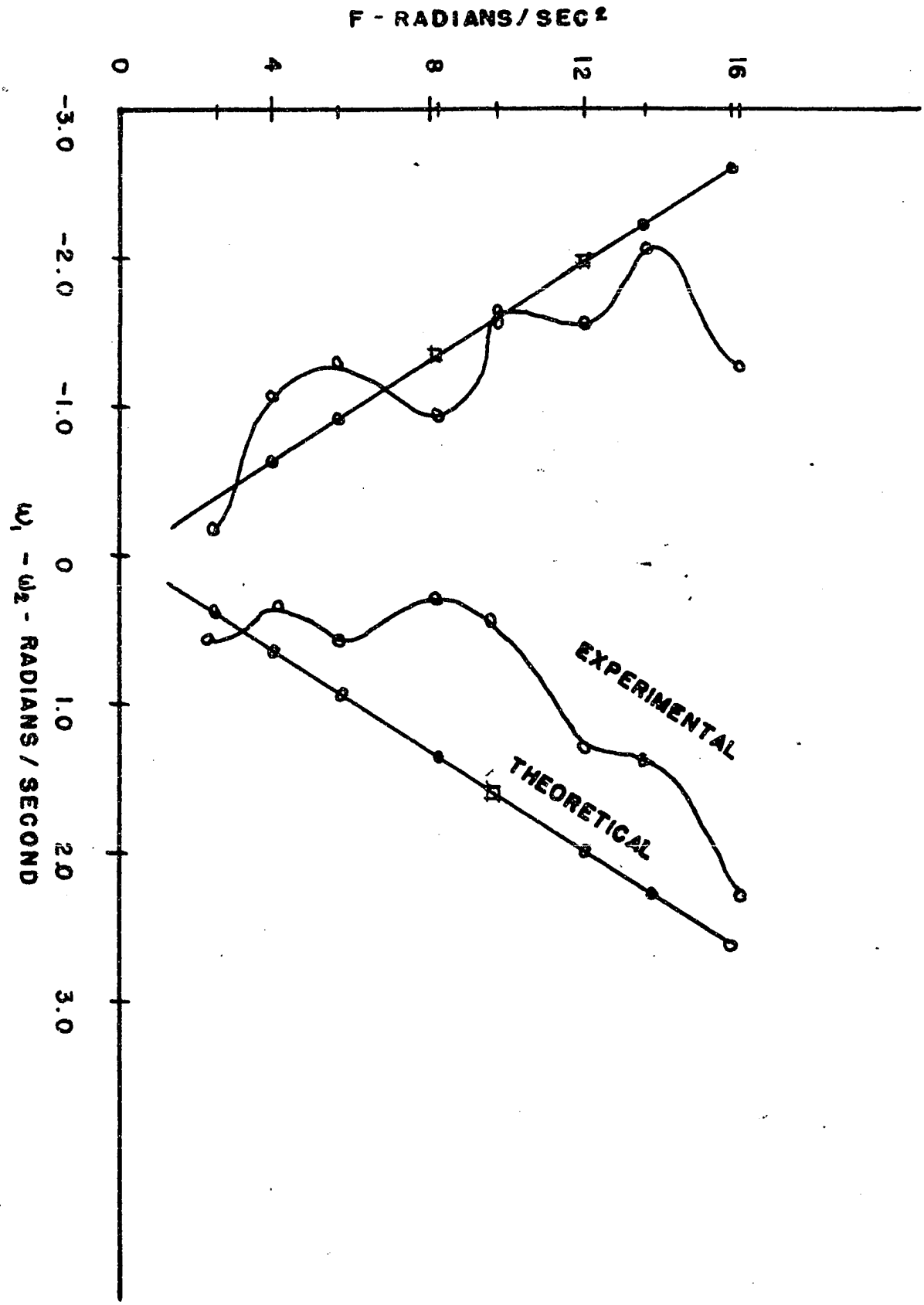

Fig. 4.15

5. A NONLINEAR SYSTEM OF TWO DEGREES OF FREEDOM

5.1 Introduction

Having successfully obtained mechanical frequency entrainment for a forced self-excited nonlinear van der Pol system of one degree of freedom, we now turn our attention to the problem of frequency entrainment in a nonlinear system of two degrees of freedom. For this purpose we consider the double torsion pendulum illustrated in fig. 5.1, and assume that two nonlinear forces act upon the system one on each plate such that we have a coupled double self-excited van der Pol system. The differential equations of motion are

$$\begin{aligned} \ddot{\theta} - \alpha_1\dot{\theta} + \omega_1^2\theta + k_1(\theta-\varphi) + \beta_1\theta^2\dot{\theta} &= 0 \\ \ddot{\varphi} - \alpha_2\dot{\varphi} + \omega_2^2\varphi - k_2(\theta-\varphi) + \beta_2\varphi^2\dot{\varphi} &= 0 \end{aligned} \qquad (5.1)$$

where $\alpha_1=\frac{a_1}{I_1}$, $\beta_1=\frac{b_1}{I_1}$, $\alpha_2=\frac{a_2}{I_2}$, $\beta_2=\frac{b_2}{I_2}$, $\omega_1^2=\frac{k_1'}{I_1}$, $\omega_2^2=\frac{k_2'}{I_2}$, $k_1=\frac{k'}{I_1}$, $k_2=\frac{k'}{I_2}$

A second electro-mechanical analog is utilized in order to represent the φ equation in eq (5.1). The difference amplifier and displacement function generators as described by Ludeke and Evans[9] have been employed in order to obtain the coupling necessary. Variations in the magnitudes of k_1 and k_2 are accomplished by potentiometers in the output of the difference amplifier. Coils attached to the analog shafts in permanent radial magnets are used to introduce

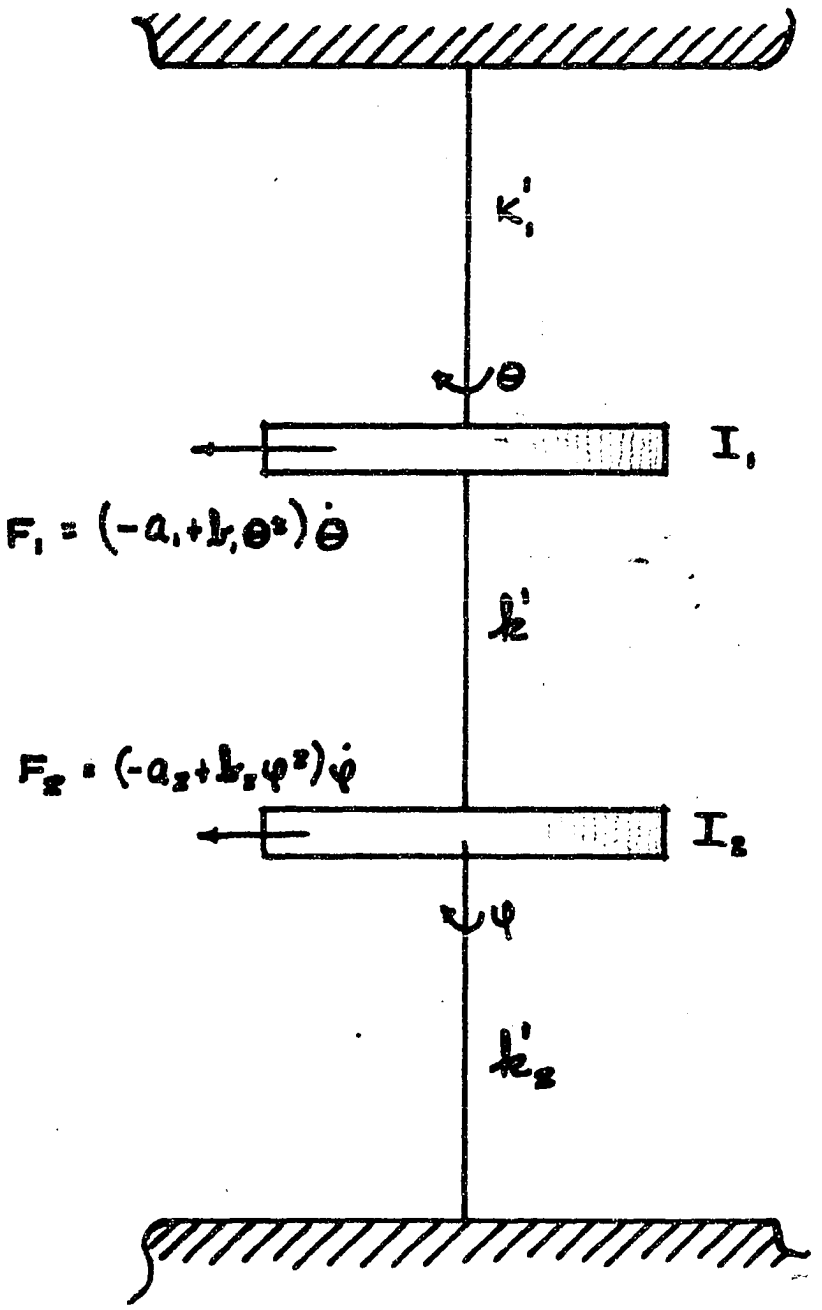

Fig. 5.1

the respective coupling torques into the analogs. Fig. 5.2 illustrates the complete analog for the two degree of freedom system, and fig. 5.3 is the block diagram of the analog.

5.2 The Reduced Linear System

For the purpose of gaining a certain amount of physical understanding of the above nonlinear system, we consider first eqs (5.1) reduced to the linear case, where $\beta_1 = \beta_2 = 0$, and α_1 and α_2 are now considered positive for convience. We have

$$\begin{aligned} \ddot{\theta} + \alpha_1\dot{\theta} + \omega_1^2\theta + k_1(\theta - \varphi) &= 0 \\ \ddot{\varphi} + \alpha_2\dot{\varphi} + \omega_2^2\varphi - k_2(\theta - \varphi) &= 0 \end{aligned} \tag{5.2}$$

which have the solutions

$$\begin{aligned} \theta &= A e^{-u_1 t}\sin(v_1 t + \gamma_1) + B e^{-u_2 t}\sin(v_2 t + \gamma_2) \\ \varphi &= cA e^{-u_1 t}\sin(v_1 t + \gamma_1) + dB e^{-u_2 t}\sin(v_2 t + \gamma_2) \end{aligned} \tag{5.3}$$

where A, B, γ_1, γ_2 are the integration constant, c and d amplitude ratio factors, and u_1, u_2, v_1, v_2 are the real parts of the two pairs of conjugate complex roots $p = -u_1 \pm iv_1$; $= -u_2 \pm iv_2$, of the characteristic equation

$$\begin{aligned} p^4 + (\alpha_1 + \alpha_2)p^3 + (\omega_1^2 + \omega_2^2 + k_1 + k_2 + \alpha_1\alpha_2)p^2 + [\alpha_2(\omega_1^2 + k_1) + \alpha_1(\omega_2^2 + k_2)]p \\ + (\omega_1^2 + k_1)(\omega_2^2 + k_2) - k_1 k_2 = 0 \end{aligned} \tag{5.4}$$

It is interesting to note that if the parameters of the system are such that $u_2 > u_1$ or vice verse, the system will automatically seek the mode of oscillation which has not damped out after the other mode has damped out. Figs. 5.3 and 5.4 demonstrate this phenomenon, the relative

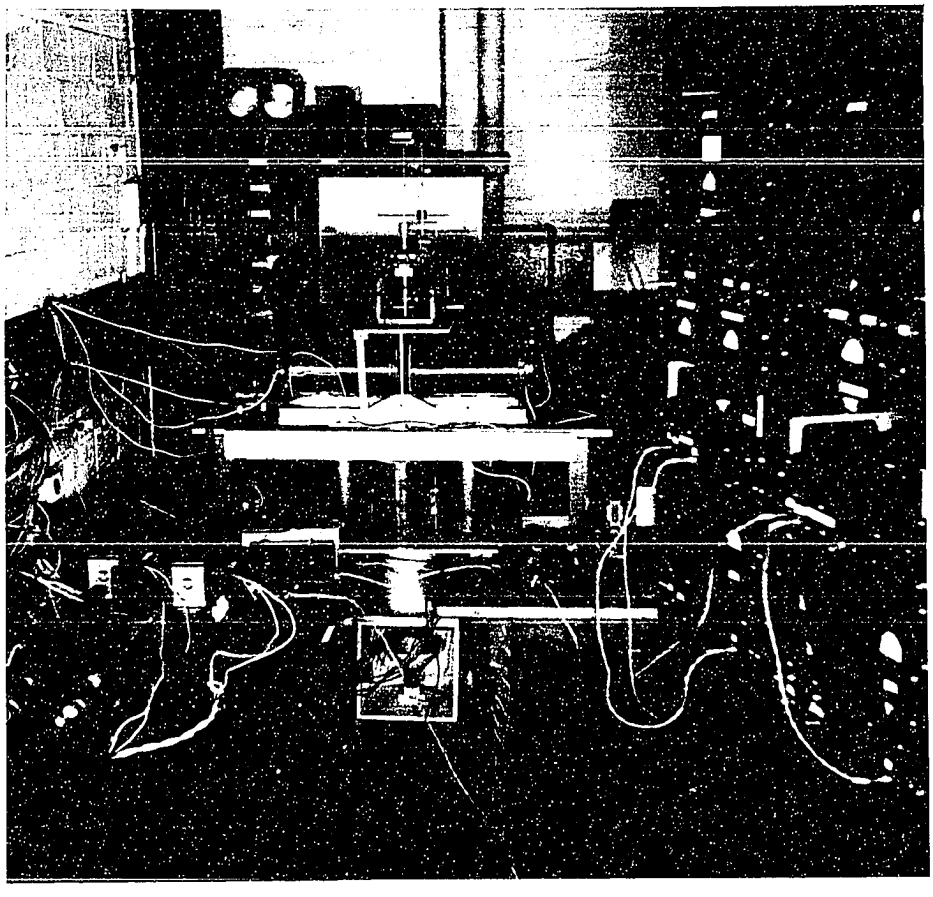

Fig. 5.2a

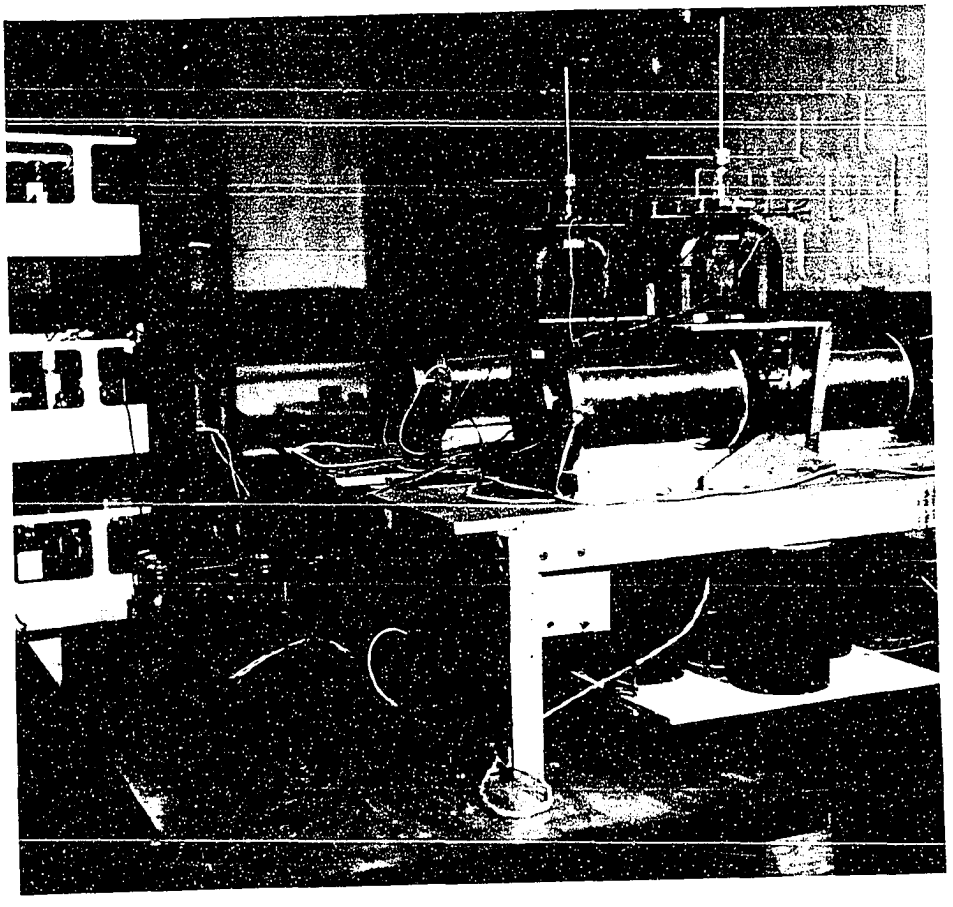

Fig. 5.2b

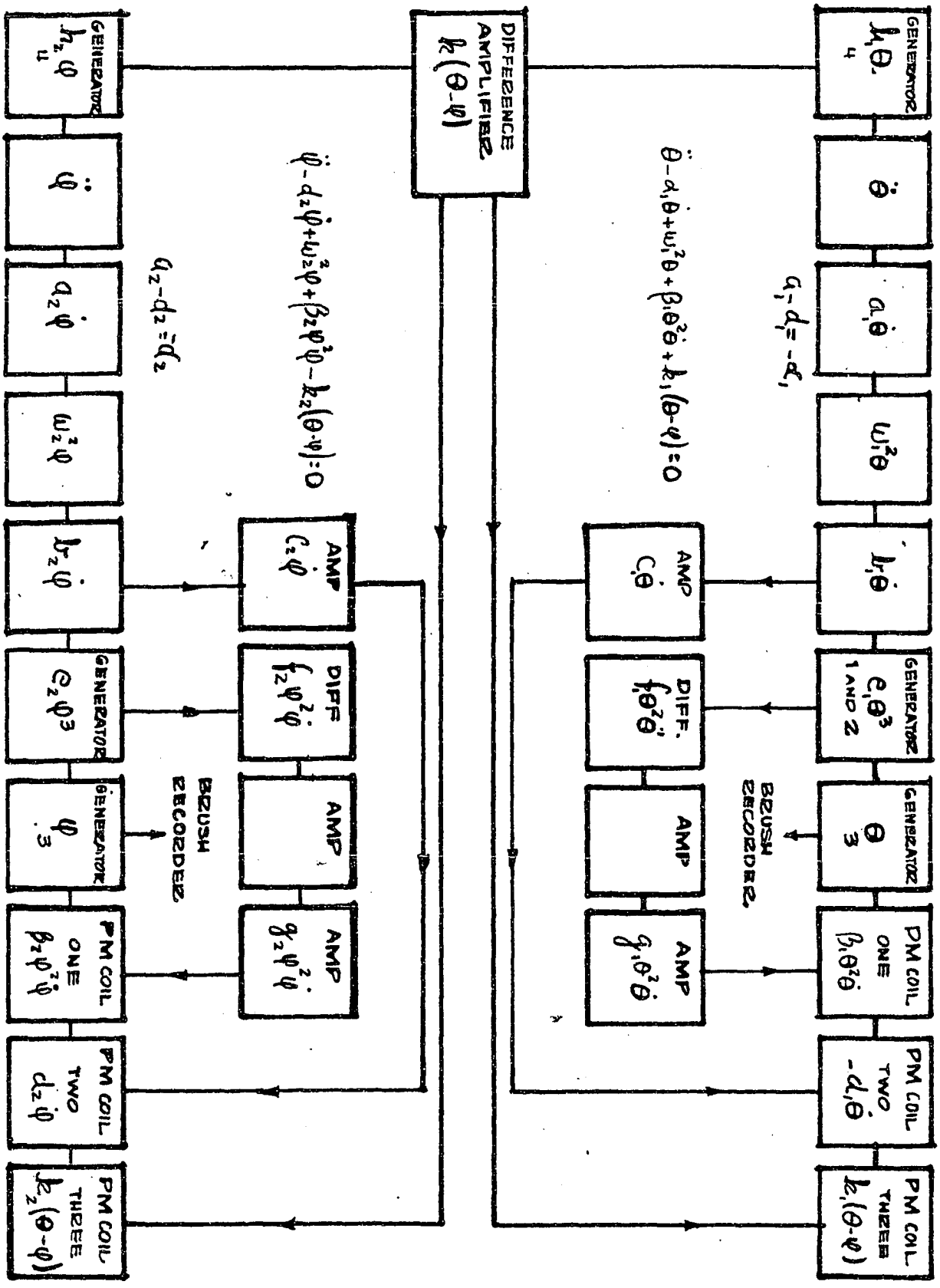

Fig. 5.3

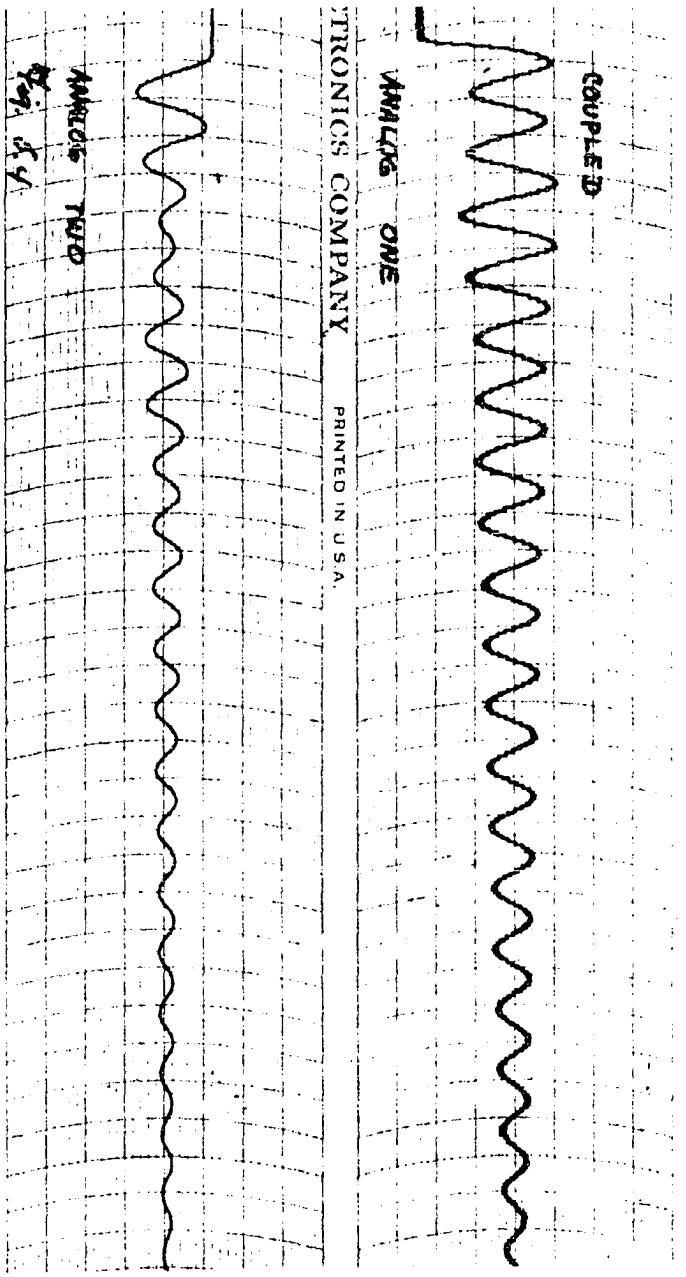

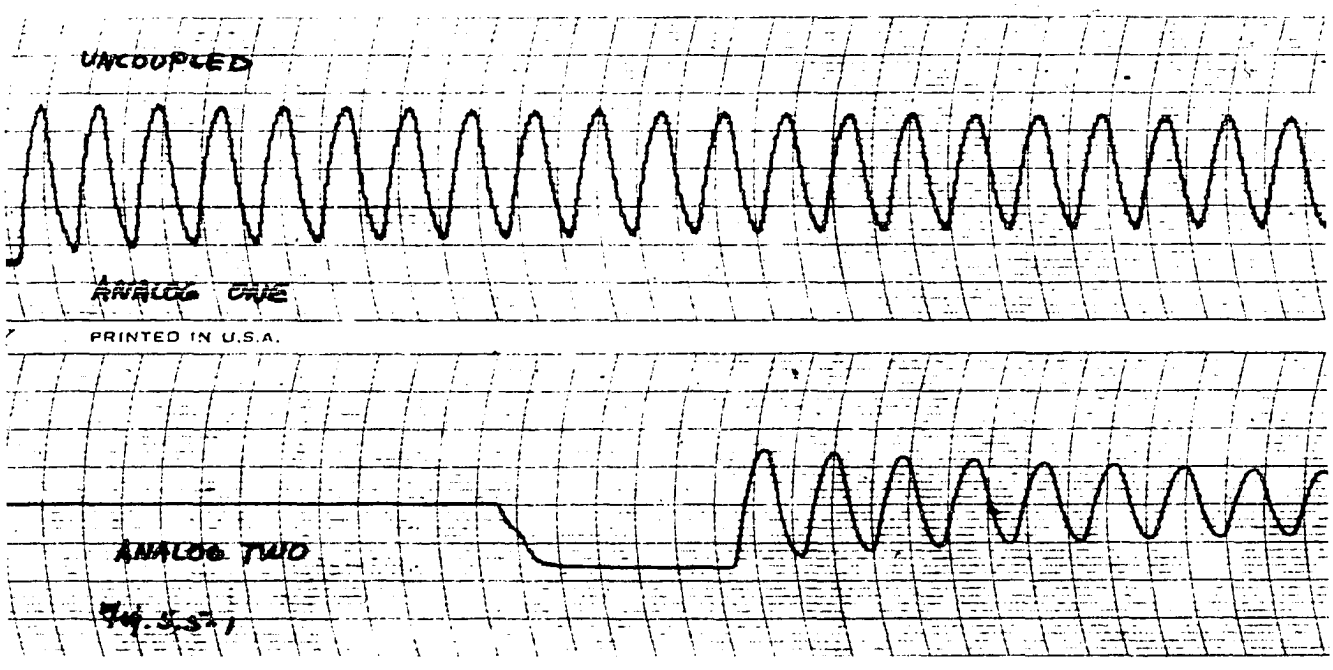

Fig. 5.5-1

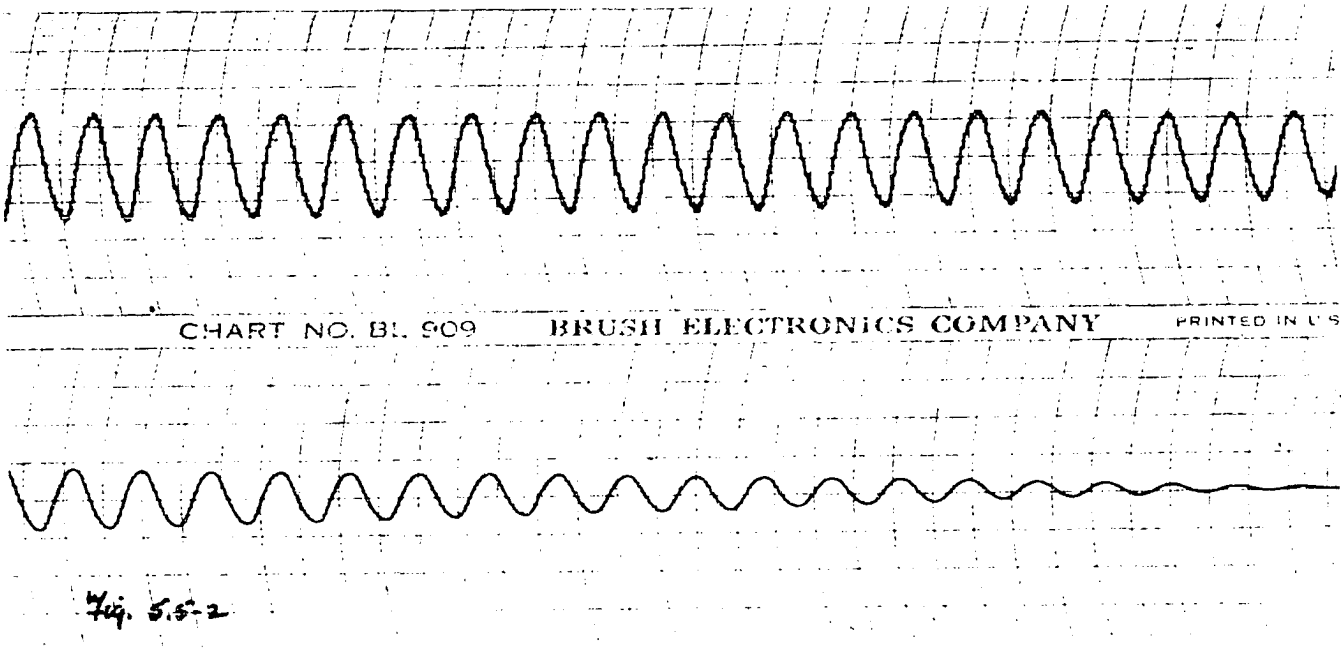

Fig. 5.5-2

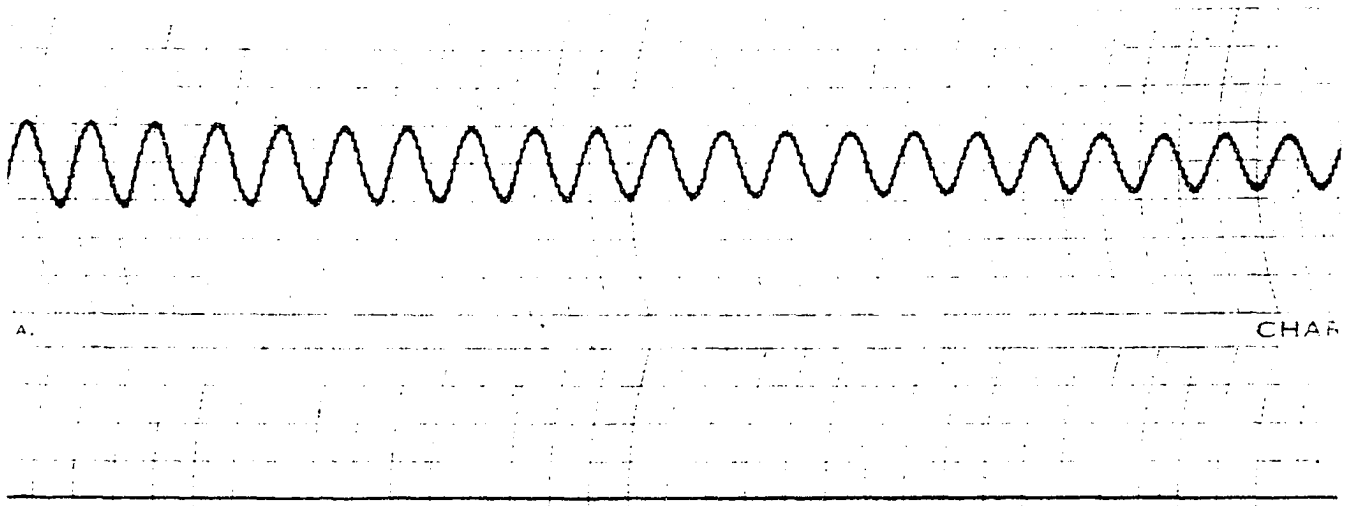

Fig. 5.5-3

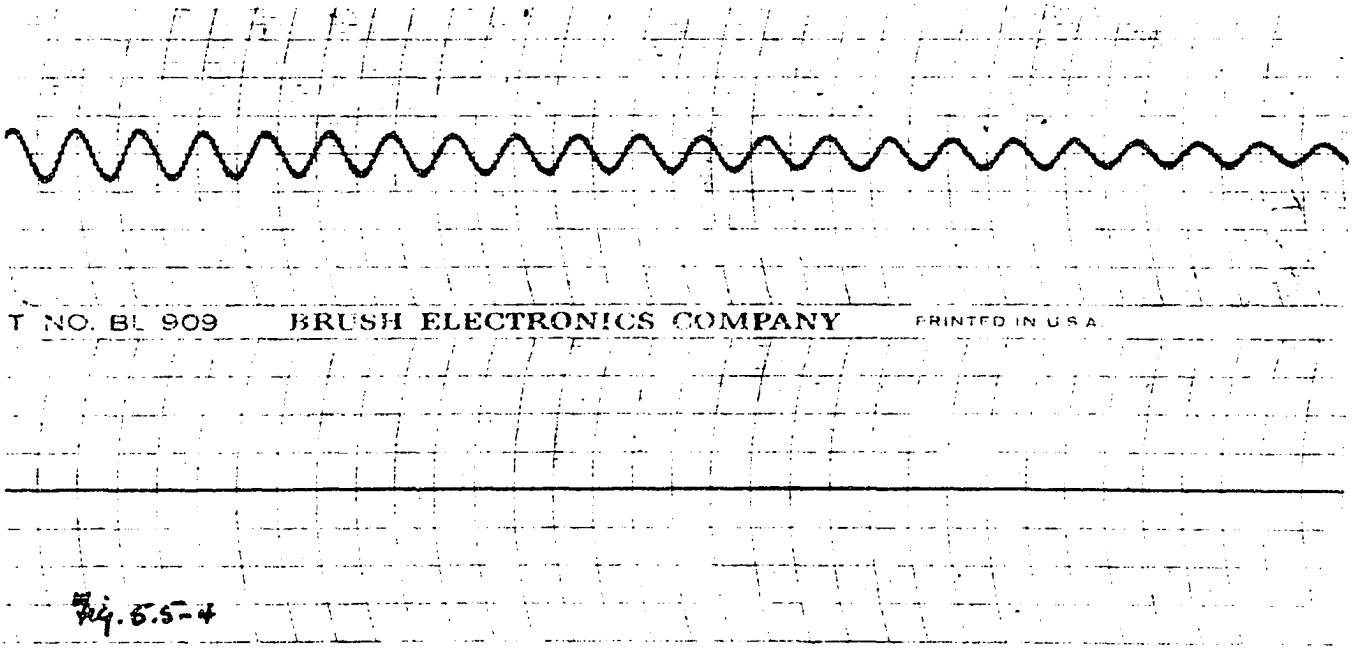

Fig. 5.5-4

damping of the uncoupled systems being demonstrated in the latter figure. u_1 and u_2, of course, depend upon all the parameters, but for the above case $k_1 \doteq k_2$, hence, the frequency and damping are instrumental in determining the magnitude of damping for the fundamental modes.

For reference in the next section we consider now the undamped linear case when $d_1 = d_2 = 0$, then eq (5.4) becomes

$$p^4 + (\omega_1^2 + \omega_2^2 + k_1 + k_2)\, p^2 + (\omega_1^2 + k_1)(\omega_2^2 + k_2) - k_1 k_2 = 0 \qquad (5.5)$$

and

$$p_{1,2}^2 = -\frac{(\omega_1^2+\omega_2^2+k_1+k_2)}{2} \pm \frac{1}{2}\left[(\omega_1^2+\omega_2^2+k_1+k_2)^2 - 4\left[(\omega_1^2+k_1)(\omega_2^2+k_2) - k_1 k_2\right]\right]^{1/2} \qquad (5.6)$$

It will be instructive to investigate the variation of the modal frequencies, $p_{1,2}$, with a variation in ω_1, the natural frequency of the first system, keeping all the other parameters fixed. For this purpose assume that $k_1 = k_2 = \omega_2^2 = 1$, then eq (5.6) becomes

$$p_{1,2}^2 = -\frac{1}{2}(\omega_1^2 + 3) \pm \frac{1}{2}(\omega_1^4 - 2\omega_1^2 + 5)^{1/2} \qquad (5.7)$$

A plot of eq (5.7) for values of ω_1 is given in fig. 5.6 from which we can see how p_1 and p_2, the principle modes of oscillation, vary by varying only the frequency parameter of one of the systems.

The variation of the modal frequencies with respect to the parameters of a linear system with damping in

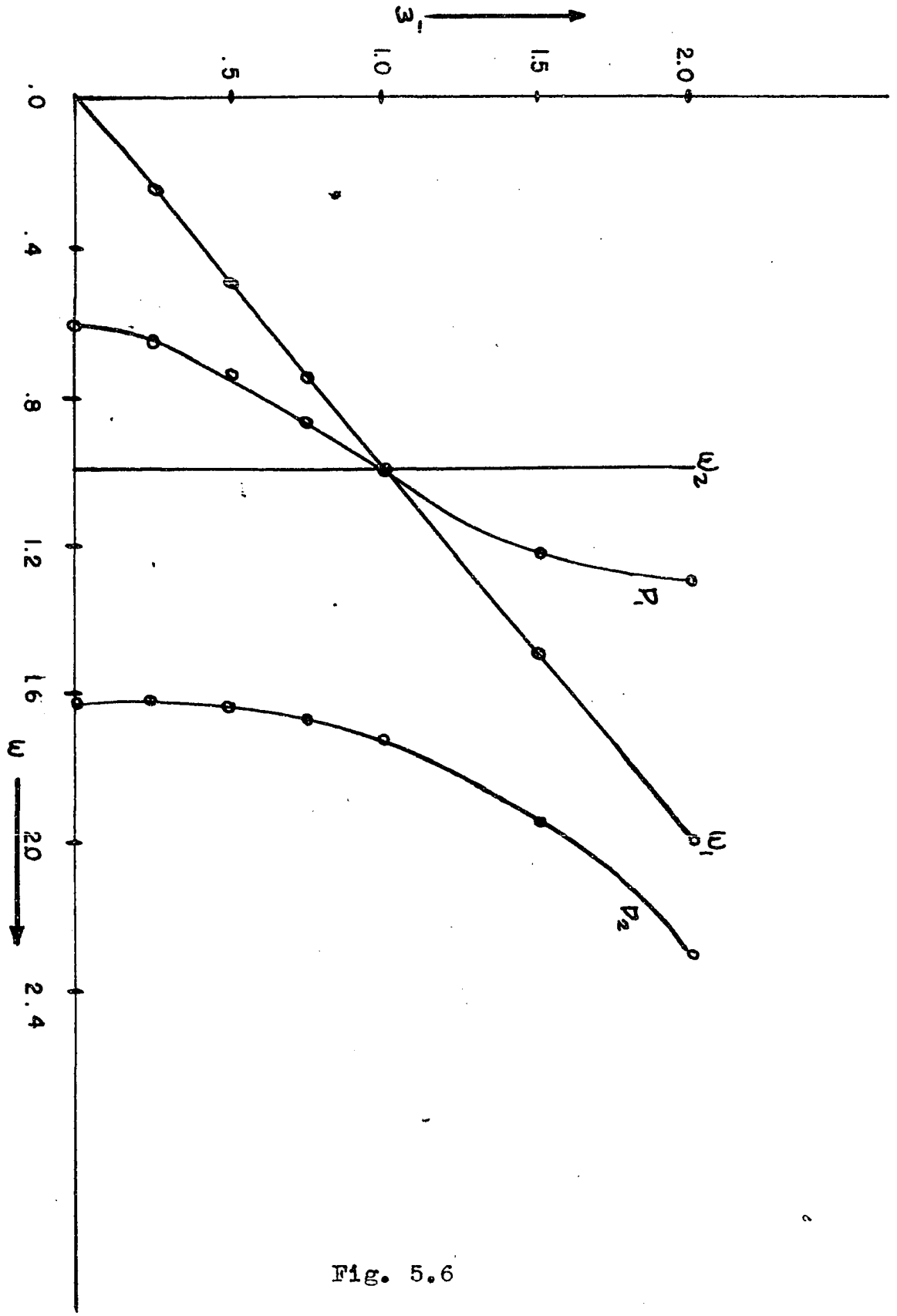

Fig. 5.6

analytical form is unobtainable, since explicit expressions of the roots of a quartic equation in terms of its coefficients not involving the fourth degree cannot be determined.

Also for future reference let us consider two more special cases of the above linear case. Suppose that $k_1 = \omega_2 = 1$ and $k_2 = 1/20$ then eq (5.6) becomes

$$p_{1,2}^2 = -\tfrac{1}{2}(\omega_1^2 + 41/20) \pm \tfrac{1}{2}(\omega_1^4 - \omega_1^2/10 + 81/400)^{1/2} \qquad (5.8)$$

a plot of which is given in fig. 5.7 for values of ω_1. Comparing with fig. 5.6 it is noted that there is a shift of the p_1 curve towards ω_2, as k_2 becomes small. Reversing this process, let $k_2 = \omega_2 = 1$ and $k_1 = 1/25$, then eq (5.6) becomes

$$p_{1,2}^2 = -\tfrac{1}{2}(\omega_1^2 + 51/25) \pm \tfrac{1}{2}(\omega_1^4 - 98/25\,\omega_1^2 + 2501/625)^{1/2} \qquad (5.9)$$

and a plot of this relation demonstrates in fig. 5.8 that p_1 and p_2 shift towards the ω_1 line as k_1 becomes small. These results will be of use in the next section.

5.3 The Nonlinear System

With the experimental arrangement as outlined in section 5.1, a number of observational experiments of the nonlinear analoged system were performed. The results are Figs. 5.9 to 5.12, and they are representative of the behavior of the nonlinear system for various values of the parameters. Of course, these initial investigations

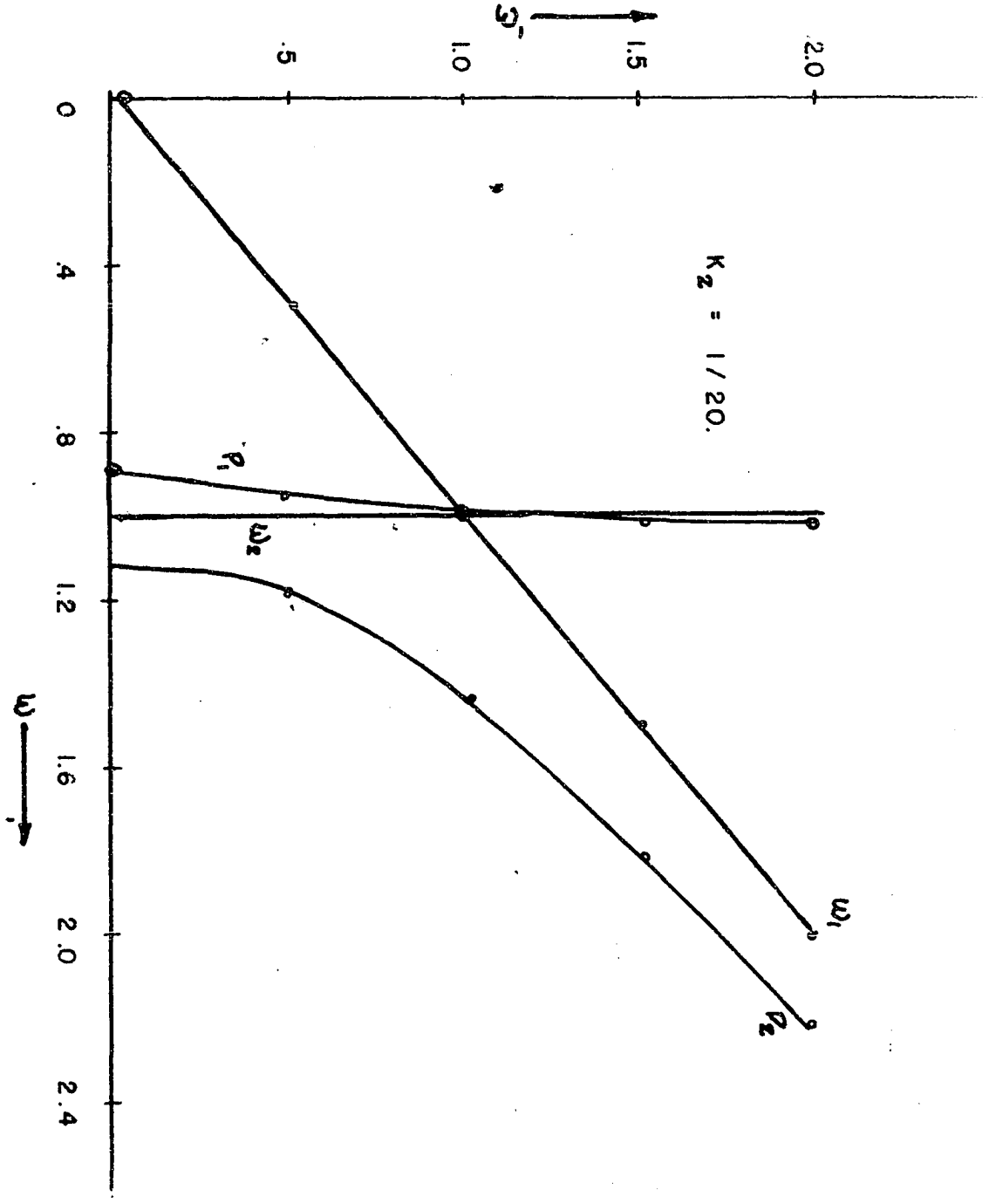

Fig. 5.7

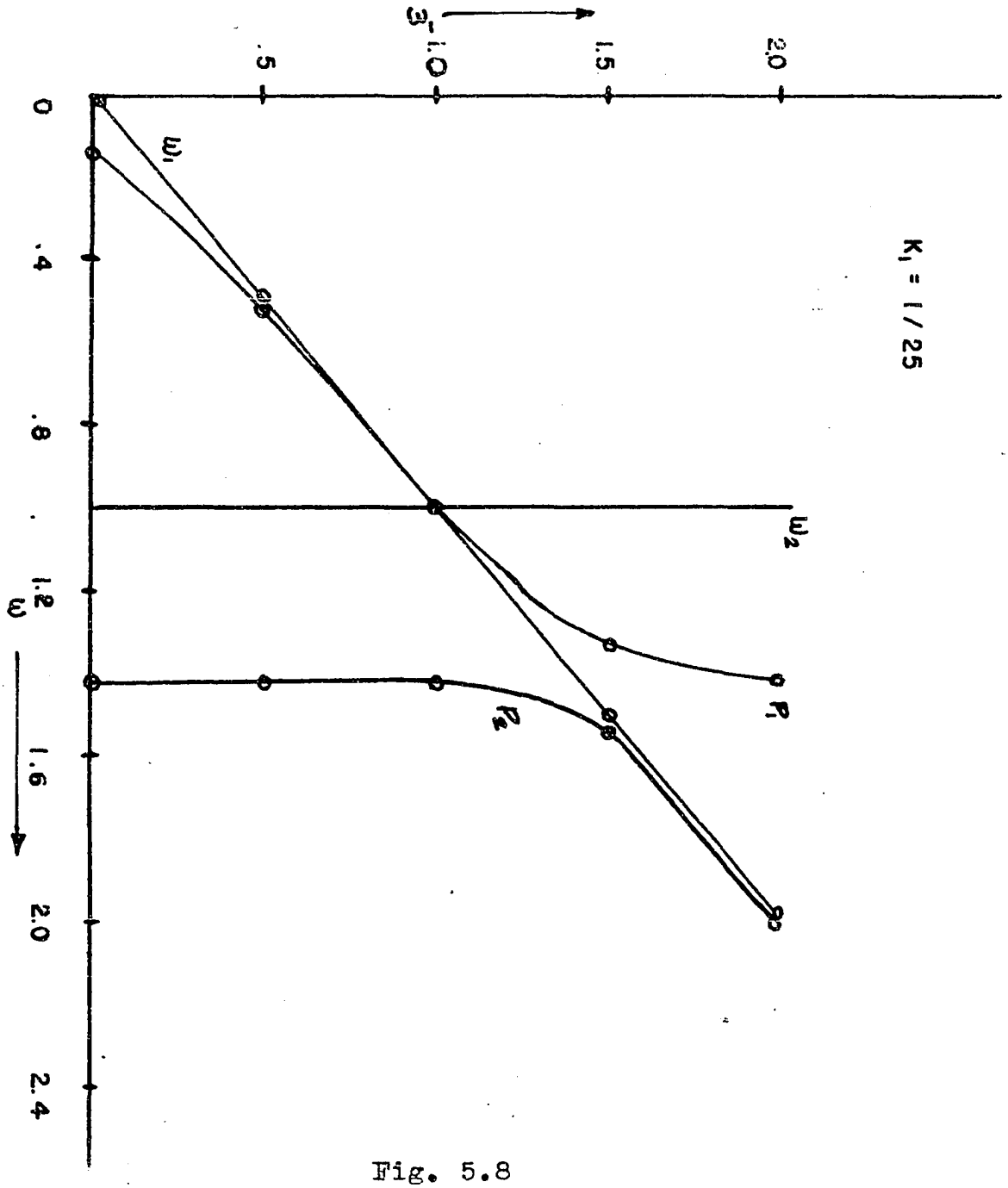

Fig. 5.8

along with the linear considerations suggested a number of quantitative experiments which, having been performed, are employed to substantiate the following interpretations of the initial investigations. After this discussion the quantitative experiments will be considered.

In Fig. 5.9 the natural frequency of the nonlinear system on analog one, ω_1, is varied through the frequency ω_2 beginning at $\omega_1 > \omega_2$, $k_1 > k_1$. The one subscripts are associated with analog one and the twos with analog two. The sequence of charts is a continuous record of the behavior of the system as the frequency ω_1 is altered at the indicated points on the charts. At all other points ω_1 is fixed. In chart 2 the system has been given an arbitrary initial displacement at the point indicated. Note that the system has settled into its previous motion as indicated in chart 3. In chart 4 ω_1 was decreased a slight amount, resulting in a change in the variations of the amplitudes of the limit cycles as indicated in chart 5. In chart 6 ω_1 was again decreased a slight amount, resulting in the system becoming synchronized in phase. This is the same thing as saying that the system is vibrating in one of its modes of oscillation. The limit cycle amplitudes are now constant. In chart 7 an arbitrary displacement is given to the system after which the system settled into its previous motion. Chart 8 indicates a

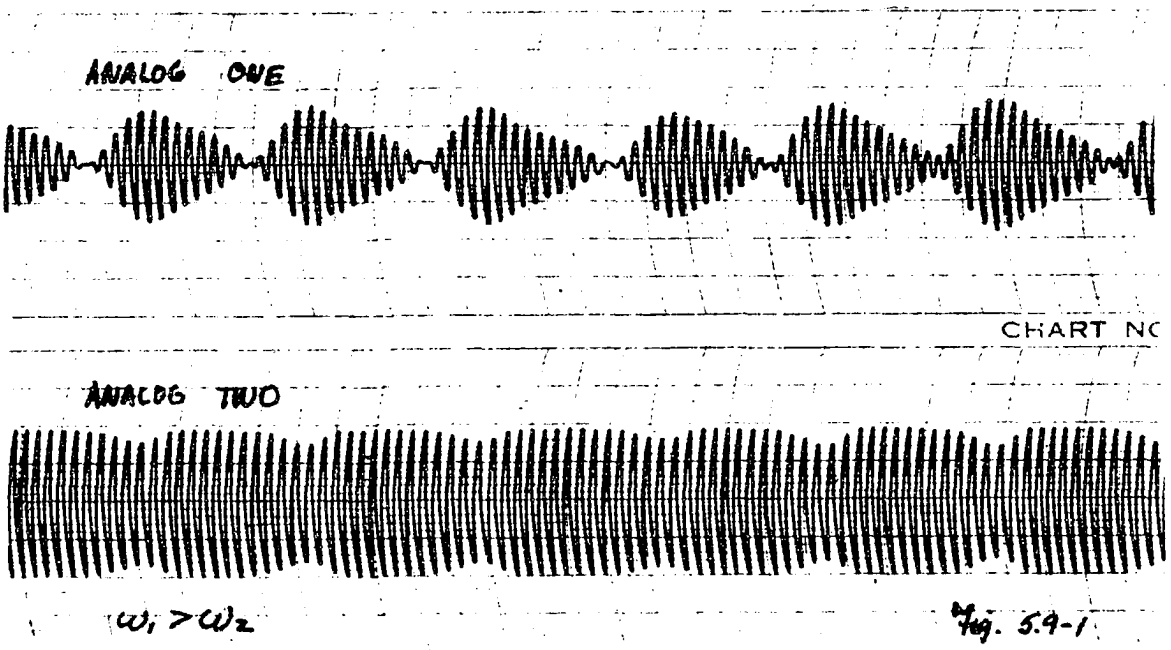

Fig. 5.9-1

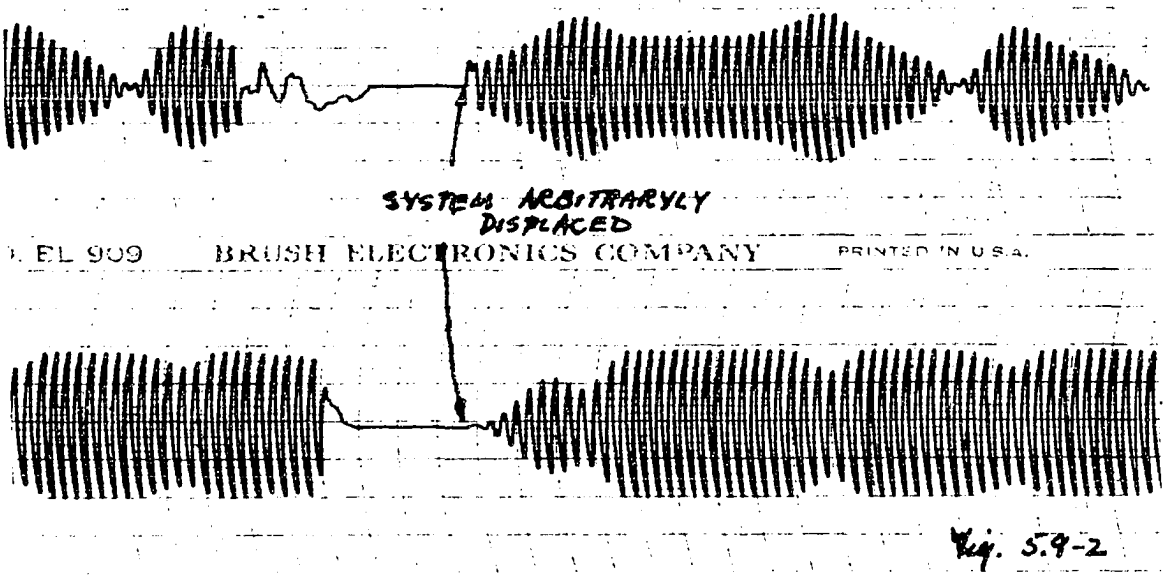

Fig. 5.9-2

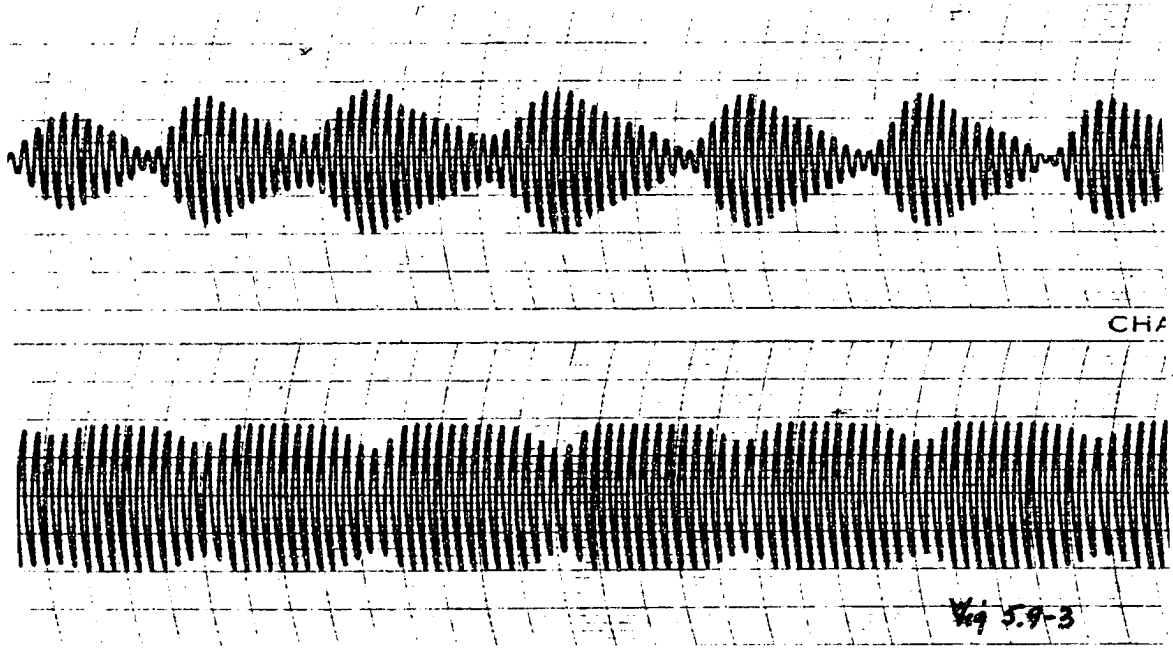

Fig 5.9-3

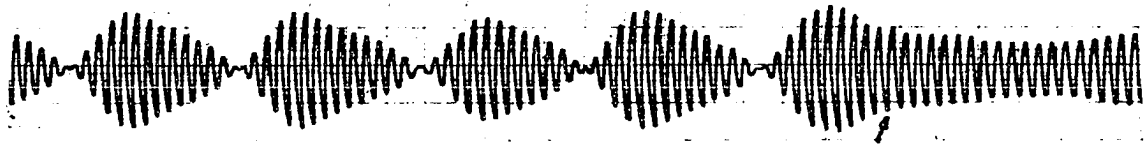

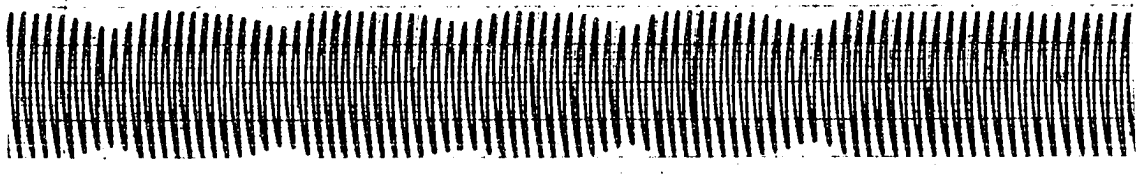

Fig. 5.9-4

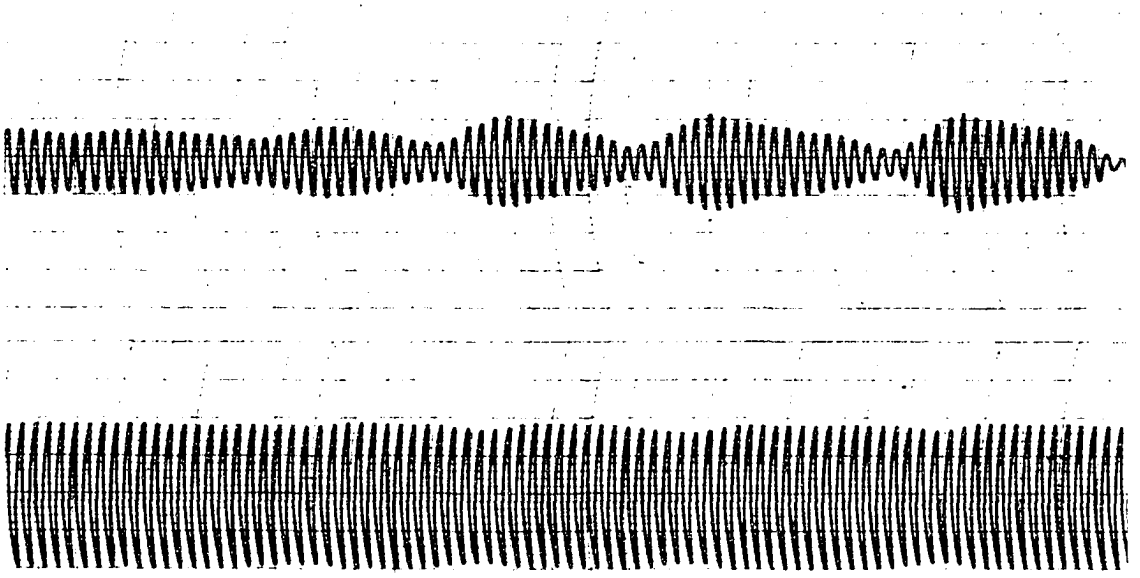

Fig. 5.9-5

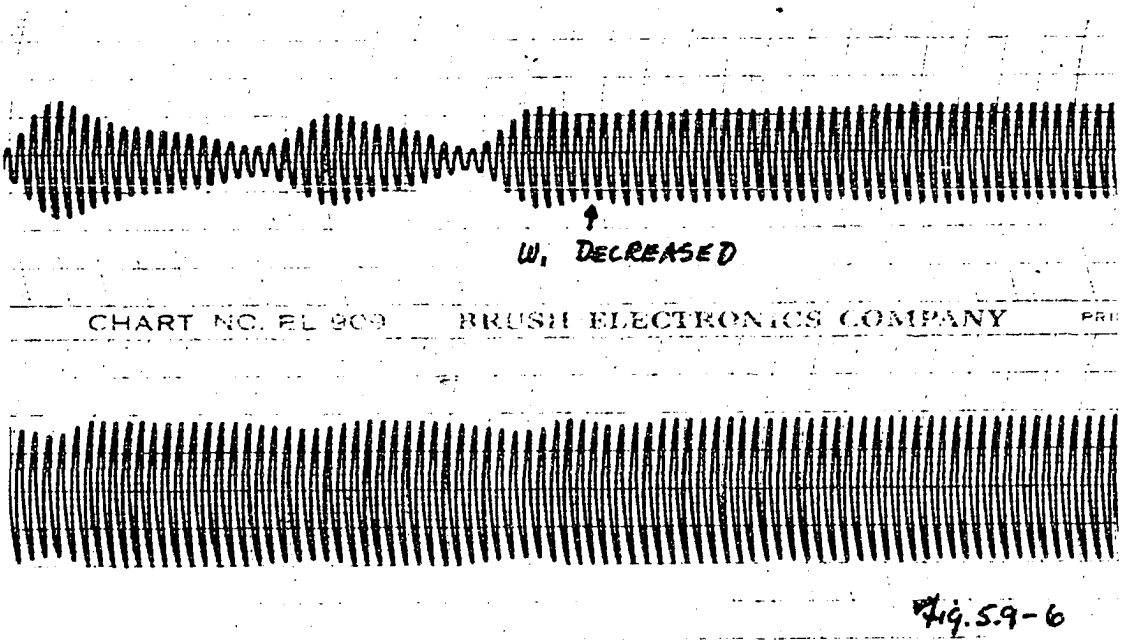

Fig. 5.9-6

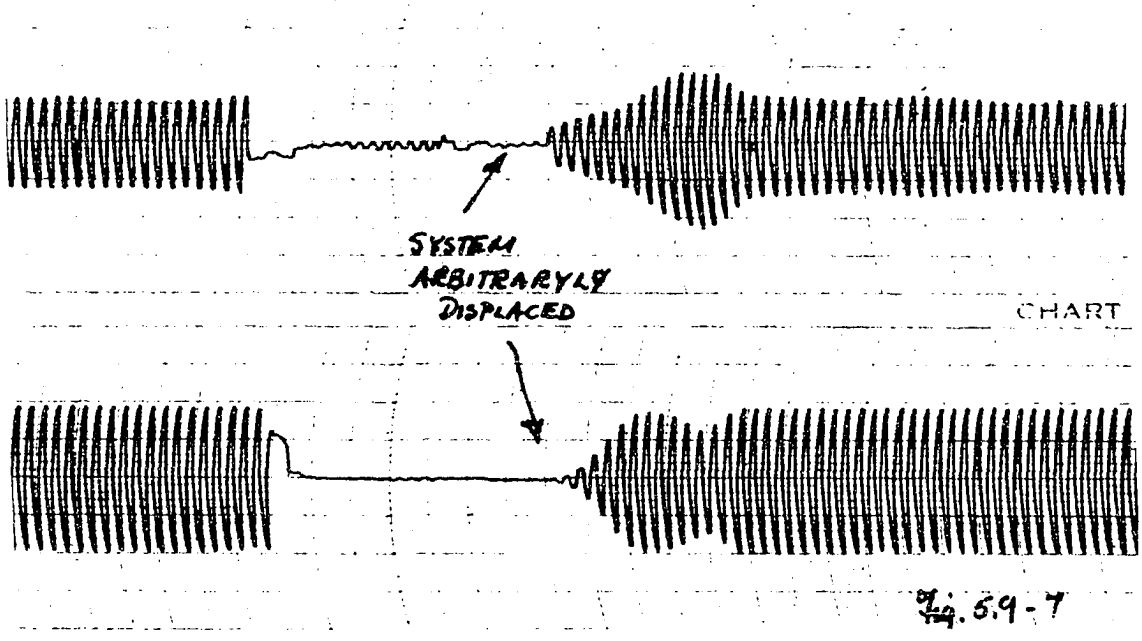

Fig. 5.9-7

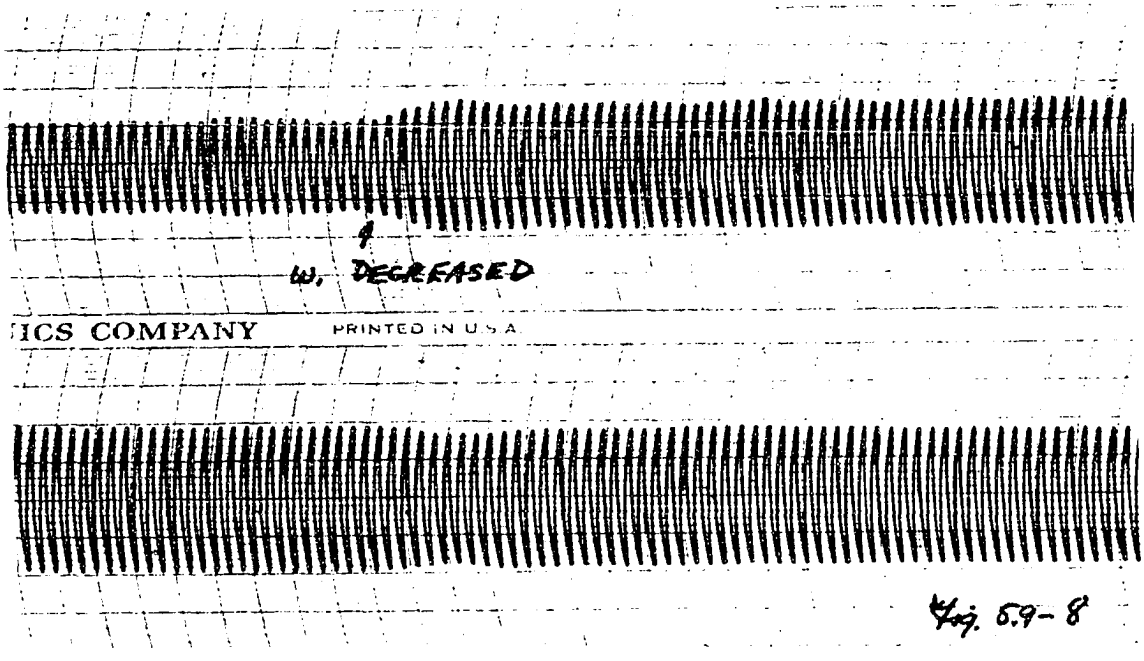

Fig. 5.9-8

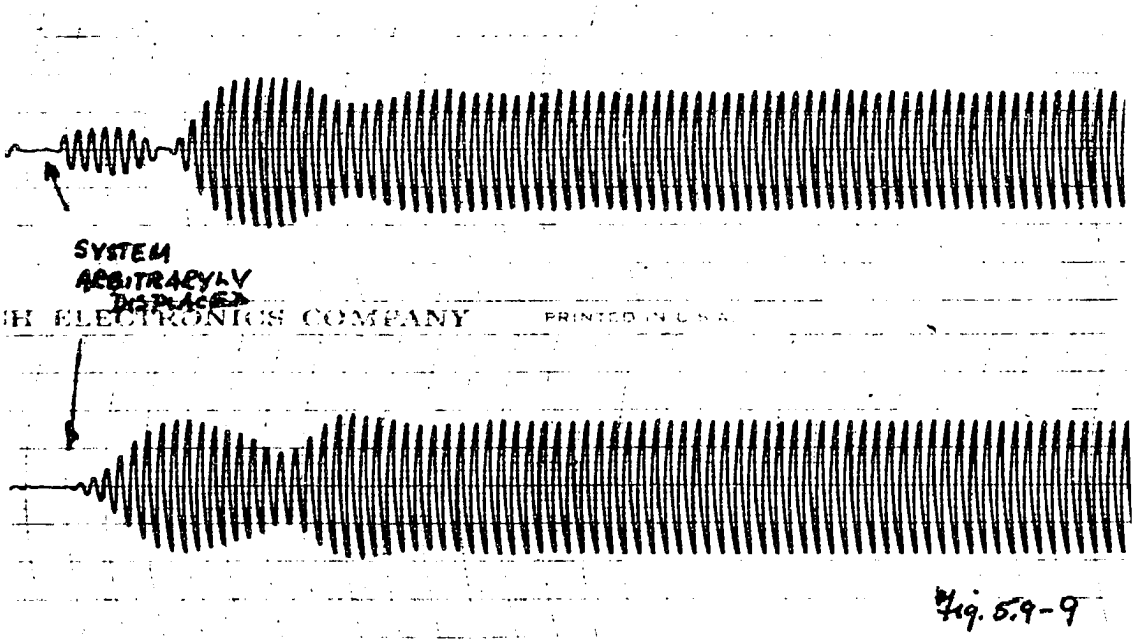

H ELECTRONICS COMPANY PRINTED IN U.S.A.

Fig. 5.9-9

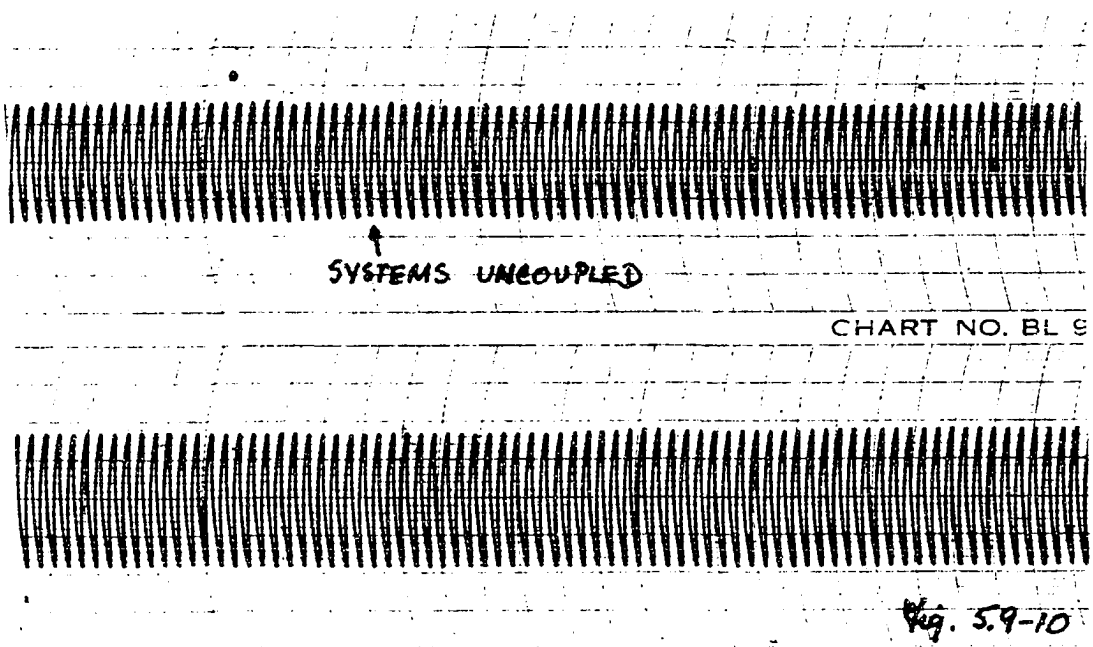

CHART NO. BL 9

Fig. 5.9-10

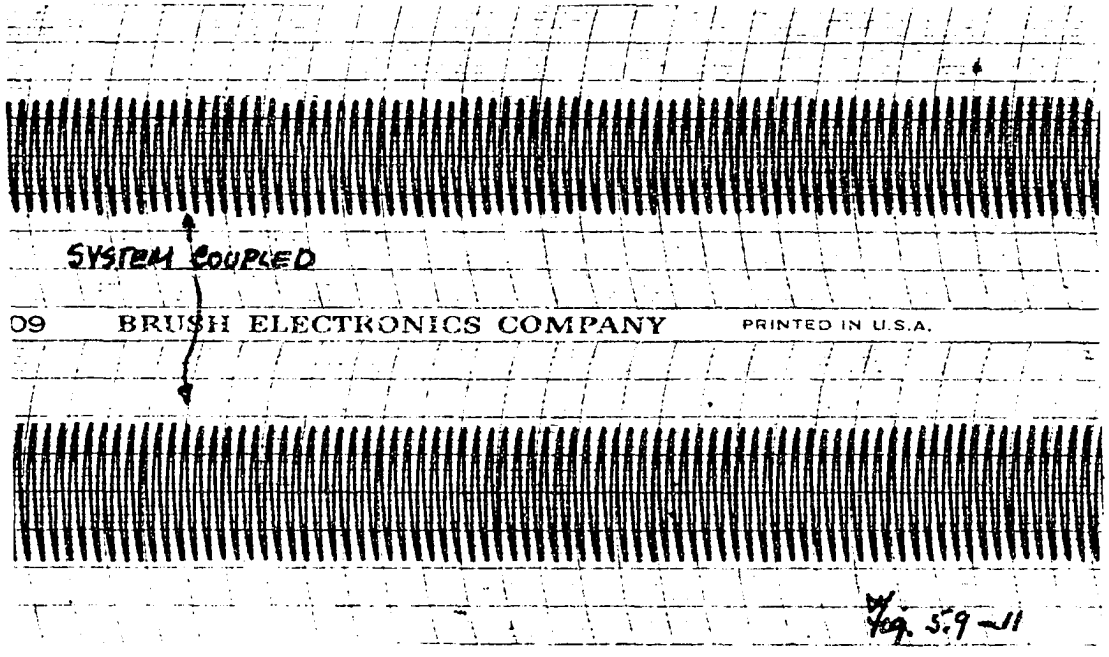

Fig. 5.9-11

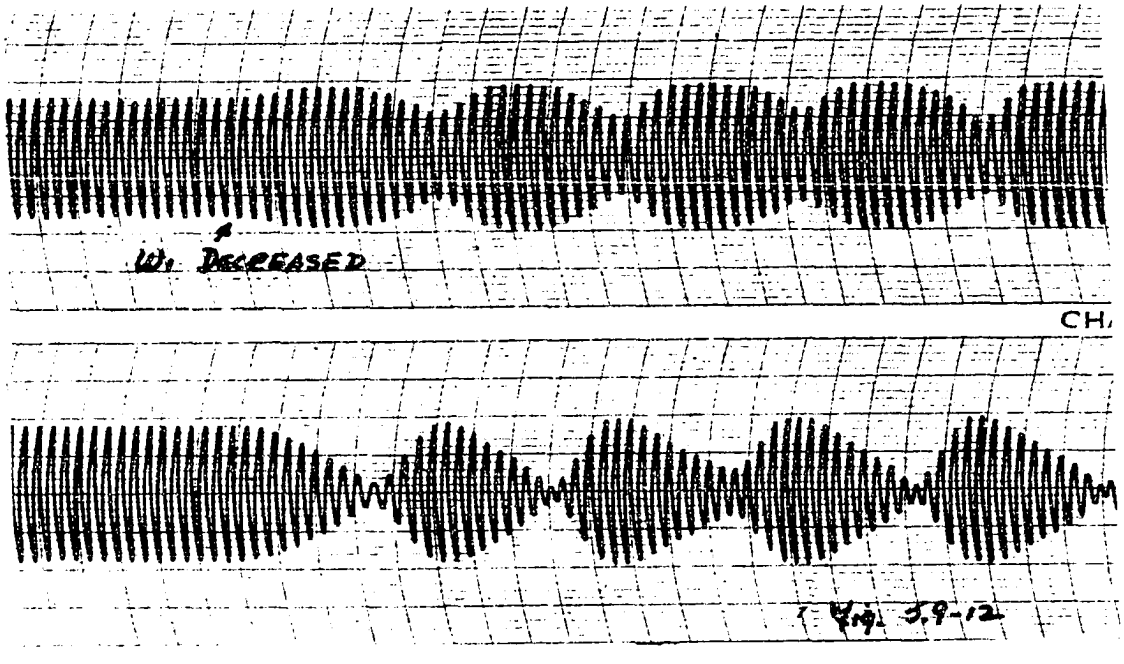

Fig. 5.9-12

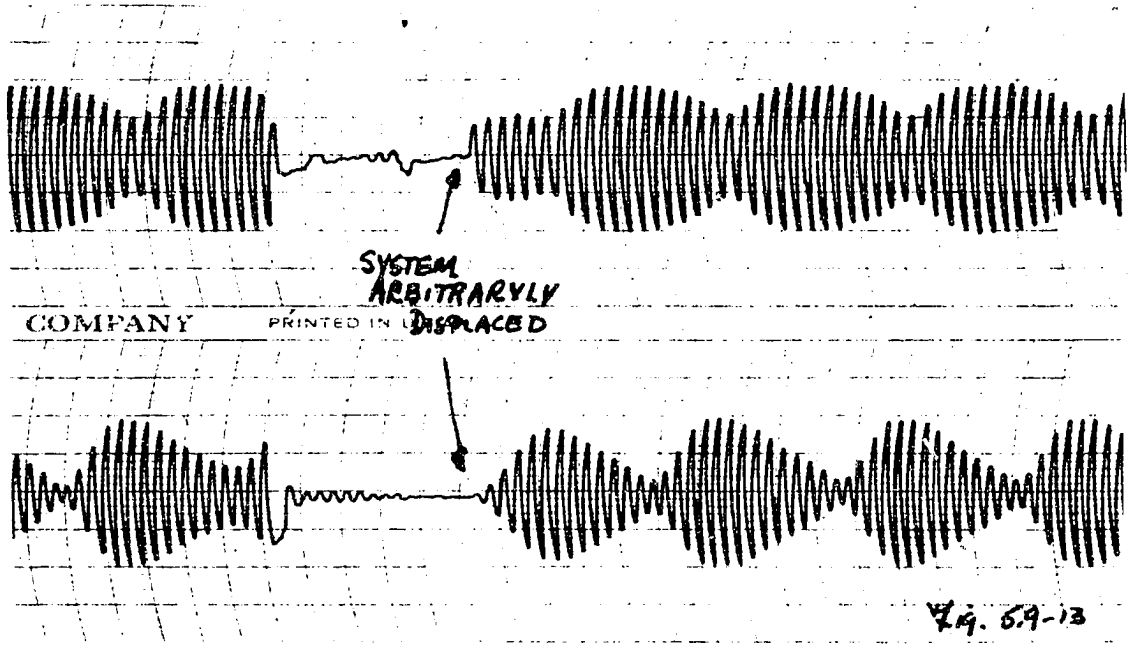

Fig. 6.9-13

change in the maximum amplitudes of the limit cycles with a change in ω_1. At this new value of ω_1 the system is again given an arbitrary displacement in chart 9; after which the system again settled into its previous behavior. In chart 10 the systems have been uncoupled electrically at the point indicated, and recoupled in chart 11 at the indicated time. Chart 12 shows the reappearance of the varying amplitudes as ω_1 is further decreased. Chart 13 demonstrates the resulting behavior for an arbitrary displacement at this value of ω_1.

Fig. 5.10 is a repeat of the previous experiment, $\omega_1 < \omega_2$ initially, ω_1 having been varied at the points indicated and the system having been coupled and uncoupled electrically at the points also indicated. At all times where the system was coupled and had constant amplitudes, the two systems were in phase in this experiment and also in the previous experiment.

Considering now fig. 5.11, in this case $k_2 > k_1$ and $\omega_1 < \omega_2$ initially, ω_1 was varied at the indicated points. In chart 3 for ω_1 such that the limit cycle amplitudes are constant, a phase difference exists between the two systems. In chart 4 after an arbitrary displacement the phase difference is again noted. In chart 6 ω_1 has reached a point where the two systems are now out of phase. This out of phase motion was again achieved after an arbitrary displacement

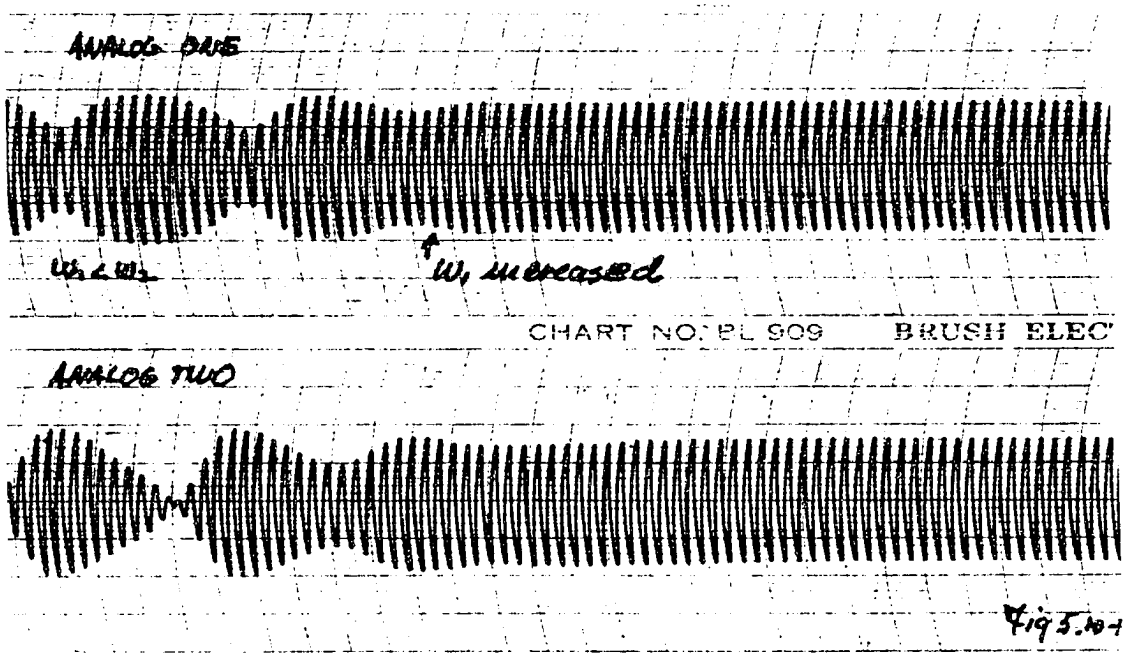

Fig 5.10-1

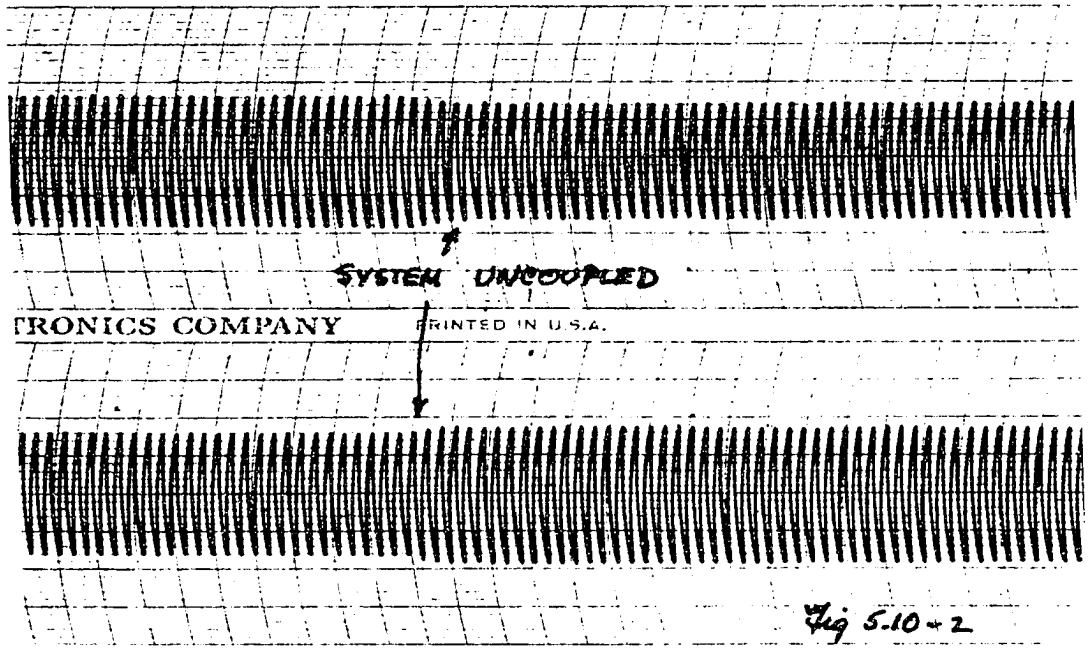

Fig 5.10-2

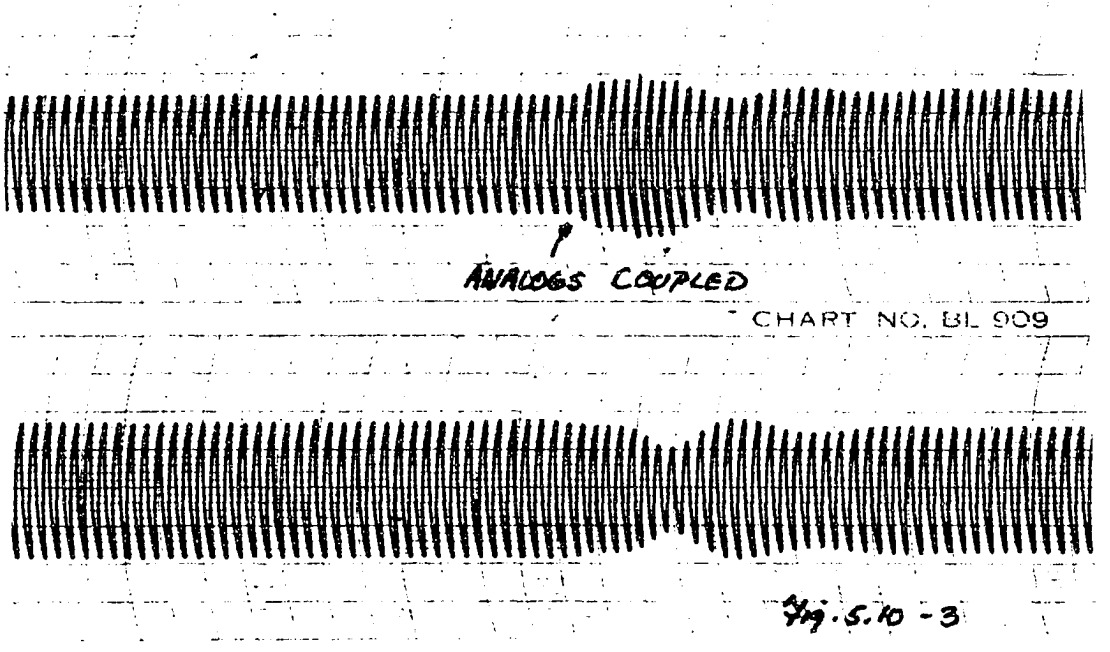

Fig. 5.10-3

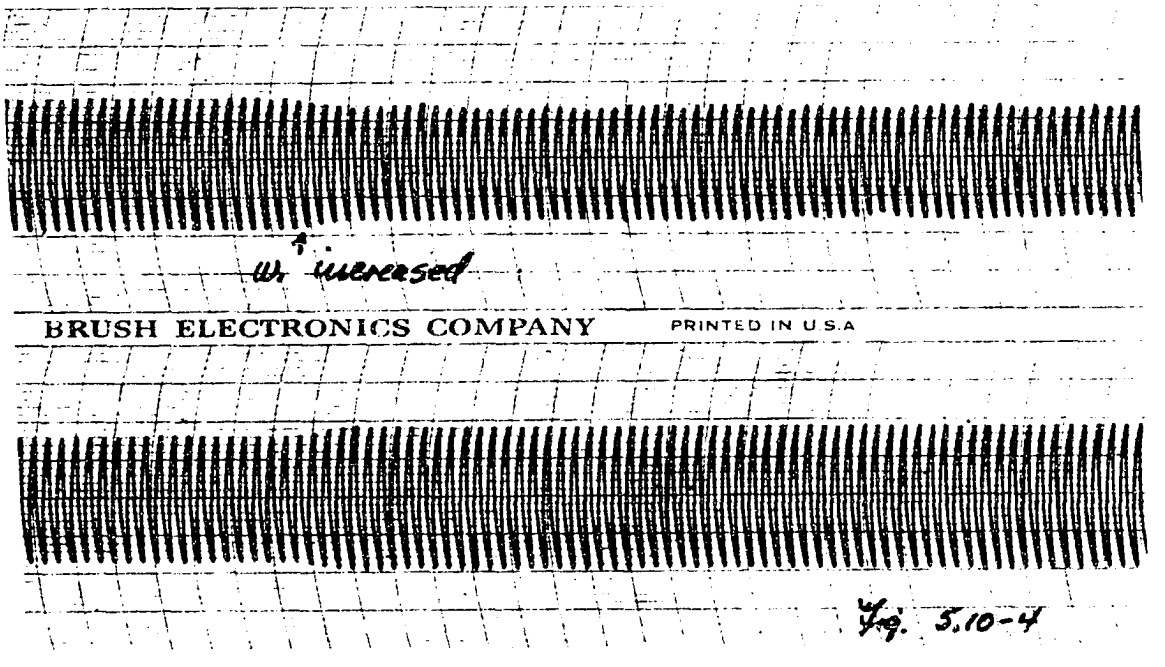

Fig. 5.10-4

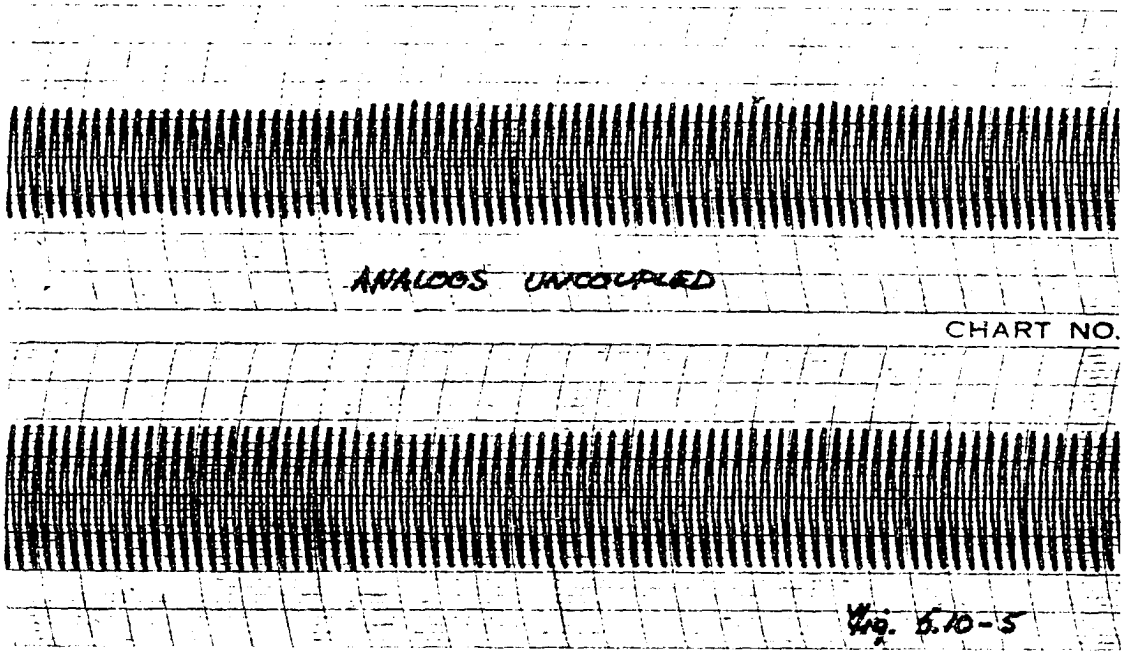

Fig. 5.10-5

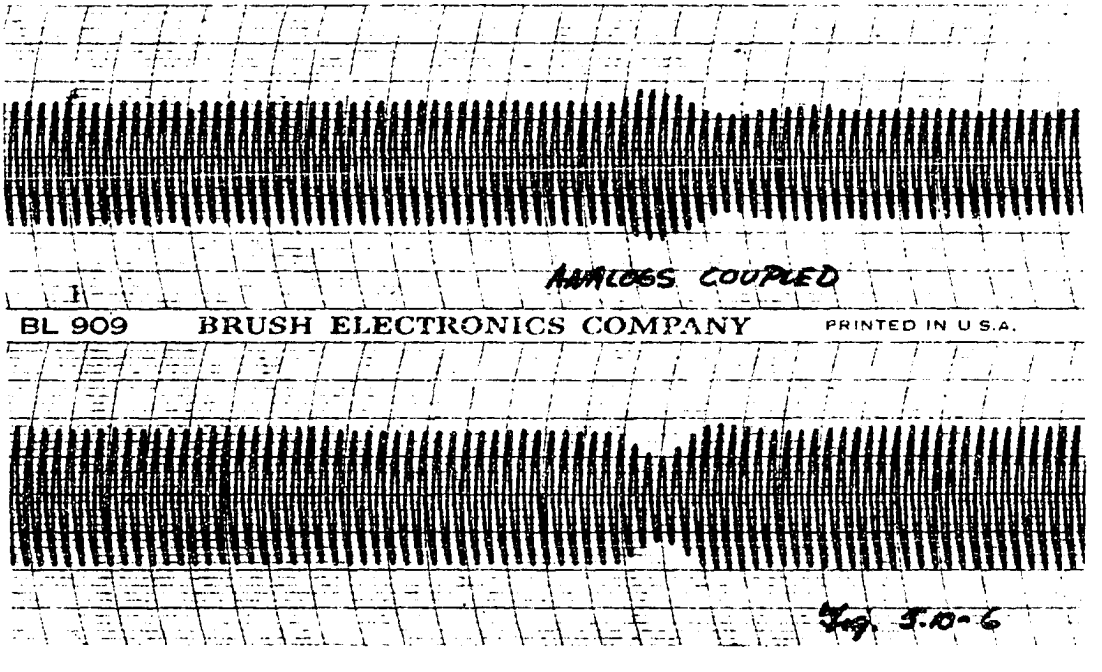

Fig. 5.10-6

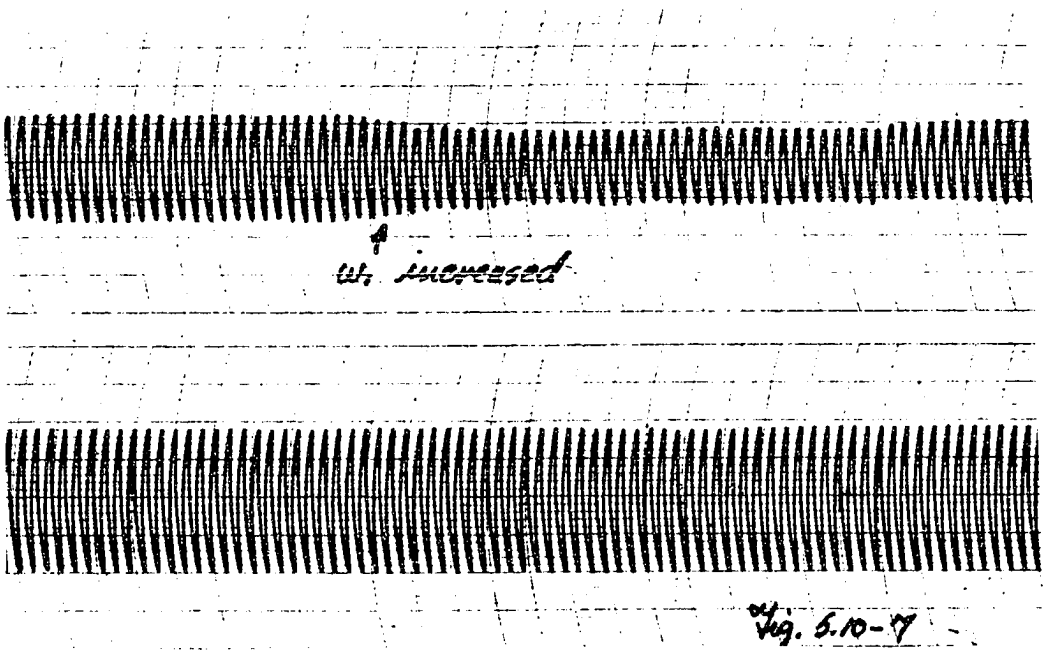

Fig. 5.10-7

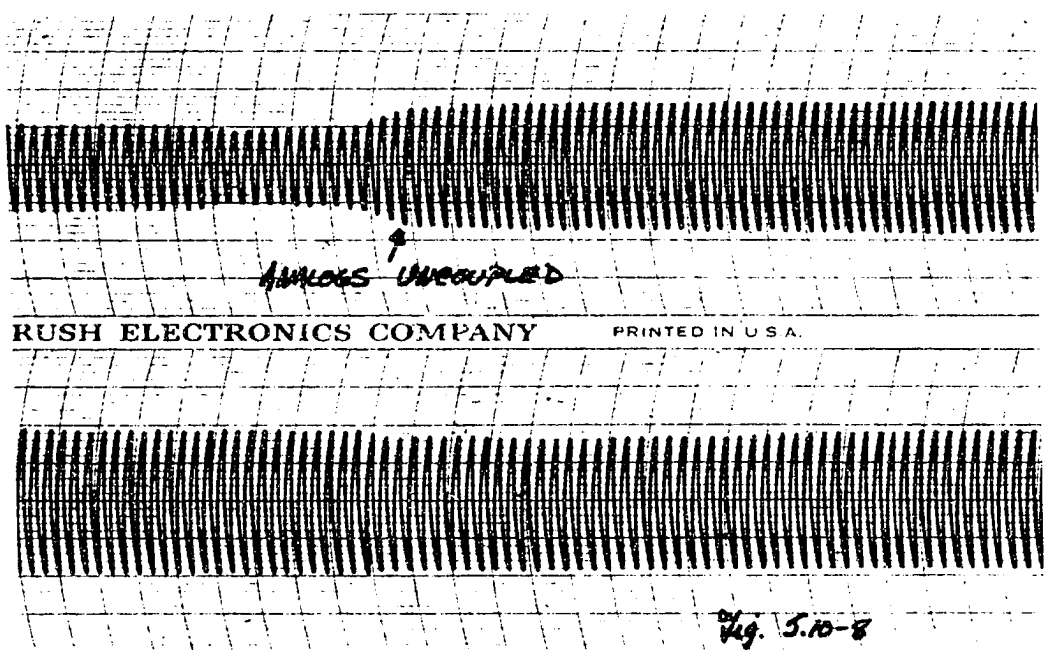

Fig. 5.10-8

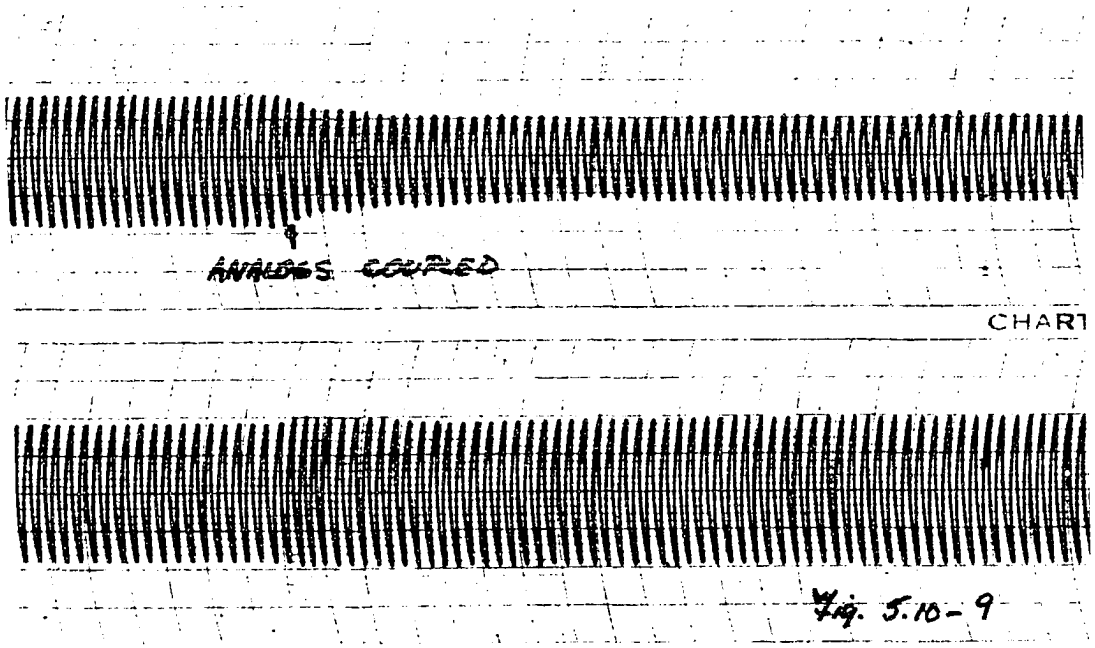

Fig. 5.10-9

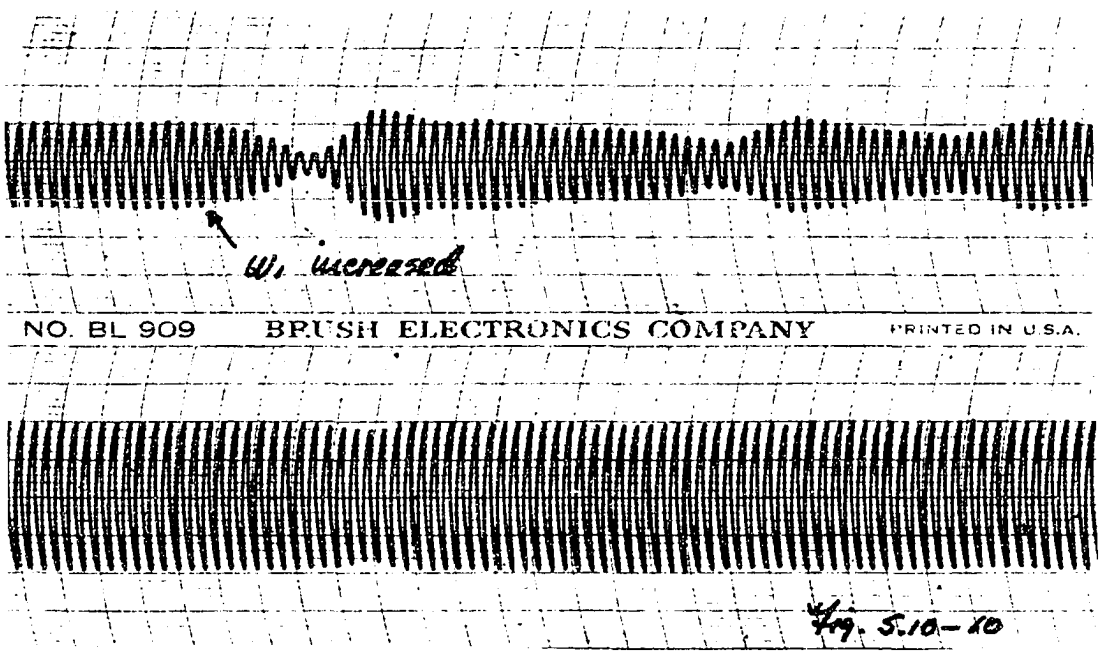

Fig. 5.10-10

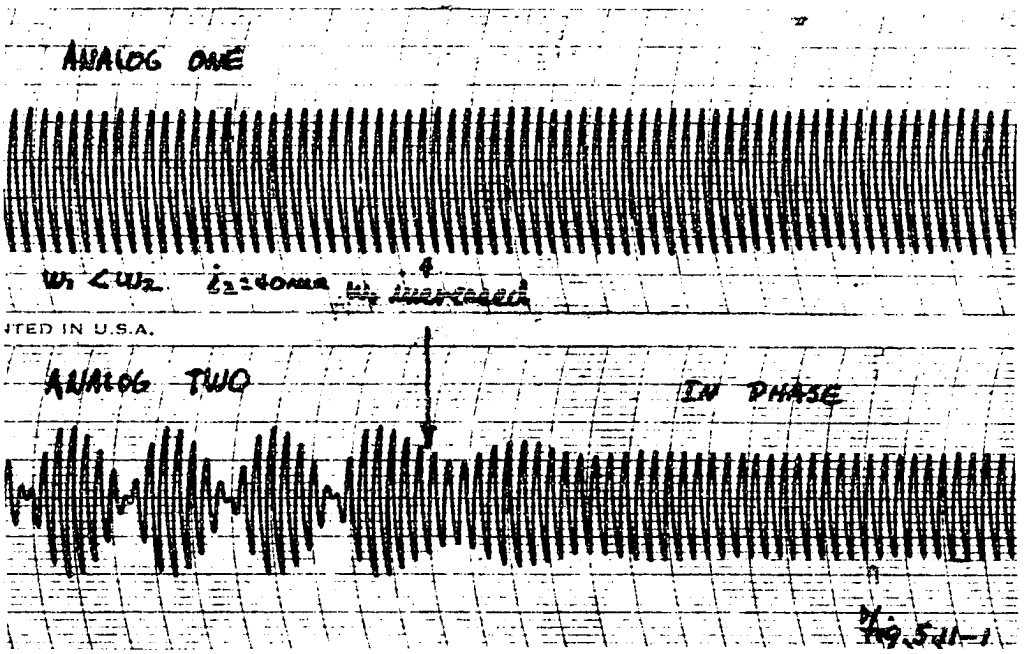

Fig. 5.11-1

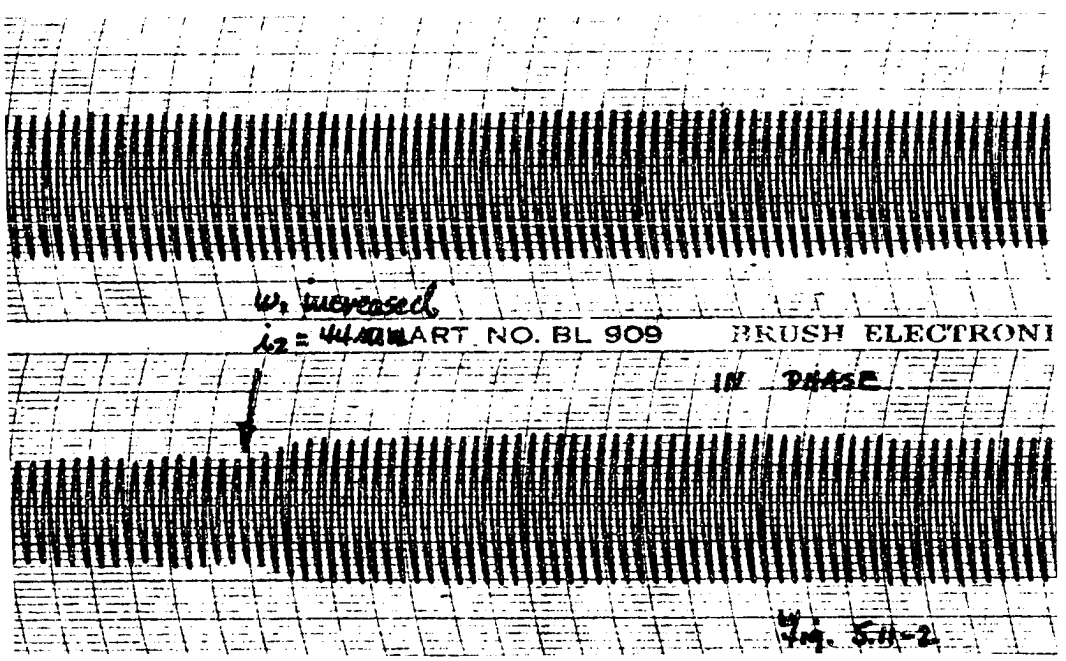

Fig. 5.11-2

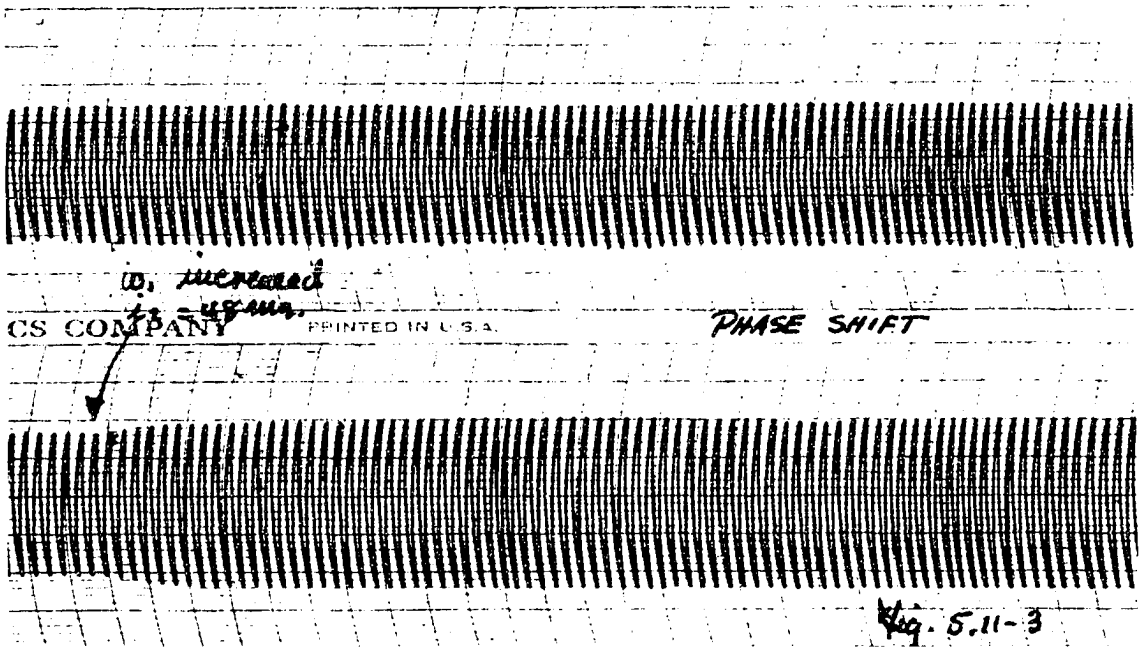

Fig. 5.11-3

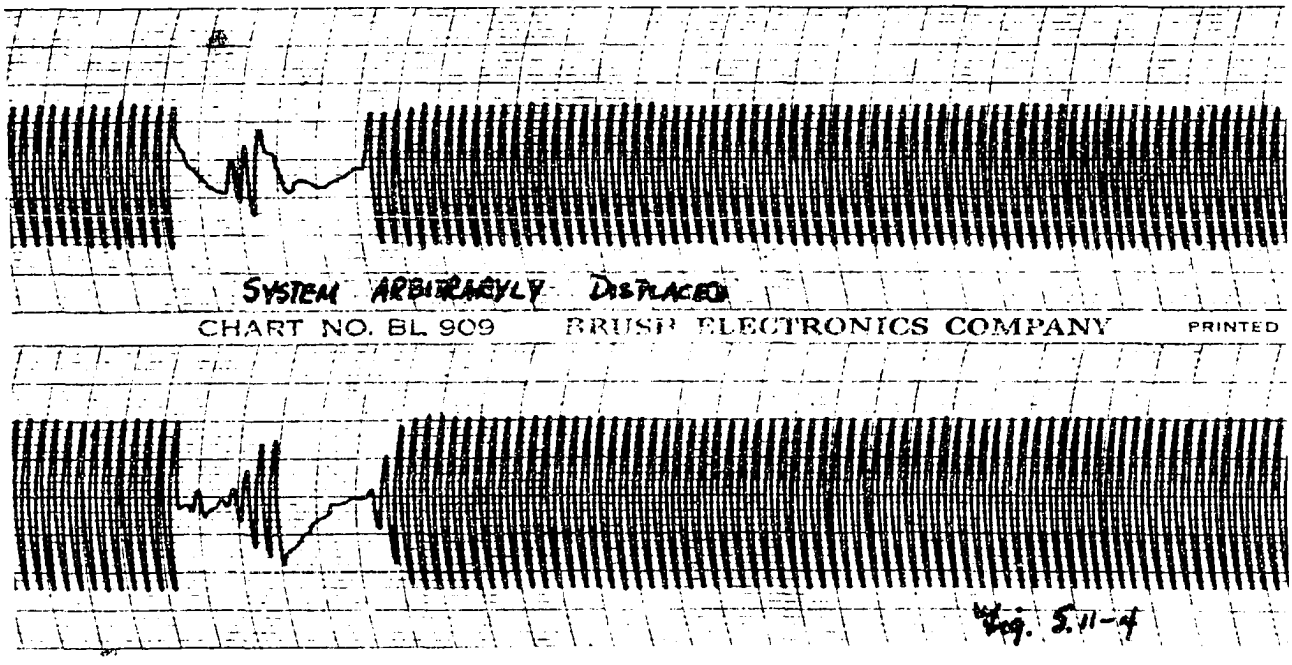

Fig. 5.11-4

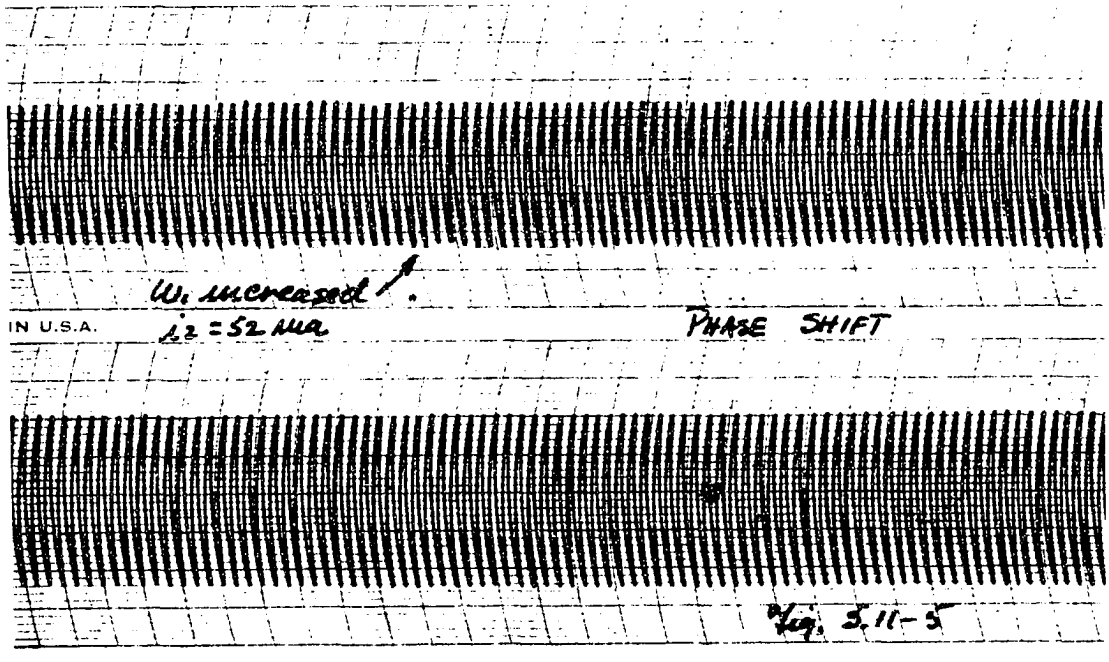

Fig. 5.11-5

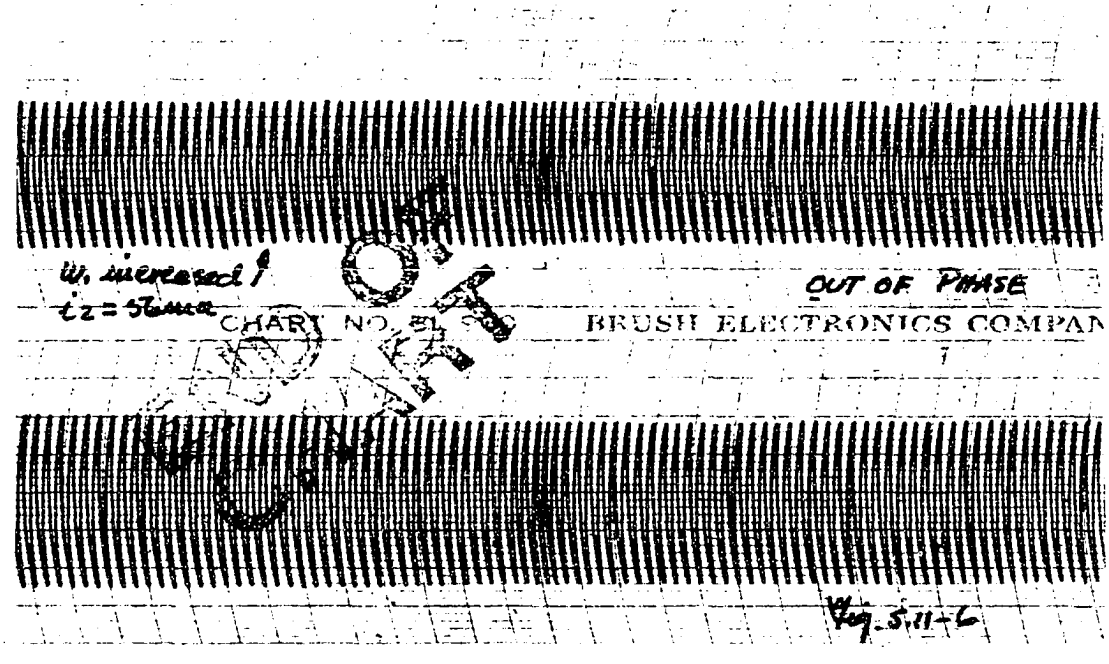

Fig. 5.11-6

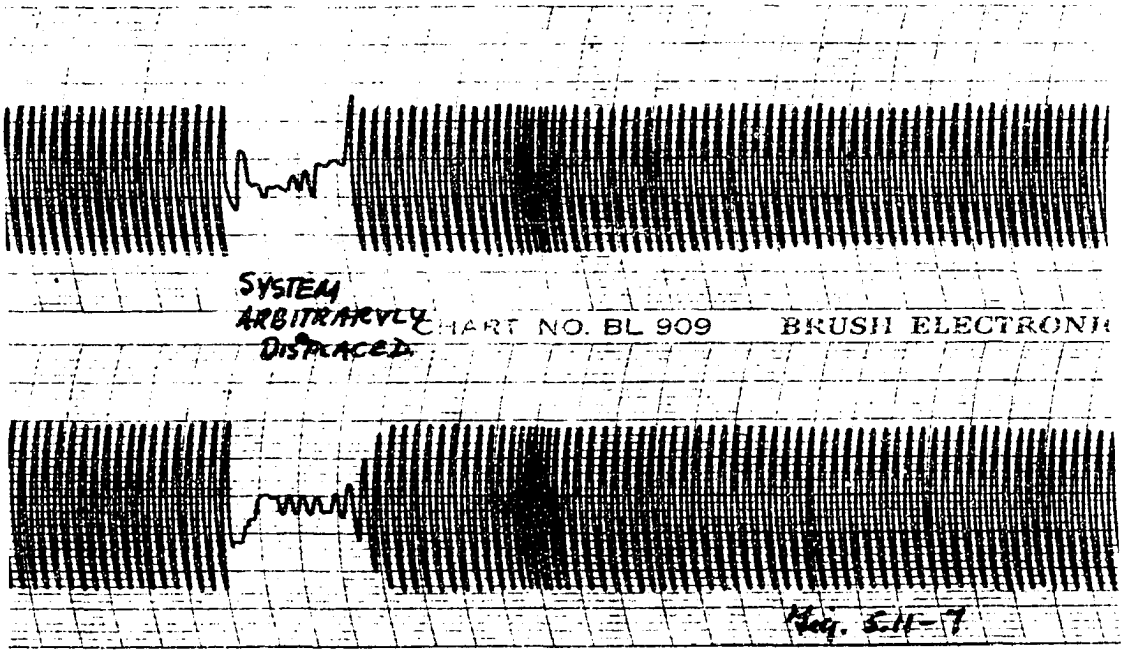

Fig. 5.11-7

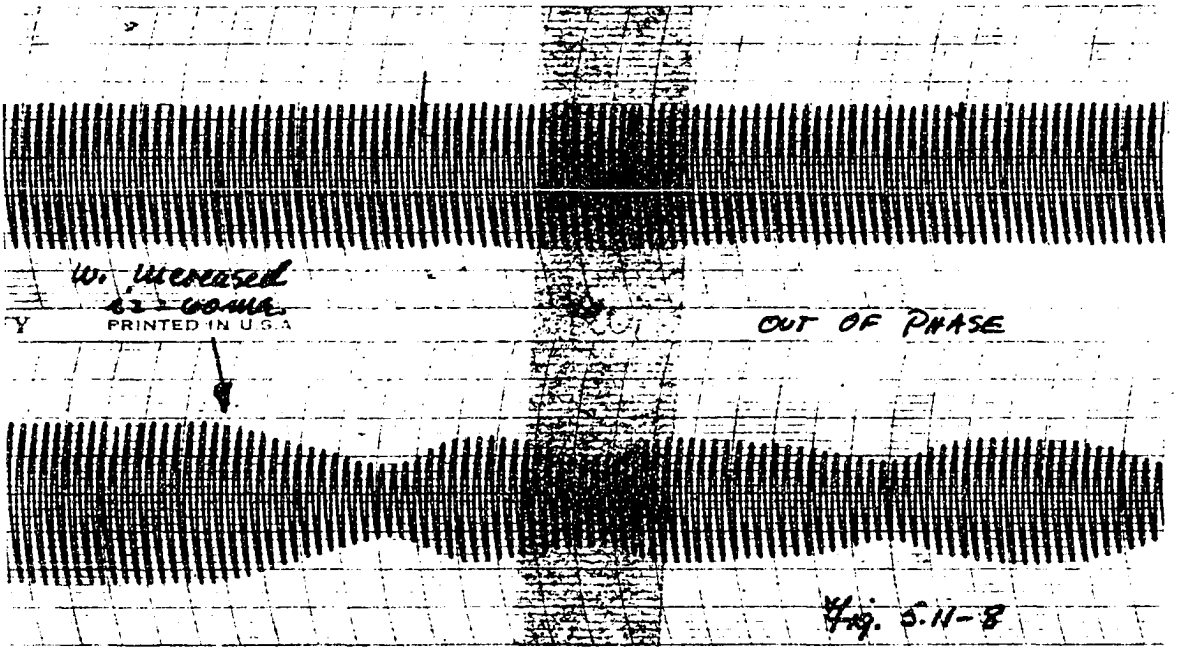

Fig. 5.11-8

in chart 7. Chart 8 demonstrates the reappearance of the varying amplitudes for an increased ω_1, $\omega_1 > \omega_2$.

Fig. 5.12 is a repeat of the latter experiment with $\omega_1 > \omega_2$ initially, and $\omega_1 > \omega_2$ finally.

It is important to note from these observations that (1) the shift in phase for $k_2 > k_1$ is predicted by the linear theory, (see fig. 5.8). As ω_1 is varied the system slips from one mode to the other; (2) For a range of ω_1, irregardless of the relative coupling magnitudes and initial transitions, the system automatically seeks one or the other modes of oscillation, and has maximum vibrating amplitudes of constant magnitude for specific frequencies of ω_1 within this range. This phenomenon is not predictable from the linear theory.

Experiments identical to the ones above however, this time quantitative in nature, were performed for the cases (1) $k_2 > k_1$ and (2) $k_2 \cong k_1$. The results are shown in the following figures: for $k_2 > k_1$ figs. 5.13 and 5.14 and for $k_2 \cong k_1$ figs. 5.15 to 5.19. The frequencies involved were measured directly from the Brush recordings. The similarity to the same type of curves for the linear cases is apparent and in figs. 5.13 and 5.17 the linear case has been plotted along with the experimental nonlinear case. All frequencies are plotted as a function of ω_1, the natural frequency of the system on analog one. For convenience ω_1 also has been plotted.

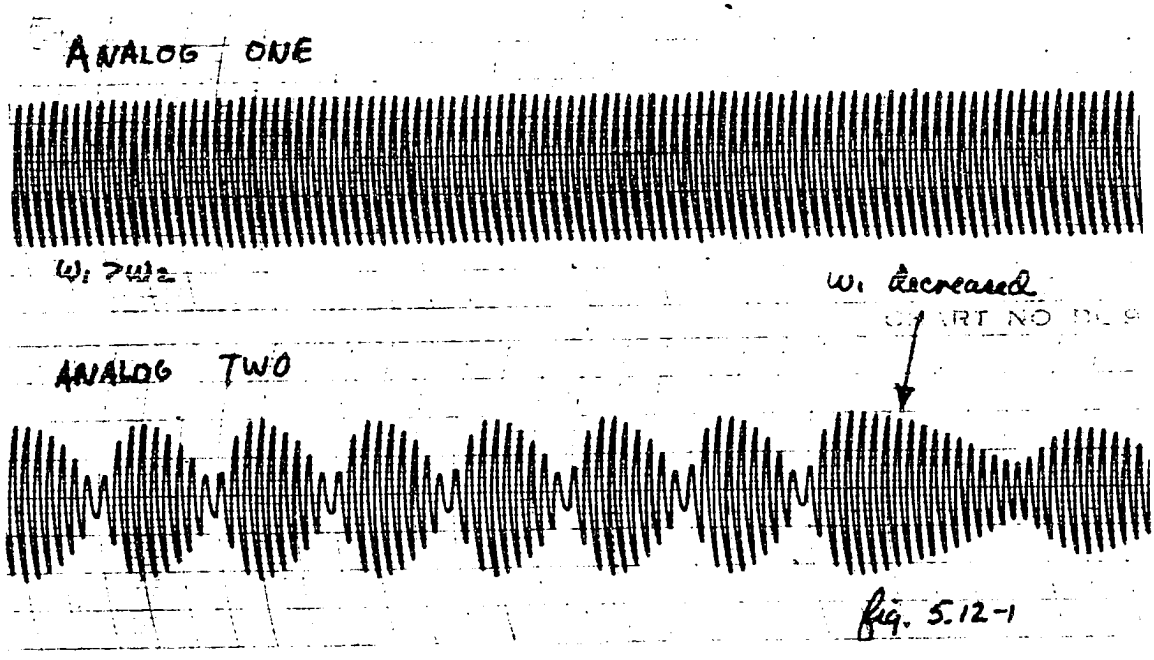

Fig. 5.12-1

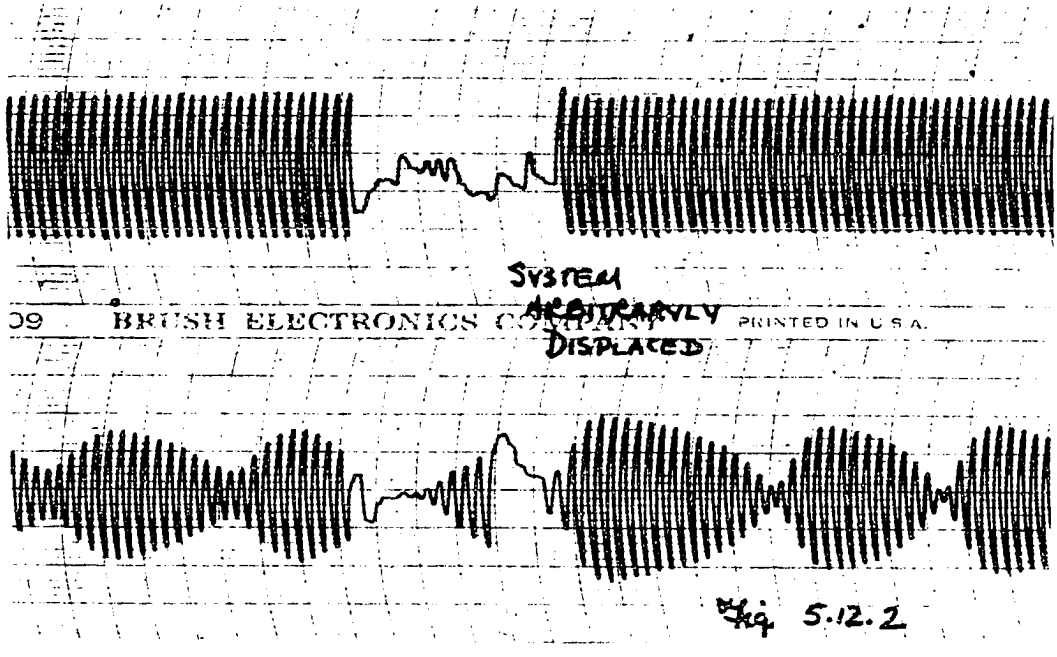

Fig. 5.12.2

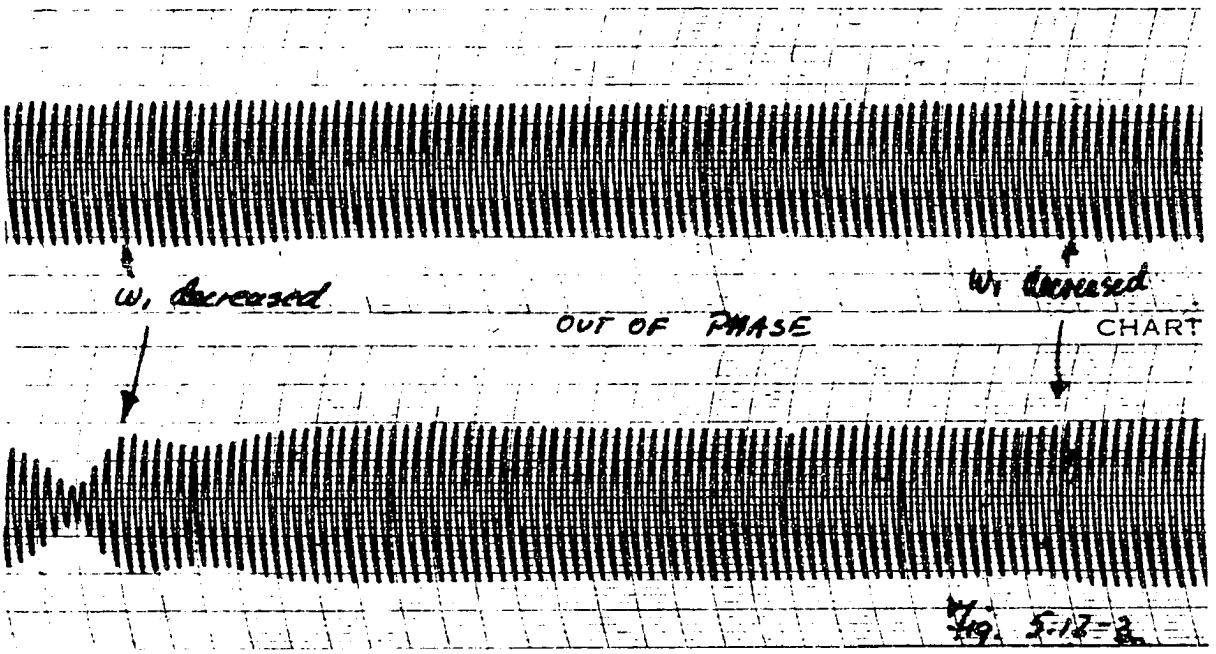

Fig. 5.12-3

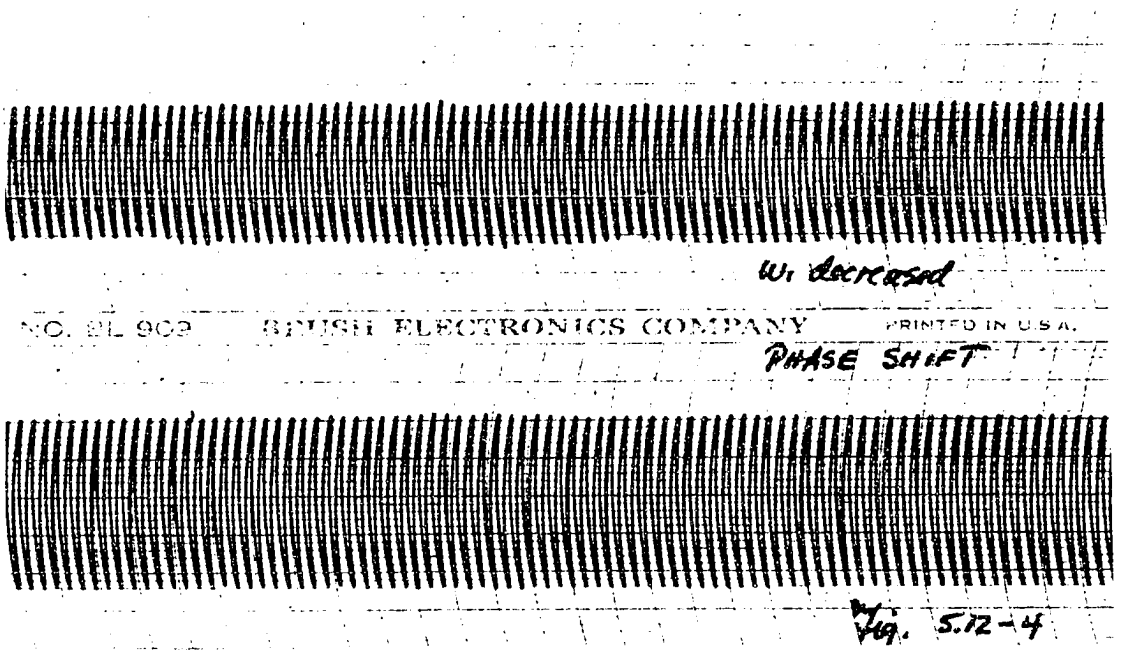

Fig. 5.12-4

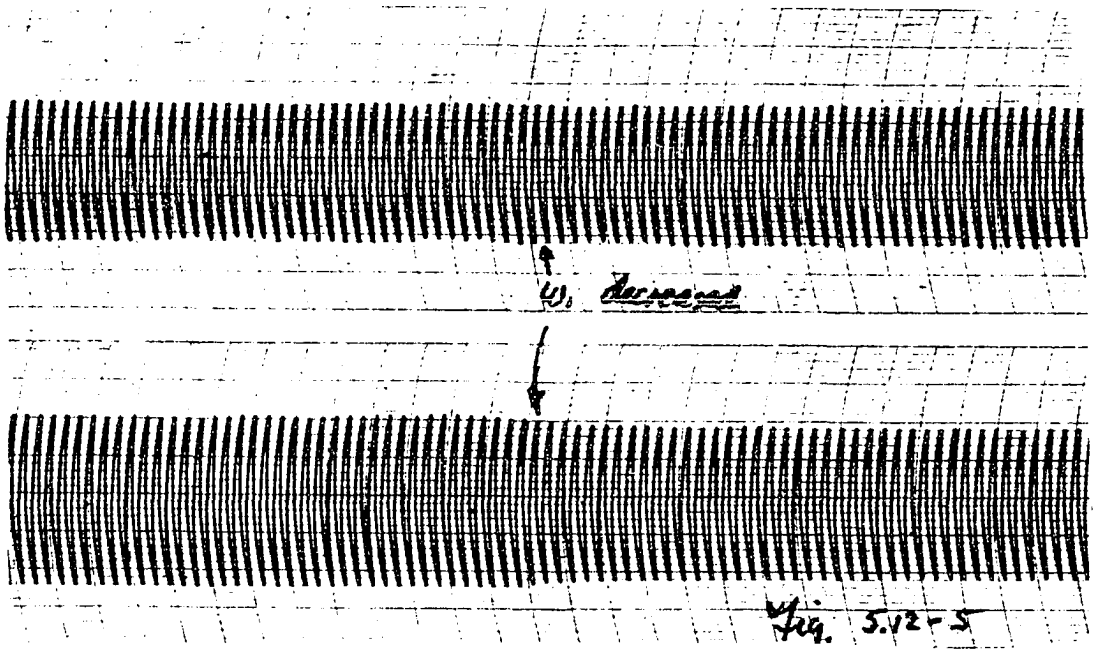

Fig. 5.12-5

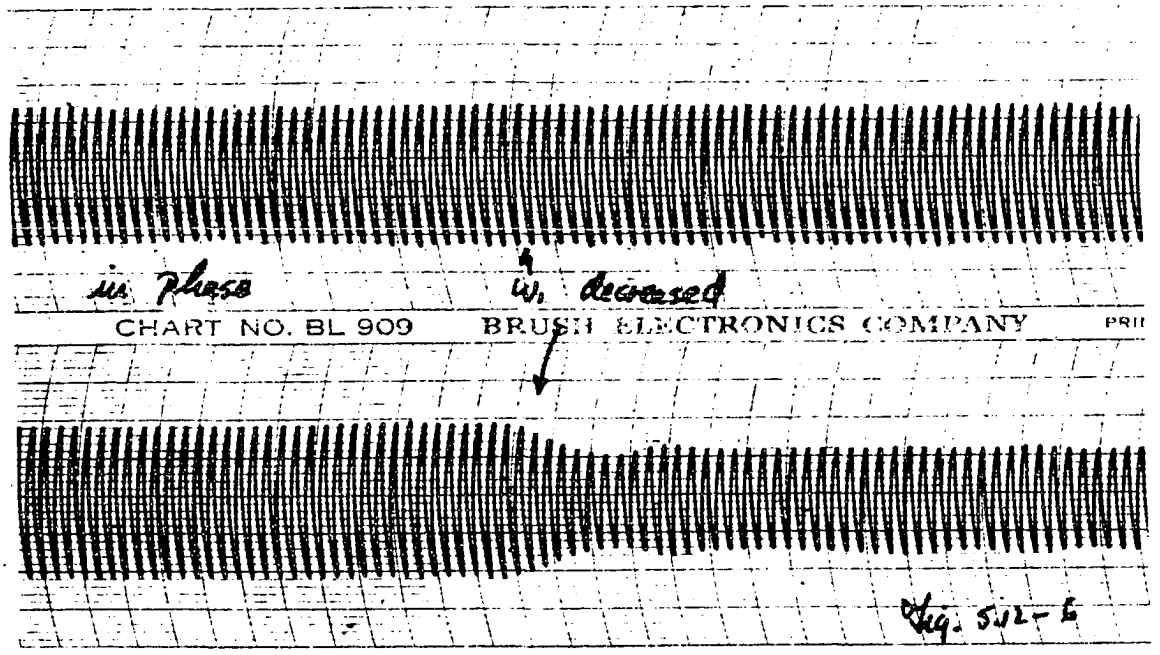

Fig. 5.12-6

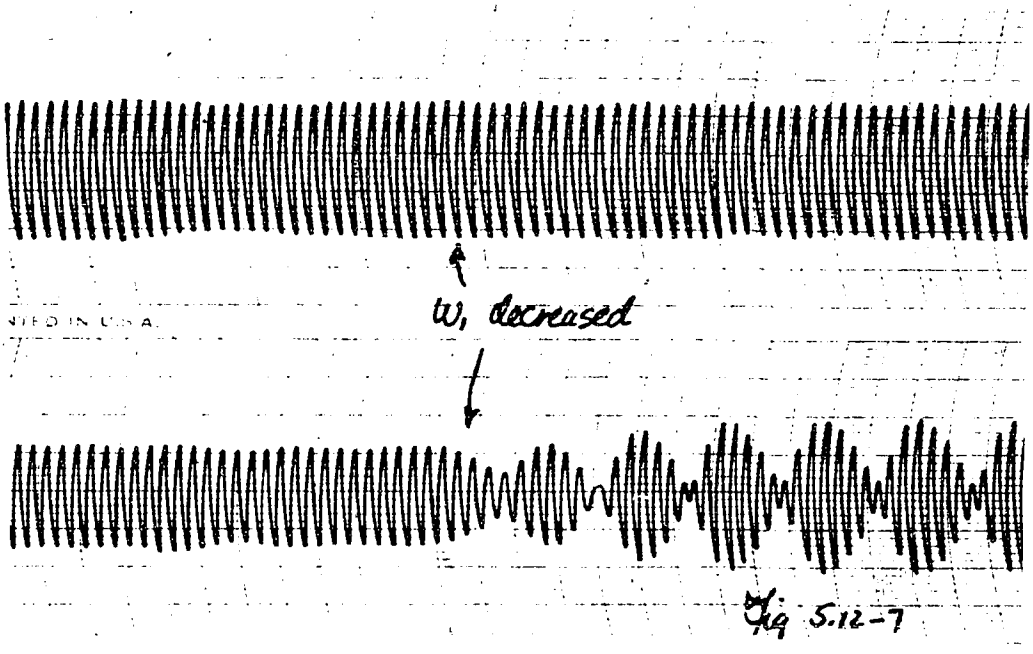

Fig 5.12-7

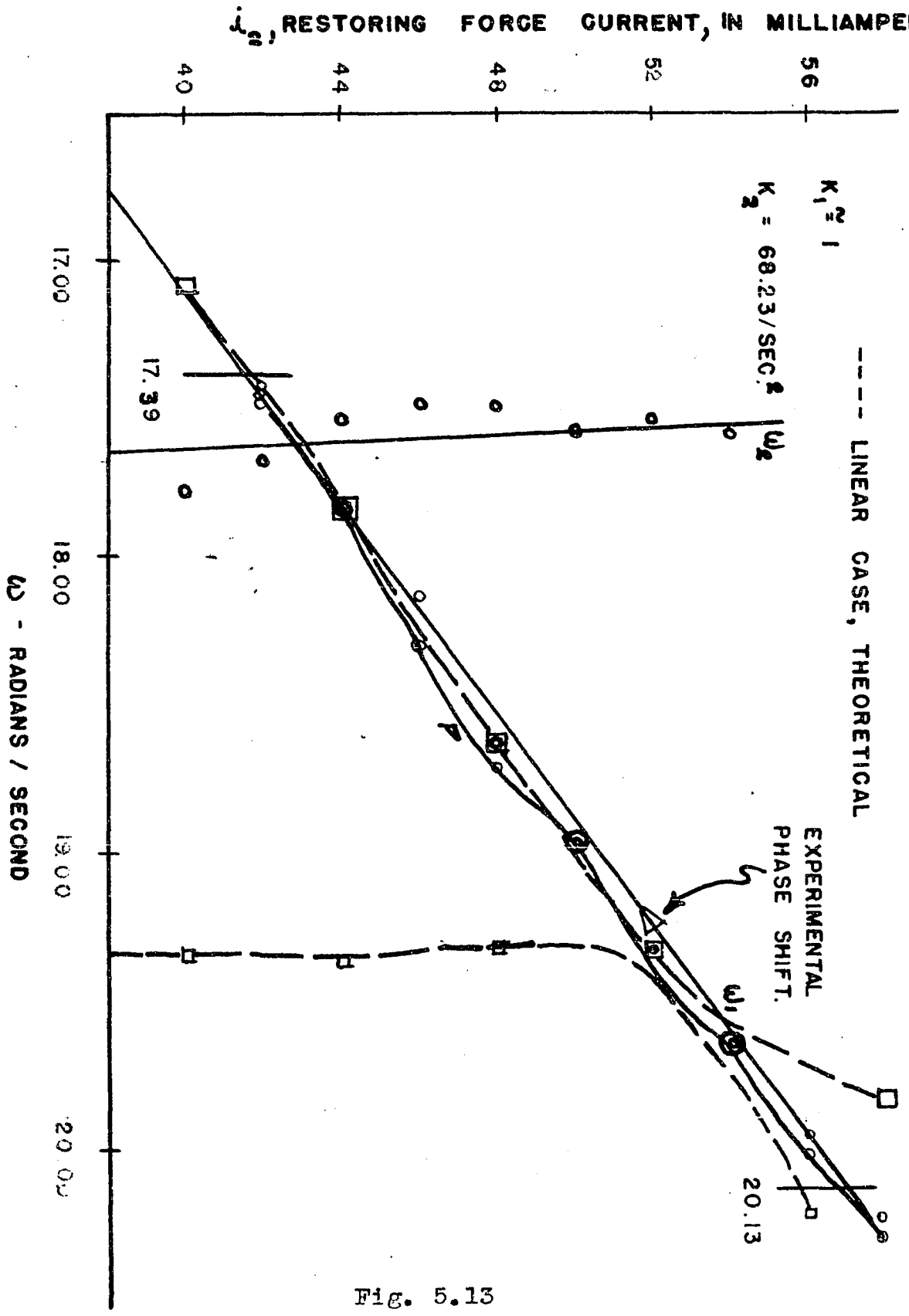

Fig. 5.13

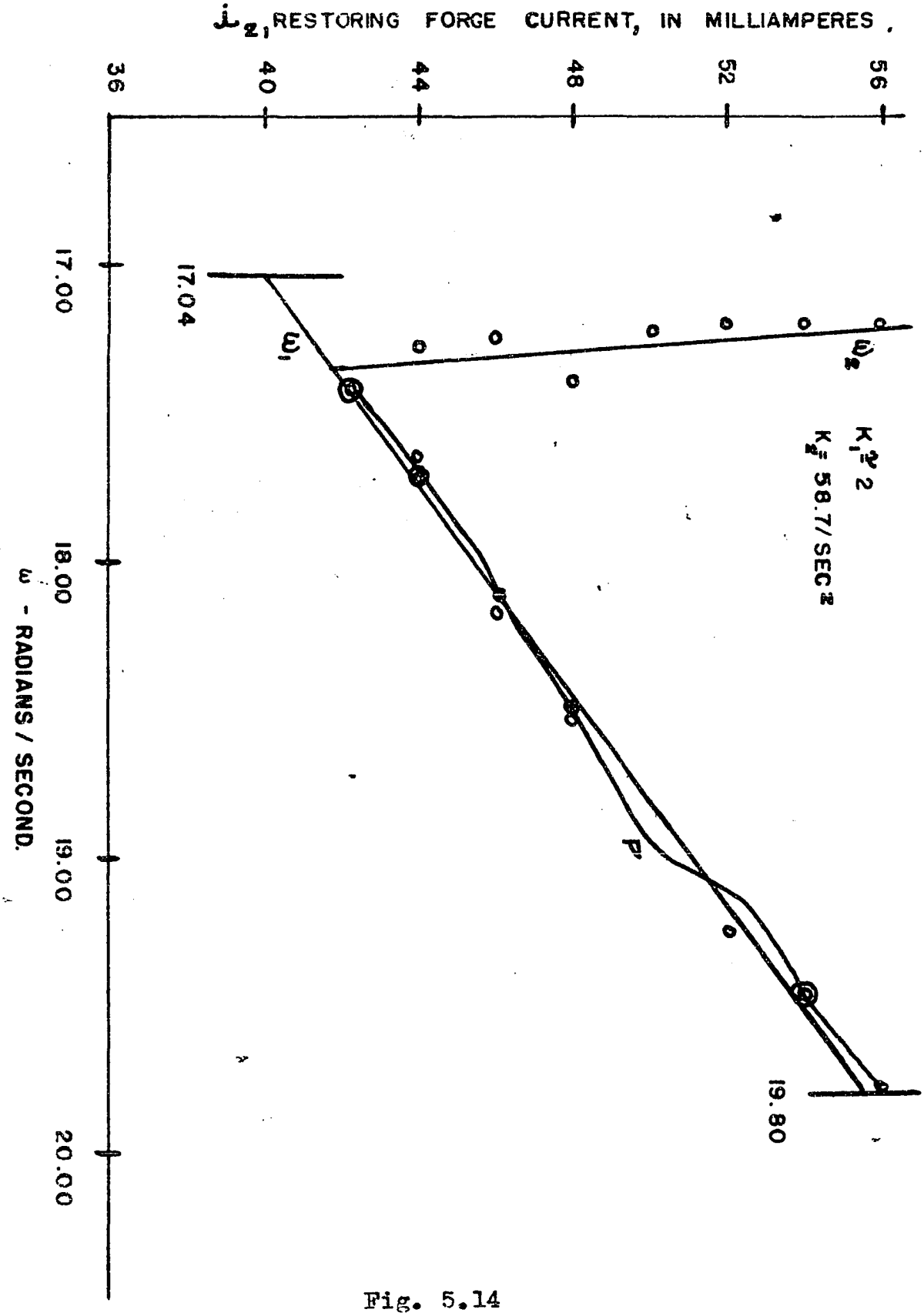

Fig. 5.14

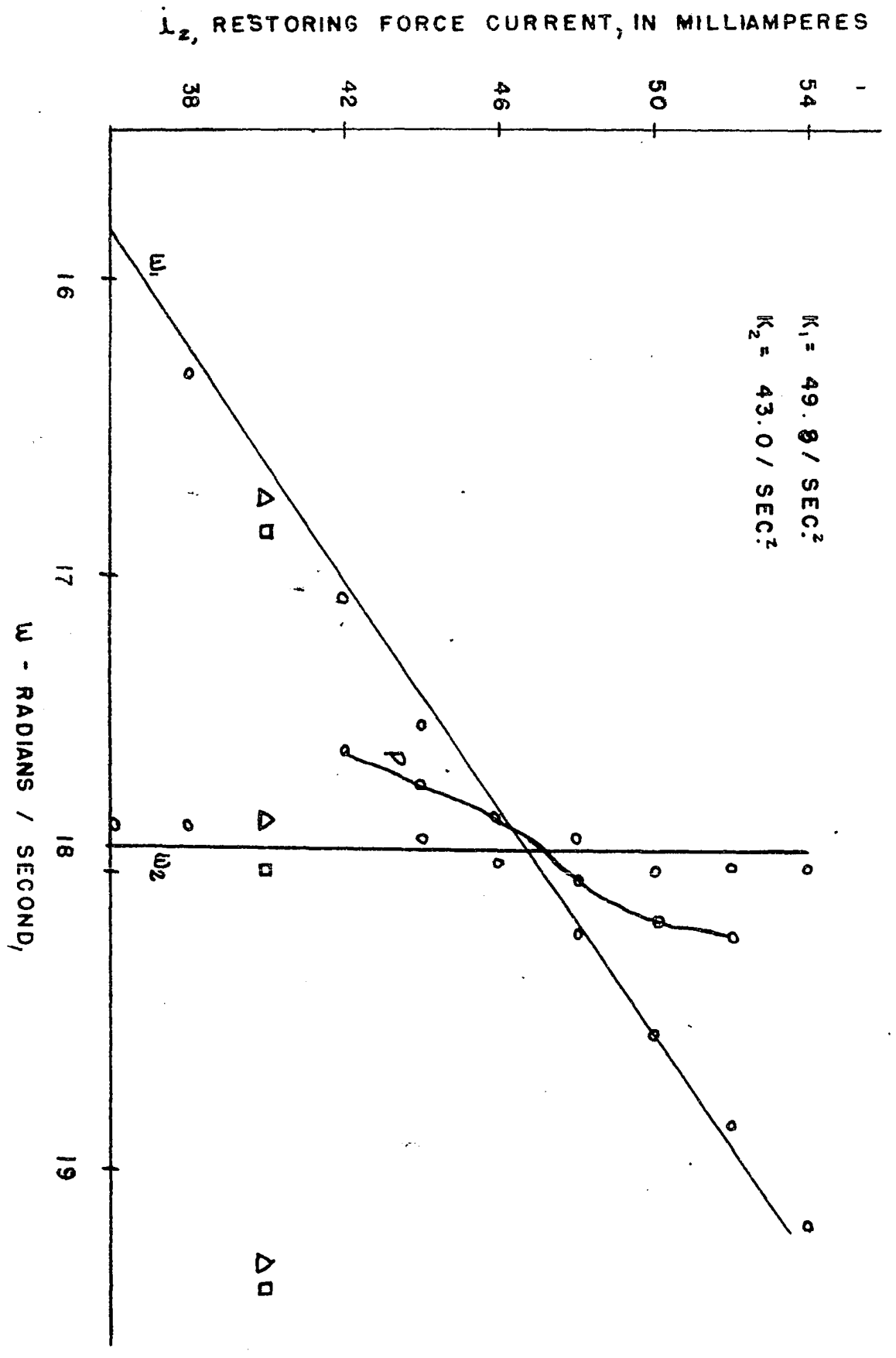

Fig. 5.15

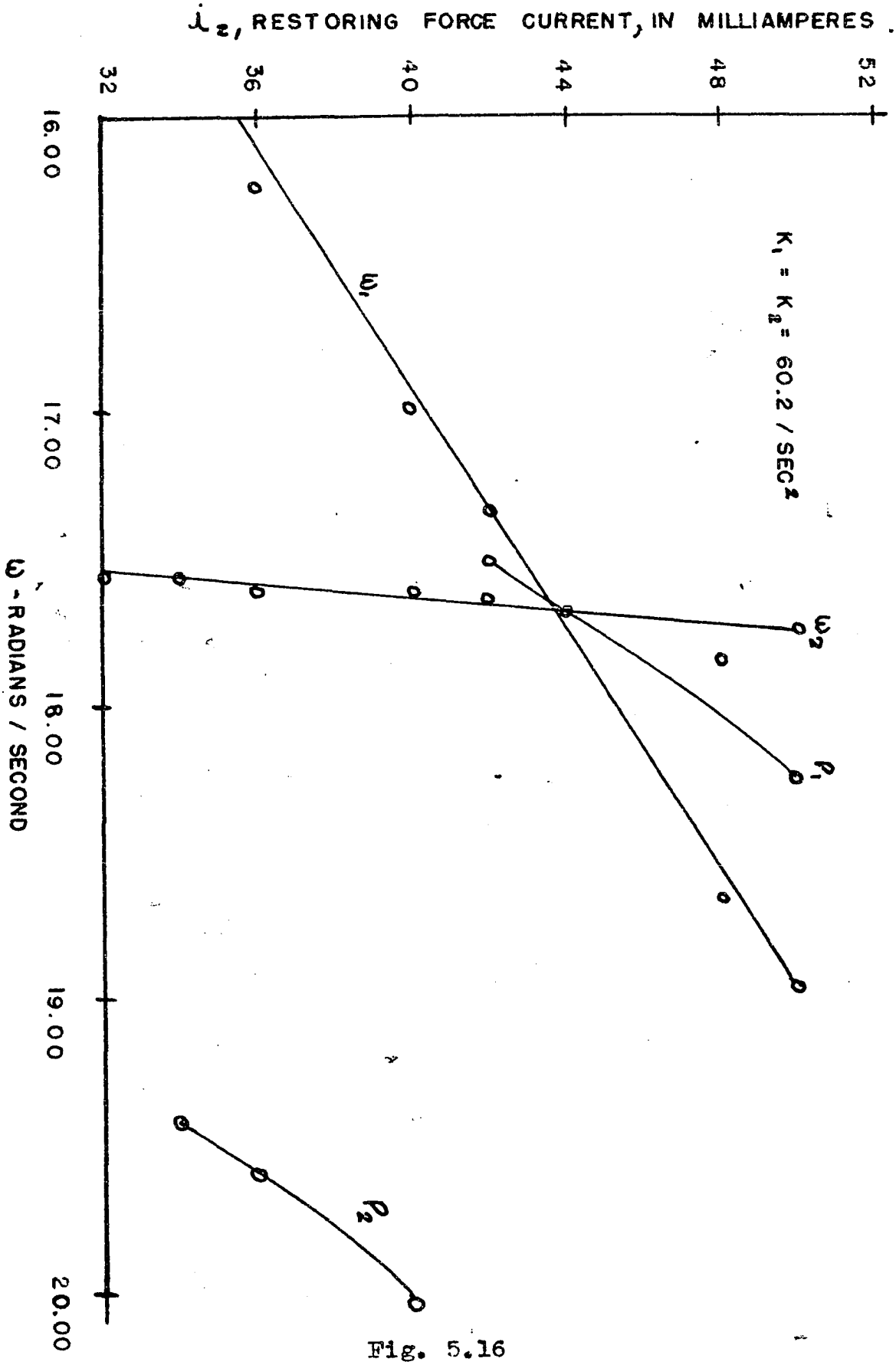

Fig. 5.16

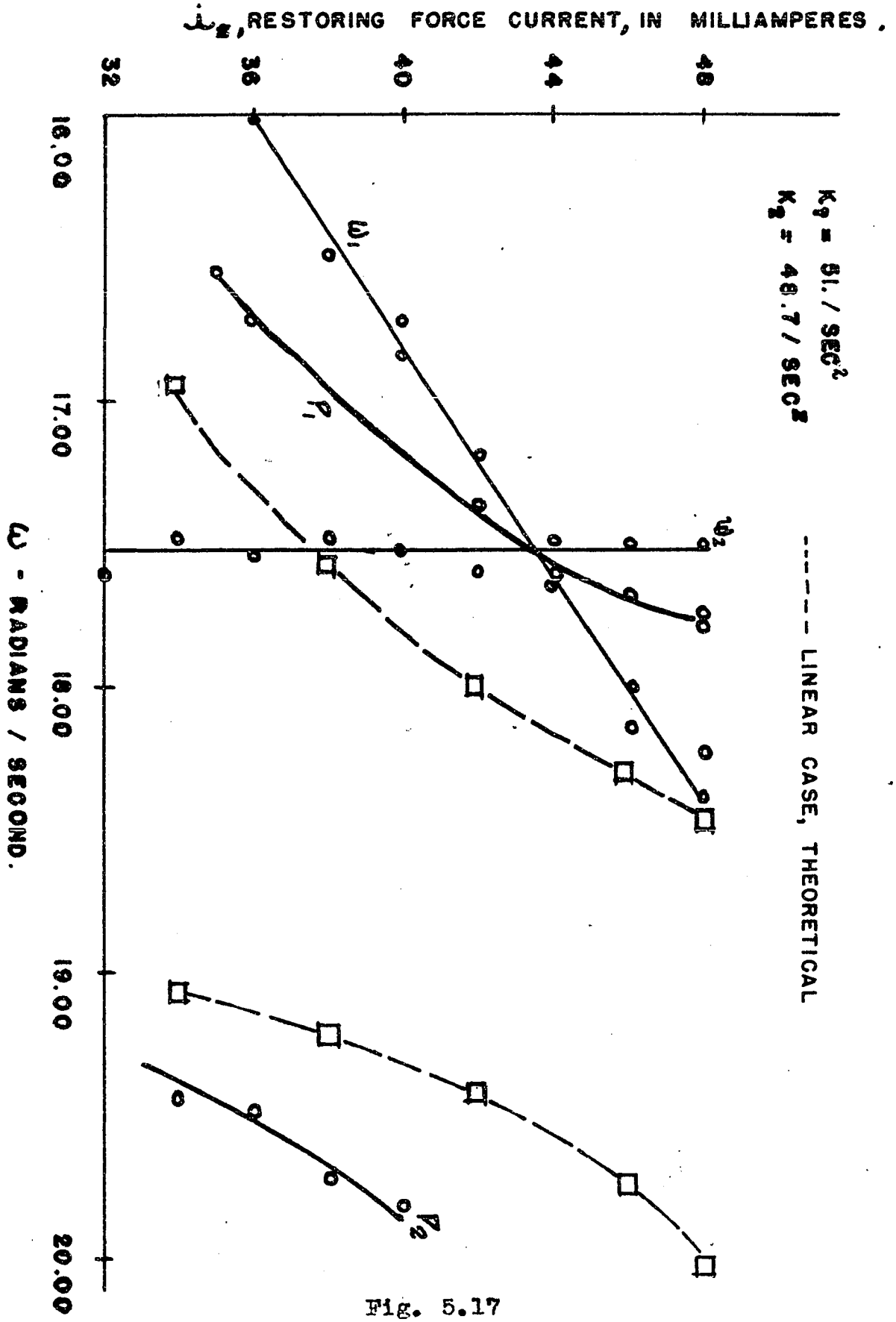

Fig. 5.17

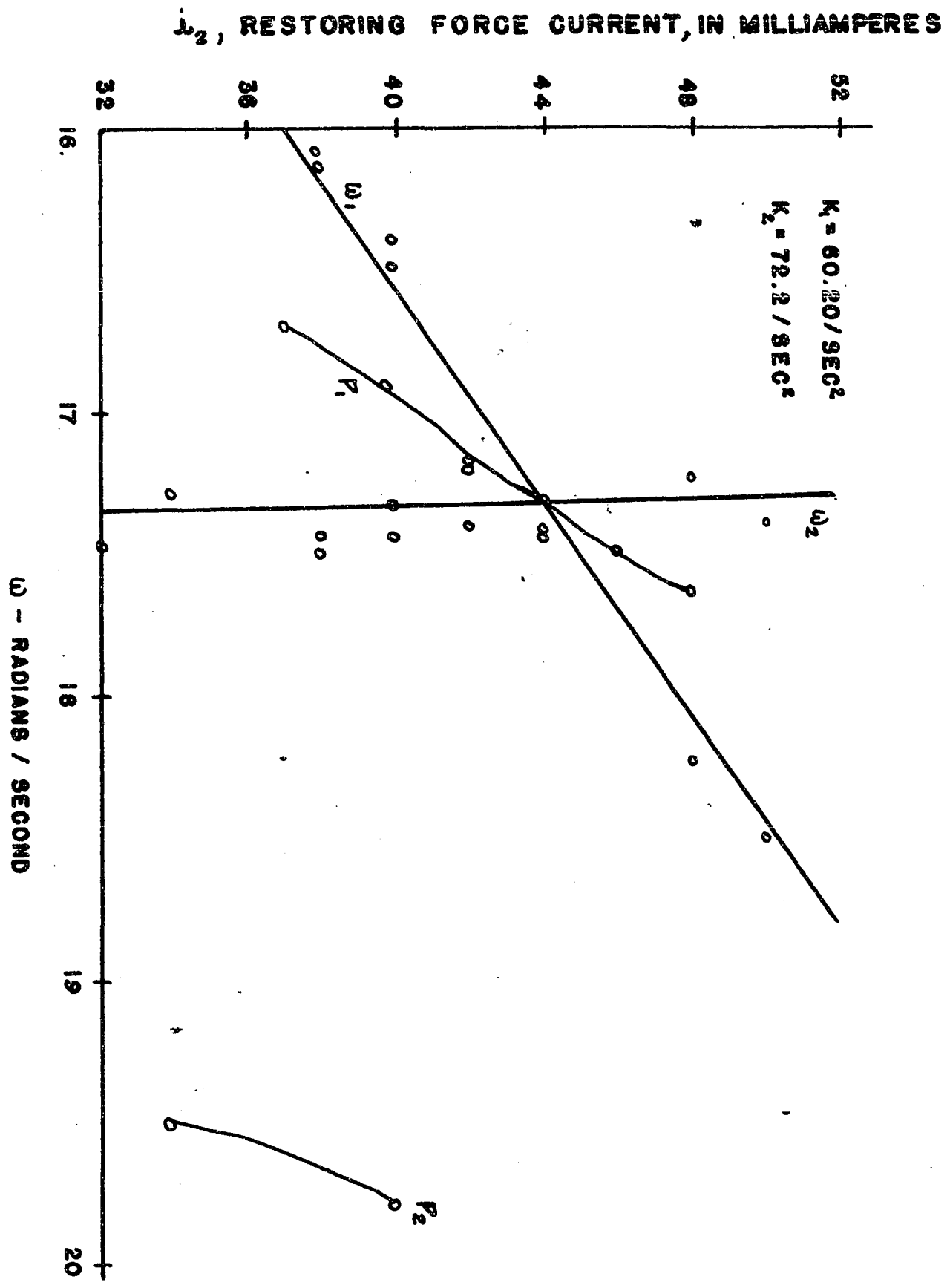

Fig. 5.18

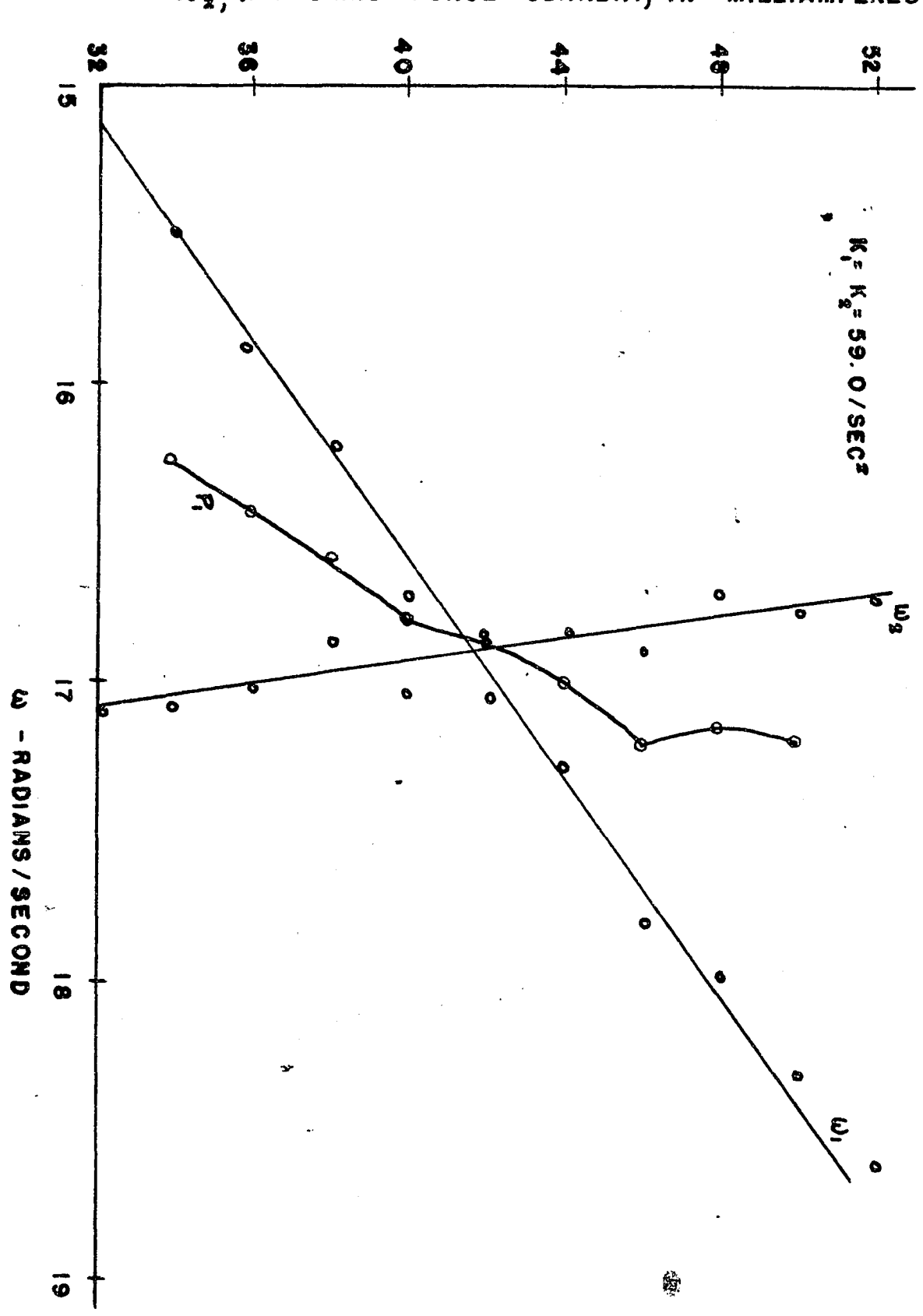

Fig. 5.19

Considering first fig. 5.13 it is noted that very little difference exists between the linear and nonlinear case, the phase shift even occurring at approximately the predicted point. The second mode was not obtained in this particular case due to the fact that the amplitudes of vibration exceeded the limits of the analog. It is further noted that a constant amplitude of the limit cycle is only obtained for a portion of the predicted linear range for the first mode in the vicinity of ω_1 .

In fig. 5.17 a shift in the modal curves is indicated for the nonlinear case when compared to the linear case. In this instance two modes of oscillation were obtainable and there is no predominance of one mode over the other for an arbitrary excitation of the system. It was noted that the relative phase upon coupling usually determined in which mode the system became excited.

It is again important to emphasize that in all these experiments there is a range of ω_1 for which the nonlinear system automatically becomes self-excited with constant amplitude regardless of the initial transitions and regardless in which mode the system is oscillating.

6. CONCLUSIONS

The experimental observations and theoretical considerations that have been presented in the previous section now make it possible to assert a number of conclusions in regards to the problem of frequency entrainment applied to nonlinear systems of two degrees of freedom. However, since the one degree of freedom entrainment phenomena has been considered in the process of investigating the latter, it will be advantageous to discuss this case first.

By the experimental results and theoretical considerations that have been presented in section 4, it has been shown that the magnitude of the range of frequency within which the forcing function drives and controls the behavior of the nonlinear system, which it is driving, is dependent upon the amplitude of the forcing function, and also is a function of the nonlinearity and damping in the system as described by the approximate relation eq. (4.6). Theoretically, there is the restriction that $\alpha < 1$ for this function, and the experimental results have been limited to this restriction.

It has been shown also that a specialized form of mechanical frequency entrainment is obtainable experimentally, and in a form which can be investigated quantitatively. It seems plausible that, if the proper procedures are followed parametrically, jump and hysteresis phenomena

as discussed by Stoker, Cartwright, and Littlewood [12]. could be obtained and investigated. It would also be advantageous to experimentally investigate the effects of increased magnitudes of nonlinearity. Subharmonic response is also a likelihood. A further field of possible investigation lies in large nonlinearity for the homogeneous van der Pol system, which, of course, leads to relaxation oscillations.

The fact that the behavior of a mechanically self-excited nonlinear system of two degrees of freedom for magnitudes of nonlinearity that are small is very similar to that of a linear undamped system of two degrees of freedom with the same parametric restrictions, leads to the conclusion that the present concept of frequency entrainment, which physically requires a forcing function, is not completely applicable to systems of two degrees of freedom. To have a complete physical understanding of the behavior of such a nonlinear system, and to include all energy states, it is necessary to consider the system as a whole and not as certain parts effecting other parts of the system, as has been done in the past. It has been shown that two modes of oscillation exist for the nonlinear system and that there is a region of ω_1 in the vicinity of ω_2 for which the nonlinear system will automatically seek one or the other modes of oscillation, and within which the amplitudes of the limit cycles remains constant at specific values of ω_1. There are no varying

amplitudes at any value of the frequency w_1 within the above frequency range. This latter phenomenon is similar to the entrainment of a one degree of freedom system, and an attempt to explain it by the suppression concept is a natural procedure and is satisfactory under certain conditions, however, for identical parameters in each half of the nonlinear system that has been considered, one would expect from the definition of frequency entrainment to have no motion when the system is synchronized due to the fact that each half would suppress the other half. This has not been obtained experimentally. Because the forcing function concept breaks down for the above case, and because the synchronization effect occurs in two modes, it is clear that a more general definition and understanding of frequency entrainment is required in order to present a true physical understanding of the self synchronization phenomenon encountered in nonlinear systems of two degrees of freedom. This requires a successful analytical nonlinear theory which proposes a problem of considerable magnitude. Many difficulties are encountered in attempting to extend the present nonlinear theories of one degree of freedom to nonlinear systems of two degrees of freedom.

The present concept of frequency entrainment might be considered satisfactory for the special case of one

coupling constant being smaller than the other. However, even then the phase shift that occurs is not predictable.

It is of interest to note that the synchronization of the various systems of two degrees of freedom, Huygens' clocks, etc., can be primarily interpreted by the linear theory, i.e. for systems almost identical parametrically and with small nonlinearities, one would expect a modal frequency to exist between the natural frequencies of the uncoupled systems. However, the automatic existence of the coupled systems in a particular mode demonstrates the synchronization phenomenon that has been obtained experimentally above. It is of further interest to note that a type of self-synchronization occurs in the two degree of freedom linear damped case when the modal damping terms are strongly unequal as has been demonstrated among the above experiments.

It has been shown that only linear coupling is necessary between the two self oscillating systems for the self-synchronization phenomenon to occur.

The fact that a mechanical self-synchronization phenomenon in a nonlinear system of two degrees of freedom has been obtained in a quantitative experimental form provides the opportunity for further investigation and makes plausible the success of the attainment of a complete physical understanding of this self-synchronization phenomenon.

REFERENCES

(1.) Minorsky, N., "Introduction to Nonlinear Mechanics", Edwards, Ann Arbor, 1947.

(2.) Stoker, J. J., "Nonlinear Vibrations", Interscience, New York, 1950.

(3.) Ibid., p. 171

(4.) Minorsky, N., "Introduction to Nonlinear Mechanics", p. 341.

(5.) van der Pol, B., "Forced Oscillations in a Circuit with Nonlinear Resistance", Philosophical Magazine, Vol. 3, No. 13 January 1927.

(6.) Lord Rayleigh, "Theory of Sound".

(7.) Vincent, J. H., "On Some Experiments in Which Two Neighboring Maintained Circuits Effect a Resonating Circuit", Proceedings of the Physical Society, London, Vol. 32, Part 2, February 1919.

(8.) Ludeke, C. A. and Morrison, C. L., "Analog Elements for Solving Nonlinear Differential Equations", Journal of Applied Physics, Vol. 24, No. 3, March 1953.

(9.) Ludeke, C. A. and Evans, R. T., "A Coupling Analog for Nonlinear Systems with More Than One Degree of Freedom", Journal of Applied Physics, Vol. 24, No. 2, February 1953.

(10.) Myklestad, No. O., "Vibration Analysis", McGraw-Hill, New York, 1944, p. 98.

(11.) Stoker, J. J., "Nonlinear Vibrations".

(12.) Ibid., p. 185.

ACKNOWLEDGMENT

The author wishes to express his appreciation to Dr. C. A. Ludeke for his untiring guidance, stimulating discussions, and valuable suggestions, and also to Dr. D. A. Wells for his helpful discussions. Discussions with Mr. William Pong also have been of assistance and are gratefully acknowledged. Construction assistance by Mr. Allan Chace is gratefully appreciated.

BIBLIOGRAPHY

Andronow and Chaikin, "Theory of Oscillations", Princeton, 1949.

Andronow, A. and Witt, A., "Zur Theorie des Mitnehmens von van der Pol", Archiv fur Electrotechnik, 24, 1930, p. 99.

Andronow, A., and Witt, A., "Sur la theorie mathematique des systemes auto-oscillaloires a deux degrees de liberte", Technical Physics of the USSR (Leningrad) 1, 249, 1934.

Appelton, E. V., "The Automatic synchronization of Triode Oscillators", Proceedings of the Cambridge Philosophical Society, London, 21, 1922.

Appelton, E. V., and van der Pol, B., "Oscillation Hysteresis in the Triode", Philosophical Magazine, 43, 177, 1922.

Cartwright, M. L., and Littlewood, J. E., Journal of London Mathematical Society, 20, 180, 1945.

Cartwright, M. L., and Littlewood, J. E., Annals of Mathematics, 48, 490, 1947.

Cartwright, M. L., Proceedings of Cambridge Philosophical Society, 45, 495, 1949.

Cartwright, M. L., Journal of Institute of Electrical Engineers, 95, 88, 1948.

Kryloff, N., and Bogoliuboff, N., "Sur le phenomene de l'entrainement in radiotechnique", Comptes Rendus, 194, 1064, 1932.

McLachlan, N. W., "Ordinary Nonlinear Differential Equations", Oxford, London, 1950.

Migulin, V., "Resonance Effects in a Nonlinear System with Two Degrees of Freedom", Journal of Technical Physics of the USSR, 4, 10, 1937.

Minorsky, N., "Introduction to Nonlinear Mechanics", Edwards Brothers, Ann Arbor, 1947.

Moller, H. G., "Uber storungsfreien Gleictistromempfung mit dem Schwingandion", Zeitschrift fur drahtlos Telegraphie und Telephonie, 17, 1921.

van der Pol, B., "Oscillation Hysteresis in a Triode Generator", Philosophical Magazine, 6, 43, 700, 1922.

van der Pol, B., "Forced Oscillations in a Circuit with Nonlinear Resistance", Philosophical Magazine, 3, 13, 1927.

Rayleigh, Lord, "On Maintained Vibrations", Philosophical Magazine, 5th Series, 15, April 1883.

Strutt, J. W., (Lord Rayleigh), "The Theory of Sound", Vol. II, 223, Dover Publications, 1945.

Stoker, J. J., "Nonlinear Vibrations", Interscience, New York, 1951.

Theodorchik, K. and Chaikin, E., "Acoustical Entrainment", Journal of Technical Physics of the USSR, 2, 111, 1932.

Vincent, J. H., "On Some Experiments in Which Two Neighboring Maintained Circuits Affect a Resonating Circuit", Proceedings of the Physical Society, London, 32, part 2, 84, 1919.